

This item was submitted to Loughborough University as a PhD thesis by the author and is made available in the Institutional Repository (<https://dspace.lboro.ac.uk/>) under the following Creative Commons Licence conditions.



For the full text of this licence, please go to:
<http://creativecommons.org/licenses/by-nc-nd/2.5/>

LOUGHBOROUGH UNIVERSITY

Special Vector Configurations in Geometry and Integrable Systems

by

Veronika Schreiber

A thesis submitted in partial fulfillment for the
degree of Doctor of Philosophy

Department of Mathematical Sciences

May 27, 2014

Declaration of Authorship

I, Veronika Schreiber, declare that this thesis titled, Special Vector Configurations in Geometry and Integrable Systems and the work presented in it are my own. I confirm that:

- This work was done wholly or mainly while in candidature for a research degree at this University.
- Where any part of this thesis has previously been submitted for a degree or any other qualification at this University or any other institution, this has been clearly stated.
- Where I have consulted the published work of others, this is always clearly attributed.
- Where I have quoted from the work of others, the source is always given. With the exception of such quotations, this thesis is entirely my own work.
- I have acknowledged all main sources of help.
- Where the thesis is based on work done by myself jointly with others, I have made clear exactly what was done by others and what I have contributed myself.

Signed:

Date:

Abstract

The main objects of study of the thesis are two classes of special vector configurations appeared in the geometry and the theory of integrable systems.

In the first part we consider a special class of vector configurations known as the \vee -systems, which appeared in the theory of the generalised Witten-Dijkgraaf-Verlinde-Verlinde (WDVV) equations. Several families of \vee -systems are known, but their classification is an open problem. We derive the relations describing the infinitesimal deformations of \vee -systems and use them to study the classification problem for \vee -systems in dimension 3. In particular, we prove that the isolated cases in Feigin-Veselov list admit only trivial deformations. We present the catalogue of all known 3D \vee -systems including graphical representations of the corresponding matroids and values of ν -functions.

In the second part we study the vector configurations, which form vertex sets for a new class of polyhedra called affine B -regular. They are defined by a 3-dimensional analogue of the Buffon procedure proposed by Veselov and Ward. The main result is the proof of existence of star-shaped affine B -regular polyhedron with prescribed combinatorial structure, under partial symmetry and simpliciality assumptions. The proof is based on deep results from spectral graph theory due to Colin de Verdière and Lovász.

Acknowledgements

Foremost, I would like to express my gratitude to my advisor Professor Alexander Petrovich Veselov, who provided me with excellent supervision and continuous support. I would also like to thank him for his patience, motivation and enthusiasm. I could not have imagined having a better advisor and mentor for my Ph.D study.

My sincere thanks also goes to the academic and support staff in the Maths department at Loughborough University.

I thank my fellow students, in particular Graham Kemp and Mariano Galvagno for stimulating discussions, encouragement and friendship.

Last but not the least, I thank my family for their love and tremendous support throughout every journey of my life.

Contents

Declaration of Authorship	1
Abstract	2
Acknowledgements	3
1 Introduction	6
I V-SYSTEMS IN DIMENSION 3	14
2 V-systems and matroids	15
2.1 V-systems: definition and constructions	15
2.1.1 Subsystems and restrictions of V-systems	17
2.1.2 Generalised root systems and their deformations	19
2.2 Vector configurations and matroids	22
3 Deformations and classification	29
3.1 Classification of V-systems of A_3 and B_3 types	29
3.2 Deformations of V-systems	33
3.3 ν -function, uniqueness and rigidity conjectures	38
3.4 Matroidal structure of V-systems	40
3.4.1 Extensions and degenerations of V-systems	41
3.4.2 V-systems and harmonic bundles with two orthogonals	43
3.4.3 V-systems and matroid duality	45
II BUFFON TRANSFORMATION FOR POLYHEDRA	48
4 Buffon transformation	49
4.1 Buffon transformation for polygons.	49
4.2 Buffon transformation for polyhedra	53

5	Spectral graph theory and proof of theorem 4.6	60
5.1	Graphs and matrices	60
5.2	Colin de Verdière number and null space representation	63
5.3	Proof of Theorem 4.6	71
5.4	On the symmetry assumption	72
6	Representation theory and affine B-regular polyhedra	75
6.1	The symmetry groups of Platonic solids and their characters	75
6.2	Examples of Buffon realizations of polyhedra	77
7	Conclusion	106
A	Catalogue of all known real 3-dimensional \vee-systems	109
B	Mathematica implementation of linearised \vee-conditions	134
	Bibliography	137

Chapter 1

Introduction

The five Platonic solids were object of fascination and study since the ancient time. Hundreds of Neolithic stone models of them have been found in Scotland. They play a special role of basic elements in Plato's ideal world.

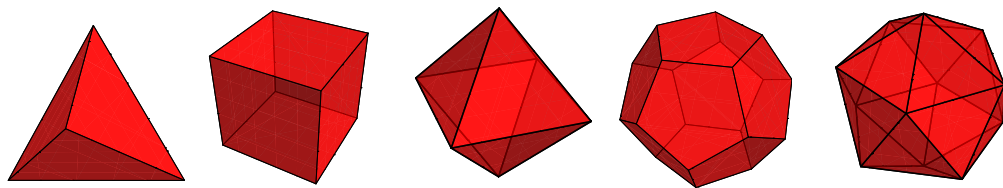


FIGURE 1.1: The 5 Platonic solids: tetrahedron, cube, octahedron, dodecahedron, icosahedron.

Kepler and Poincaré are usually credited for the discovery of all 4 regular star polyhedra. Schläfli (1814-1895) introduced the concept of regular polytopes in higher dimensions. Coxeter (1907-2003), who is commonly considered as greatest geometer of 20th century, continued this work and made major contributions far beyond the theory of polytopes.

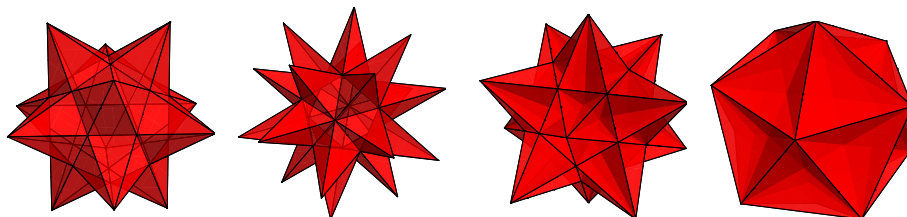


FIGURE 1.2: Kepler - Poincaré polyhedra: small stellated dodecahedron, great stellated dodecahedron, great icosahedron, great dodecahedron.

The symmetries of regular polytopes are particular cases of the *Coxeter groups*, which are finite groups generated by the hyperplane reflections. Such groups are all classified and can be described by the corresponding *Coxeter root systems*, which are the sets of the normals to the mirror hyperplanes. By definition such a system \mathcal{R} consists of non-zero vectors in Euclidean space such that for any $\alpha \in \mathcal{R}$ the reflection $s_\alpha : x \rightarrow x - \frac{2(\alpha, x)}{(\alpha, \alpha)}\alpha$ leaves \mathcal{R} invariant, i. e. $s_\alpha \mathcal{R} = \mathcal{R}$.

These systems play an important role in various areas of Mathematics. In particular, in the crystallographic case they coincide with the Weyl groups of simple complex Lie algebras [3].

The geometric meaning of the root systems for basic classical Lie superalgebras was clarified by V. Serganova [42], who introduced the notion of *generalised root systems* in the presence of the isotropic roots. The problem is that for an isotropic root one can not define the reflection. Serganova proposed the following replacement of the invariance condition in this case: if $\alpha \in \mathcal{R}$ is an isotropic root, then for any $\beta \in \mathcal{R}$ such that $(\beta, \alpha) \neq 0$ at least one of the vectors $\beta + \alpha$ or $\beta - \alpha$ belongs to \mathcal{R} . A generalised root system is called *irreducible* if it does not admit a representation as a direct orthogonal sum of two non-empty generalised root systems. A remarkable result obtained by Serganova states that the class of irreducible root systems with isotropic roots includes all root systems of the basic classical Lie superalgebras (with the exception of the superalgebra $B(0, n)$ which has no isotropic roots). Any generalised root system \mathcal{R} has a partial symmetry described by the finite group W_0 generated by the reflections with respect to the non-isotropic (real) roots of \mathcal{R} .

The list of the irreducible generalised root systems consists of the classical series $A(n, m)$, $B(n, m)$, $D(n, m)$, $C(n, m)$, $BC(n, m)$, and the exceptional cases $AB(1, 3)$ (also known as $F(4)$), $G(1, 2)$ (also known as $G(3)$) and $D(2, 1, \lambda)$ with the parameters $\lambda = (\lambda_1, \lambda_2, \lambda_3)$ satisfying the relation $\lambda_1 + \lambda_2 + \lambda_3 = 0$.

Based on the notion of the generalised root systems Sergeev and Veselov [43] introduced the notion of the *deformed root systems* and studied the related generalised quantum Calogero-Moser problems. The first family of the deformed Calogero-Moser systems corresponding to the deformation $A_n(m)$ of the root system A_n was described in an earlier work by O. Chalykh, M. Feigin and A. P. Veselov in 1996 [4].

A more general class of vector configurations appeared in relation with the Witten-Dijkgraaf-Verlinde-Verlinde (WDVV) equation. The WDVV equations play an important role in 2D topological field theory and $N = 2$ SUSY Yang-Mills theory [9, 31]. The generalised WDVV equations have the form

$$F_i F_k^{-1} F_j = F_j F_k^{-1} F_i \quad \text{with } i, j, k = 1, \dots, n$$

where F_m are $n \times n$ matrices constructed from the third partial derivatives of the unknown function $F = F(x^1, \dots, x^n)$:

$$(F_m)_{pq} = \frac{\partial^3 F}{\partial x^m \partial x^p \partial x^q}.$$

A geometric theory of the WDVV equation was developed by Dubrovin, who put it in the foundation of the theory of Frobenius manifolds [9, 10].

A new important notion of \vee -system was introduced by Veselov [49], who considered a special class of solutions of WDVV equation by taking the ansatz

$$F^{\mathcal{A}} = \sum_{\alpha \in \mathcal{A}} (\alpha, x)^2 \log(\alpha, x)^2,$$

where \mathcal{A} denotes a finite set of collinear vectors $\alpha \in \mathbb{R}^n$ corresponding to the (positive part) of a root system. The systems must satisfy certain relations, called the \vee -conditions, which turned out to hold not only for the root systems but also for their deformations [49]. The formal definition is as follows.

Let V be a real vector space and $\mathcal{A} \subset V^*$ be a finite set of vectors in the dual space V^* (covectors) spanning V^* . To such a set one can associate the following *canonical form* $G_{\mathcal{A}}$ on V :

$$G_{\mathcal{A}}(x, y) = \sum_{\alpha \in \mathcal{A}} \alpha(x)\alpha(y),$$

where $x, y \in V$, which establishes the isomorphism

$$\varphi_{\mathcal{A}} : V \rightarrow V^*.$$

Denote the inverse $\varphi_{\mathcal{A}}^{-1}(\alpha)$ as α^{\vee} . The system \mathcal{A} is called \vee -*system* if the following relations (\vee -*conditions*)

$$\sum_{\beta \in \Pi \cap \mathcal{A}} \beta(\alpha^\vee) \beta^\vee = \nu \alpha^\vee$$

are satisfied for any $\alpha \in \mathcal{A}$ and any two-dimensional plane $\Pi \subset V^*$ containing α and some ν , which may depend on Π and α .

Several families of \vee -systems are known including all 2-dimensional systems, Coxeter configurations and the deformed root systems, but their classification is an open problem. The main results in this direction had been found in [5, 14, 15, 13, 26]. In particular, Feigin and Veselov proved an important result that the class of \vee -systems is closed under the restriction operation [15]. The most comprehensive list of known \vee -systems together with their geometric properties can be found in [14, 15].

In the first part of this thesis we present some arguments in favour of the completeness of Feigin-Veselov list. In order to state precisely the classification problem we use the language of the theory of matroids [36]. A matroidal approach in this context was also used by Lechtenfeld et al [26].

For a fixed matroidal structure we derive the relations describing the infinitesimal deformations of \vee -systems and use them to prove the local completeness of Feigin-Veselov list of the 3-dimensional \vee -systems. We study the properties of the corresponding matroids and the values of ν -functions on 2-flats. The conjecture is that the matroid and ν -function on 2-flats determine the \vee -system uniquely. We present a catalogue of all known 3D \vee -systems with these data and graphical representation.

In the second part we study a special class of vector configurations, which form vertex sets for a new class of polyhedra called affine B -regular. The story of the considered problem goes back to Count Buffon, a French naturalist and the translator into French of Newton's Principia.

Start with an arbitrary polygon. Generate a second polygon by joining the centres of consecutive edges. Repeat this construction (see Fig.1.3).

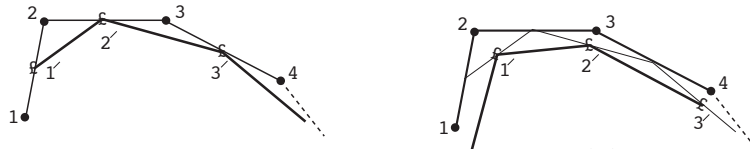


FIGURE 1.3: Buffon procedure for polygons.

It is easy to see that the process converges to a point - the centroid of the original vertices (and therefore the centroid of the vertices of any polygon in the sequence). Buffon observed a remarkable *regularisation effect* of this procedure: the limiting shape of the polygon is *affine regular*. Here a polygon is called affine regular if it is affine equivalent to a regular polygon.

In fact a similar phenomenon was already observed since Roman times. When creating mosaics Roman craftsmen achieved more regular pieces by breaking the corner, so effectively using the same procedure [1]. The explanation is based on simple arguments from linear algebra, see e.g. [2, 51] and Chapter 4.

Veselov and Ward [50] proposed a natural generalisation of the Buffon transformation for polyhedra. Let P be a simplicial polyhedron in \mathbb{R}^3 , having all faces triangular. Define its *Buffon transformation* $B(P)$ as the simplicial polyhedron with vertices $B(v)$, where for each vertex v of P the new vertex $B(v)$ is defined as the centroid of the centroids of all edges meeting at v . The question is what is the limiting shape of $B^n(P)$ as n goes to infinity.

Unfortunately, the answer in general is disappointing: the limiting shape will be one-dimensional. Indeed the same arguments from linear algebra show that this shape is determined by the subdominant eigenspace of the corresponding operator on the graph $\Gamma(P)$, which is the 1-skeleton of P (see the details below), and this eigenspace generically has dimension 1. This means that in order to have a sensible limiting shape we need to add some assumptions on the initial polyhedron P .

Let G be one of the symmetry groups $G = T, O, I$ of the Platonic solids: tetrahedron, octahedron/cube, icosahedron/dodecahedron respectively. Assume that the combinatorial structure of the initial polyhedron P is G -invariant, which means that G faithfully acts on the graph $\Gamma(P)$.

The main result of the second part of the thesis is the following theorem [40].

Theorem 1.1. *Let P be a simplicial polyhedron in \mathbb{R}^3 with G -invariant combinatorial structure. Then for a generic P the limiting shape obtained by repeatedly*

applying Buffon procedure to P is a star-shaped polyhedron P_B . The vertices of P_B are explicitly determined by the subdominant eigenspace of the Buffon operator, which in this case has dimension 3.

The explicit generation of P_B is given by the eigenspace realisation procedure applied to the subdominant eigenspace of the Buffon operator.

Recall that the polyhedron P is called *star-shaped* (not to be mixed with star polyhedra like Kepler-Poinsot) if there is a point inside it from which one can see the whole boundary of P , or equivalently, the central projection gives a homeomorphism of the boundary of P onto a sphere.

Let us call polyhedron P *affine B-regular* if $B(P)$ is affine equivalent to P . In dimension 2 this is equivalent to affine regularity. Thus the Buffon procedure produces affine B -regular version P_B from a generic polyhedron P with the above properties. As far as we know the notion of the affine regularity for polyhedra with non-regular combinatorial structures was not discussed in the literature before.

For a generic polyhedron P with combinatorial structure of a Platonic solid the explicit calculation of the subdominant eigenspace shows that the corresponding polyhedron P_B is affine regular, which means that it is affine equivalent to the corresponding Platonic solid. For the Archimedean solids, however, this is no longer true.

Note that there are plenty of polyhedra P with G -invariant combinatorial structures, which can be constructed from the Platonic solids using Conway operations [7]. In particular, one will have a simplicial polyhedron by applying to any such P the operation, which Conway called *kis* and denoted by k , consisting of building the pyramids on all the faces. Many examples of the corresponding combinatorial types can be found in chemistry and physics literature in relation with the famous Thomson problem, see e.g. [11].

The proof of the existence of star-shaped affine B -regular version of P is based on deep results from the spectral theory on graphs due to Colin de Verdière [6] and Lovász et al [47, 27, 29]. Both assumptions of the theorem, namely simpliciality and Platonic symmetry, are essential. For non-simplicial polyhedra the Buffon transformation usually breaks the faces.

The Platonic symmetry keeps the limiting shape 3-dimensional, preventing collapse to lower dimension. The dihedral symmetry is not enough: one can check

that a polyhedron with prismatic combinatorial structure will collapse to the corresponding affine regular polygon.

The star-shape property of the limiting shape is the strongest we can claim since a convex version may not exist as the following example of the triakis tetrahedron (with pyramids built on each face of the tetrahedron) shows (see Fig. 1.4).

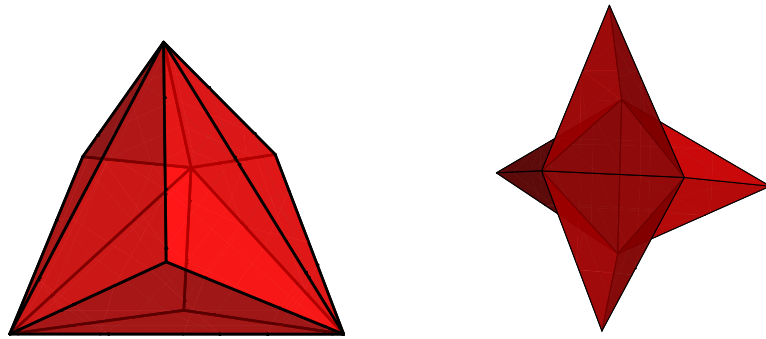


FIGURE 1.4: Triakis tetrahedron and its affine B -regular realisation (right).

The structure of the Thesis is the following.

We start with the general notions of the \vee -systems, their geometric properties and construction methods based mainly on results from [49, 48, 14]. In the second part of Chapter 2 we give a brief overview of the basic concepts from the theory of matroids [36], which provides a natural framework for the problem of classification of \vee -systems. This allows us to formalise the problem of classification by fixing first the corresponding matroidal type, and sets the tone for the rest of this part of the thesis.

In Chapter 3 we consider the problem of deformation and classification of \vee -systems. For small \vee -systems of the Coxeter matroidal type of A_3 , B_3 we show that they are completely classified by the formulae found in [5]. Figure 1.5 shows projective representations of these systems together with the \vee -system D_3 .

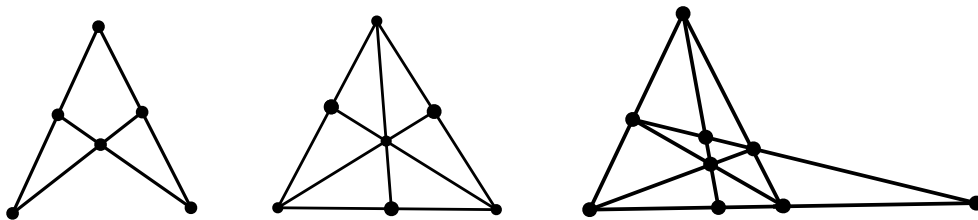


FIGURE 1.5: Projective configurations corresponding to the \vee -systems of the Coxeter type A_3 and B_3 and to the \vee -systems of type D_3 .

In order to analyse larger \vee -systems of a given matroidal type, we derive the \vee -conditions on the infinitesimal deformations. We then show that the isolated \vee -systems listed in [14] are indeed isolated.

This is followed by investigation of some characteristic properties of the functions ν defined by the \vee -conditions. We formulate the uniqueness conjecture, saying that the matroid and function ν on its flats uniquely determine the corresponding \vee -system.

The last section of the first part is an attempt to characterise the class of matroids giving rise to \vee -systems. We will refer to such matroids as \vee -realisable matroids. We list several properties of the \vee -systems based on the results of their deformations, some facts from projective geometry and observations derived from the graphical representations of the known \vee -systems.

Chapter 4 starts with a discussion of the solution of the Buffon puzzle for polygons. We explain the main ideas and relation to linear algebra. Then, in the second part of the chapter, we define the Buffon transformation for polyhedra and review the classical Steinitz theorem, which gives graph-theoretical characterisation of 1-skeletons of convex polyhedra.

In Chapter 5 we introduce the main tools from spectral graph theory: the Colin de Verdière invariant and null space realisation for polyhedral graphs studied by Lovász et al [47, 27, 29]. We then use these results and representation theory of finite groups to prove our main result.

In Chapter 6 we present the character tables for the polyhedral groups and the corresponding decomposition of the space of functions on the vertices of Platonic solids into irreducible components, and analyse their relation to the spectra of the Buffon operators for some combinatorial types. We also present the corresponding shapes of affine B -regular polyhedra.

In the Appendix A we give the catalogue of all known \vee -systems in dimension 3 together with the corresponding matroids and the values of ν -functions. In the Appendix B we describe the Mathematica implementation of the linearised \vee -conditions.

The main results of the Thesis are published in the arXiv [39],[40].

Part I

\vee -SYSTEMS IN DIMENSION 3

Chapter 2

V-systems and matroids

2.1 V-systems: definition and constructions

We study the special finite sets of covectors called V-systems introduced in [49, 48]. The motivation came from the study of certain special solutions of the generalized Witten-Dijkgraaf-Verlinde-Verlinde (WDVV) equations, playing an important role in 2D topological field theory and $N = 2$ SUSY Yang-Mills theory [9, 31].

Let V be a real vector space and $\mathcal{A} \subset V^*$ be a finite set of vectors in the dual space V^* (covectors) spanning V^* . To such a set one can naturally associate the following positive definite *canonical form* $G_{\mathcal{A}}$ on V :

$$G_{\mathcal{A}}(x, y) = \sum_{\alpha \in \mathcal{A}} \alpha(x)\alpha(y), \quad (2.1)$$

where $x, y \in V$, which establishes the isomorphism

$$\varphi_{\mathcal{A}} : V \rightarrow V^*.$$

The inverse $\varphi_{\mathcal{A}}^{-1}(\alpha)$ we denote as α^{\vee} . The system \mathcal{A} is called *V-system* if the following relations

$$\sum_{\beta \in \Pi \cap \mathcal{A}} \beta(\alpha^{\vee})\beta^{\vee} = \nu\alpha^{\vee} \quad (2.2)$$

(called *V-conditions*) are satisfied for any $\alpha \in \mathcal{A}$ and any two-dimensional plane $\Pi \subset V^*$ containing α and some ν , which may depend on Π and α . Depending on

the number of covectors contained in a given plane Π the above condition 3.6 has the following interpretation:

1. If the plane Π contains no more than one covector from \mathcal{A} , the \vee -condition is trivial.
2. If Π contains only two covectors from \mathcal{A} , say α and β , then we must have

$$G_{\mathcal{A}}(\alpha^{\vee}, \beta^{\vee}) = 0.$$

3. If Π contains more than 2 covectors then ν does not depend on α and the corresponding two forms $G_{\mathcal{A}}$ and

$$G_{\mathcal{A}}^{\Pi}(x, y) := \sum_{\alpha \in \Pi \cap \mathcal{A}} \alpha(x)\alpha(y)$$

are proportional on the plane $\Pi^{\vee} \subset V$ (see [49, 48]).

Alternatively, one can use the form G to introduce the Euclidean structure on V and to give definition of \vee -systems in more geometric terms as follows. We say that a finite subset \mathcal{A} of the Euclidean vector space V is *well-distributed*, if

$$G_{\mathcal{A}}(x, y) = \sum_{\alpha \in \mathcal{A}} \langle \alpha, x \rangle \langle \alpha, y \rangle,$$

is proportional to the Euclidean structure $\langle \cdot, \cdot \rangle$ on V . Then a finite subset \mathcal{A} of V is called a *Euclidean \vee -system* if \mathcal{A} is well-distributed, and any of its 2-dimensional subsystems is either reducible or well-distributed in the corresponding plane.

Finally, all \vee -conditions are equivalent to the flatness of the corresponding Knizhnik–Zamolodchikov-type connection (or Dubrovin’s connection)

$$\nabla_a = \partial_a + m \sum_{\alpha \in \mathcal{A}} \frac{\langle \alpha, a \rangle}{\langle \alpha, x \rangle} \alpha^{\vee} \otimes \alpha.$$

The examples of \vee -systems include all 2-dimensional systems, all Coxeter root systems as well as their deformed versions appeared in the theory of quantum Calogero–Moser systems [49, 48].

Some of the remarkable geometric properties of the \vee -system are [15]:

- A subsystem of a given V -system (see definition below) is also a V -system.
- The restriction of a V -system \mathcal{A} to a subspace defined by a subset $\mathcal{B} \subset \mathcal{A}$ is also a V -system.
- The definition of the V -systems can be extended to complex vector spaces.

We give a brief overview of these classes of V -systems as well as of their geometric properties and methods of construction. For more details we refer to [15], [14].

2.1.1 Subsystems and restrictions of V -systems

V -systems obtained from restrictions of Coxeter systems appeared in [13, 14].

Let \mathcal{A} be a given V -system in a real vector space \mathbf{V}^* and $\mathbf{W} \subset \mathbf{V}^*$ a vector subspace spanned by a subset $\mathcal{B} \subset \mathcal{A}$. \mathcal{B} is called a *subsystem* of \mathcal{A} if $\mathcal{B} = \mathcal{A} \cap \mathbf{W}$.

Consider the linear subspace $\mathbf{W}^\vee \subset \mathbf{V}$, which corresponds to \mathbf{W} under the identification through the form 2.1.

Theorem 2.1. [13] *The subsystem $\mathcal{B} \subset \mathcal{A}$ as a set of covectors on $\mathbf{W}^\vee \subset \mathbf{V}$ is a V -system.*

The subspace $\mathbf{L}_\mathcal{B}$ in V defined as

$$\mathbf{L}_\mathcal{B} = \{v \in \mathbf{V} \mid \beta(v) = 0, \forall \beta \in \mathcal{B}\}$$

gives rise to the following statement.

Theorem 2.2. [14] *The restriction of a V -system \mathcal{A} to the subspace $\mathbf{L}_\mathcal{B}$ is a V -system.*

As pointed out in [13], subsystems of the Coxeter systems do not give new V -systems. Restrictions of the Coxeter root systems A_n and B_n were discussed in [14]. Restrictions of the exceptional Coxeter systems lead to a number of interesting three-dimensional V -systems.

The list of all V -systems coming from restrictions of exceptional Coxeter root systems was given in [14]. It consists of 42 different vector configurations. 19

of these systems span a three-dimensional space. They are labeled by a pair (G, H) , denoting by G the original Coxeter group and by H its parabolic subgroup generated by the set of reflections $\{s_\beta : \beta \in \mathcal{B}\}$.

Here we consider the \vee -systems of F_4 -type. We follow the treatment provided in [14].

Consider the configuration

$$\mathbf{F}_4 = \begin{cases} e_i \pm e_j, & 1 \leq i < j \leq 4, \\ 2\Lambda e_i, & 1 \leq i \leq 4, \\ \Lambda(e_1 \pm e_2 \pm e_3 \pm e_4). \end{cases} \quad (2.3)$$

The parameter $\Lambda \in \mathbb{R}$ appears due to an additional orbit on the root system F_4 .

The set $\mathcal{B} = \{2\Lambda e_1\}$ is a one-dimensional subsystem of the \vee -system F_4 . The restriction of F_4 to the corresponding subspace

$$\mathbf{L}_{\mathcal{B}} = \{x \in \mathbb{R}^4 : 2\Lambda e_1(x) = 0\}$$

gives the \vee -system $\mathbf{F}_3(\Lambda)$ consisting of 13 covectors:

$$\mathbf{F}_3(\Lambda) = \begin{cases} e_i \pm e_j, & 1 \leq i < j \leq 3, \\ \sqrt{4\Lambda^2 + 2}e_i, & 1 \leq i \leq 3, \\ \Lambda\sqrt{2}(e_1 \pm e_2 \pm e_3). \end{cases} \quad (2.4)$$

Another possible choice for the one-dimensional subsystem is

$$\tilde{\mathcal{B}} = \{e_1 - e_2\}.$$

This leads to a \vee -system which is equivalent to 2.4 up to a linear transformation [14]. Fig.2.1 shows a graphical representation of the 3-dimensional \vee -system of type F_3 as projective configuration.

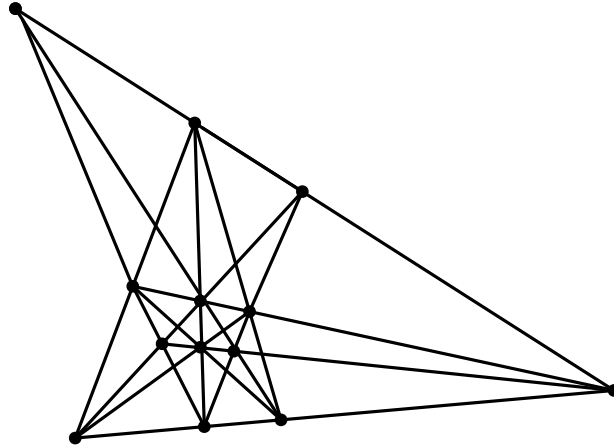


FIGURE 2.1: Graphical realisation of the \vee -system F_3 in the projective plane.

2.1.2 Generalised root systems and their deformations

V. Serganova introduced [42] *generalised root systems* in the presence of the isotropic roots. For isotropic roots reflections are not defined. Serganova proposed the following notion.

Let V be a vector space with a non-degenerate bilinear form \langle, \rangle .

The finite vector set \mathcal{R} in $V \setminus \{0\}$ is called a *generalised root system* if the following conditions are satisfied:

1. \mathcal{R} spans V and $\mathcal{R} = -\mathcal{R}$;
2. if $\alpha, \beta \in \mathcal{R}$ and $\langle \alpha, \alpha \rangle \neq 0$ then $\frac{2\langle \alpha, \beta \rangle}{\langle \alpha, \alpha \rangle} \in \mathbf{Z}$ and $s_\alpha(\beta) = \beta - \frac{2\langle \alpha, \beta \rangle}{\langle \alpha, \alpha \rangle} \alpha \in \mathcal{R}$;
3. if $\alpha \in \mathcal{R}$ and $\langle \alpha, \alpha \rangle = 0$ then for any $\beta \in \mathcal{R}$ such that $\langle \alpha, \beta \rangle \neq 0$ at least one of the vectors $\beta + \alpha$ or $\beta - \alpha$ belongs to \mathcal{R} .

A generalised root system \mathcal{R} is called irreducible if it can not be presented as a direct sum of two non-empty generalised root systems. The set of reflections corresponding to the non-isotropic roots generates a finite group W_0 that describes the partial symmetry of \mathcal{R} .

Serganova classified all irreducible generalised root systems. The list consists of classical series $A(n, m)$ and $BC(n, m)$ and three exceptional cases $G(1, 2)$, $AB(1, 3)$

and $D(2, 1, \lambda)$, which essentially coincides with the list of basic classical Lie super-algebras.

Sergeev and Veselov [43] introduced a class of *admissible deformations* of generalised root systems, when the bilinear form \langle, \rangle is deformed and the roots $\alpha \in R$ acquire some multiplicities m_α . They satisfy the following 3 conditions:

- 1) the deformed form B and the multiplicities are W_0 -invariant;
- 2) all isotropic roots have multiplicity 1;
- 3) the function $\psi_0 = \prod_{\alpha \in R_+} \sin^{-m_\alpha}(\alpha, x)$ is a (formal) eigenfunction of the Schrödinger operator

$$L = -\Delta + \sum_{\alpha \in R_+} \frac{m_\alpha(m_\alpha + 2m_{2\alpha} + 1)(\alpha, \alpha)}{\sin^2(\alpha, x)}, \quad (2.5)$$

where the brackets $(,)$ and the Laplacian Δ correspond to the deformed bilinear form B , which is assumed to be non-degenerate.

All admissible deformations of the generalised root systems were described explicitly in [43].

The connection between the class of *admissible deformations* of generalised root systems and the theory of \vee -systems becomes clear from the following theorem.

Theorem 2.3. [15] *For any admissible deformation (\mathcal{R}, B, m) of a generalised root system \mathcal{R} the set $\mathcal{A} = \{\sqrt{m_\alpha}\alpha, \alpha \in \mathcal{R}\}$ is a \vee -system whenever the canonical form*

$$G_{\mathcal{A}}(u, v) = \sum_{\alpha \in \mathcal{R}} m_\alpha \alpha(u) \alpha(v)$$

is non-degenerate.

The exceptional generalised root systems give rise to the following 3-dimensional \vee -systems [15]:

- The admissible deformation of the exceptional generalised root system $AB(1, 3)$ leads to the family of \vee -systems $AB_4(t)$, which has exactly two different three-dimensional restrictions:

$$(AB_4(t), A_1)_1 = \begin{cases} \sqrt{2(2t^2 + 1)}e_1, \sqrt{2(2t^2 + 1)}e_2, t\sqrt{\frac{2(2t^2-1)}{t^2+1}}e_3, \\ \sqrt{2}(e_1 \pm e_2), t\sqrt{2}(e_1 \pm e_3), t(e_1 \pm 2e_2 \pm e_3) \end{cases}$$

and

$$(AB_4(t), A_1)_2 = \begin{cases} (e_i + e_j), & 1 \leq i < j \leq 3 \\ \sqrt{2}e_i, & 1 \leq i \leq 3 \\ \frac{1}{\sqrt{4t^2+1}}(e_i - e_j), & 1 \leq i < j \leq 3 \\ \frac{t\sqrt{2}}{\sqrt{t^2+1}}(e_1 + e_2 + e_3) \end{cases}.$$

- The admissible deformed exceptional generalised root system $G(1, 2)$ gives for $t \notin \{0, -\frac{1}{2}\}$ the following \vee -system:

$$G_3(t) = \begin{cases} \sqrt{2t+1}e_1, \sqrt{2t+1}e_2, \sqrt{\frac{3}{t}}e_3, \\ \sqrt{2t+1}(e_1 + e_2), \sqrt{\frac{2t-1}{3}}(e_1 - e_2), \sqrt{\frac{2t-1}{3}}(2e_1 + e_2), \sqrt{\frac{2t-1}{3}}(e_1 + 2e_2), \\ e_1 \pm e_3, e_2 \pm e_3, e_1 \pm e_3, e_1 + e_2 \pm e_3. \end{cases}$$

The cases $t = 1, \frac{3}{4}, \frac{1}{2}$ correspond to the restrictions $(E_7, A_2^2), (E_8, A_5)$ and (E_6, A_1^3) , respectively. All the other \vee -systems of this family can not be obtained through deformation and restriction of the Coxeter root systems [14].

- The family of the exceptional generalised root systems $D(2, 1, \lambda)$ gives rise to the two-parameter family $D_3(t, s)$ of \vee -systems consisting of the following covectors:

$$e_1 \pm e_2 \pm e_3, \sqrt{\frac{2(s-t+1)}{t}}e_2, \sqrt{\frac{2(s-t+1)}{t}}e_3, \sqrt{2(-1+t+s)}e_1.$$

The one-parameter sub-families $D_3(t, t-1), D_3(t, -t+1), D_3(t, t+1)$ are equivalent to the family $A_3(s, s, 1, 1)$ of the restricted Coxeter root system of type A_3 .

All known examples of 3D \vee -systems are summarised in Fig. A.1 below.

2.2 Vector configurations and matroids

The combinatorial structure of the vector configurations can be described using the notion of *matroids*. The theory of matroids was introduced by Whitney in 1935, who was looking for an abstract notion generalising the linear dependence in the vector space.

We review some standard notions from this theory following mainly Oxley [36].

A *matroid* M is a pair (X, \mathcal{I}) , where X is a finite set and \mathcal{I} is a collection of subsets S of X (called the *independent sets* of M) such that:

- \mathcal{I} is non-empty
- For any $S \in \mathcal{I}$, any $S' \subset S$ one has $S' \in \mathcal{I}$.
- If $A, B \in \mathcal{I}$, $|A| = |B| + 1$ then $\exists x \in A \setminus B$ such that $B \cup \{x\} \in \mathcal{I}$.

The last property is sometimes also referred to as the *Steinitz exchange axiom* [37].

The rank of the subset $S \subset X$ is defined as $r(S) = \max_{I \in \mathcal{I}} \{|I| : I \subseteq S\}$. A *direct sum* of matroids $M_1 = (X_1, \mathcal{I}_1)$ and $M_2 = (X_2, \mathcal{I}_2)$ is defined as

$$M_1 \oplus M_2 = (X_1 \cup X_2, \{I_1 \cup I_2 : I_1 \in \mathcal{I}_1, I_2 \in \mathcal{I}_2\}).$$

A matroid is called *connected* if it can not be represented as a direct sum.

Matroids can be obtained using several (equivalent) models. The name "matroid" suggests that this structure is related to a matrix. Indeed, every matrix gives rise to a matroid. Let A be a real $r \times n$ matrix. Let $X = \{1, 2, \dots, n\}$ be the set of column labels of A , and let \mathcal{I} be the collection of subsets S of X for which the multiset of columns labelled by S is linearly independent over \mathbb{R} . Then (X, \mathcal{I}) is a matroid. A matroid obtained from the matrix A is called a *vector matroid* and is denoted by $M[A]$.

The following operations on matrix A do not affect the corresponding vector matroid $M[A]$:

1. Elementary operations with the rows

- (a) Interchange two rows
- (b) Multiply a row by a non-zero scalar
- (c) Replace a row by the sum of that row and another
- (d) Delete a zero row (unless it is the only row)
- (e) Interchange two columns

2. Multiplication of a column by a non-zero number.

Two matrices A and A' representing the same matroid M are said to be *projectively equivalent representations* of M if A' can be obtained from A by a sequence of these operations. Equivalently, one can say that $A' = CAD$, where C is an invertible $r \times r$ matrix, and D is a diagonal $n \times n$ matrix with non-zero diagonal entries.

Alternatively, one can define the *linear dependence matroid* on the set X as a family \mathcal{I}_C of minimal dependent subsets C of X (called *circuits*) through the following axioms:

- The empty set is not a circuit.
- No circuit is contained in another circuit.
- If $C_1, C_2 \in \mathcal{I}_C$ are two circuits sharing an element $e \in X$, then $(C_1 \cup C_2) \setminus e$ is a circuit or contains a circuit.

The rank of a circuit is defined as the dimension of the vector space spanned by its vectors. Circuits spanning the same d -dimensional subspace can be united in so-called d -flats. A set $F \subseteq X$ is a *flat* of the matroid M if

$$r(F \cup \{x\}) = r(F) + 1$$

for all $x \in X \setminus F$. The matroid can be labelled by listing all d -flats.

As an example consider the positive roots of the B_3 -type system. The corresponding matrix (with the first row giving the labelling) is

$$A = \begin{bmatrix} 1 & 2 & 3 & 4 & 5 & 6 & 7 & 8 & 9 \\ 1 & 1 & 0 & 0 & 1 & 1 & 1 & 0 & 0 \\ 1 & -1 & 1 & 1 & 0 & 0 & 0 & 1 & 0 \\ 0 & 0 & -1 & 1 & 1 & -1 & 0 & 0 & 1 \end{bmatrix}.$$

Here matroid M is defined on the set $X = \{1, 2, 3, 4, 5, 6, 7, 8, 9\}$, with

$$\mathcal{L}_3 = \{(4, 1, 6), (6, 2, 3), (4, 5, 2), (1, 5, 3)\},$$

$$\mathcal{L}_4 = \{(3, 4, 8, 9), (1, 2, 7, 8), (5, 6, 7, 9)\}$$

corresponding to 2-flats with 3 and 4 elements respectively. Together with the 3-flat $\mathcal{L}_9 = X$ this gives the complete list of flats.

Graphically on the projective plane we have

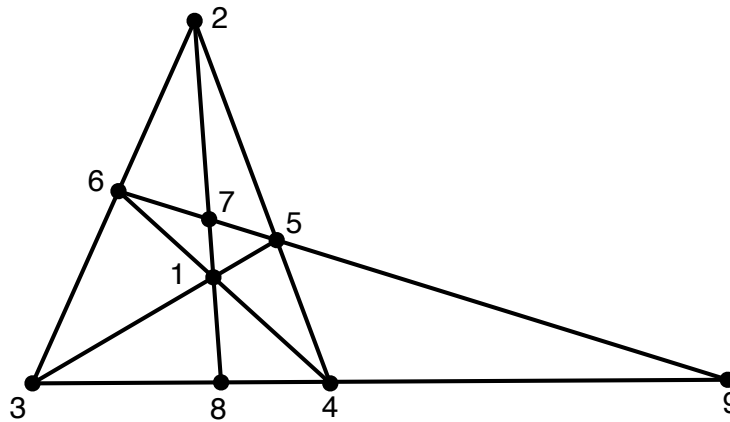


FIGURE 2.2: Graphical representation of B_3 -matroid: lines correspond to rank-2 flats

A matroid is called *simple* if it does not contain one- or two-element circuits. For vector matroids this means that no two vectors are proportional.

Number of matroids up to isomorphism grows very rapidly with $n = |X|$. The following table summarises the results for rank 3-matroids for small n [32].

n	3	4	5	6	7	8	9	10	11	12
all matroids	1	4	13	38	108	325	1275	10037	298491	31899134
simple matroids	1	2	4	9	23	68	383	5249	232928	28872972

The class of matroids we are interested in is the class of connected simple vector matroids of rank 3.

Vector matroids build the class of *realisable matroids*. The problem of finding a criterion for realisability is known to be *NP*-hard [37].

Let M be a vector matroid. We say that matroid M is *projectively rigid* if the space of all its vector realisations

$$\mathcal{R}(M) = \{A : M = M[A]\} / \sim$$

modulo projective equivalence is discrete and *strongly projectively rigid* if it consists of only one point (which means that up to projective equivalence M has a unique vector realisation).

Let G be a finite Coxeter group, which is a finite group generated by hyperplane reflections in a Euclidean space. We say that matroid M is of *Coxeter type* if it describes the vector configuration of the normals to the corresponding reflection hyperplanes for such a group (chosen one for each hyperplane).

Theorem 2.4. *The rank-3 matroids of Coxeter root systems of types A_3 , B_3 are strongly projectively rigid. The rank-3 matroid of type H_3 is projectively rigid with precisely two projectively non-equivalent vector realisations.*

Proof. Let us prove this first for B_3 case. Since the images a_1, a_2, a_3, a_4 of the elements 1,2,3 and 4 in the projective plane form a projective basis it is enough to prove that the remaining a_5, a_6, a_7, a_8, a_9 can be constructed uniquely. From the matroid structure we can see that a_5 must be an intersection point of the lines (2-flats) (a_1a_3) and (a_2a_4) . We denote this as

$$a_5 = (a_1a_3) \wedge (a_2a_4)$$

using the general lattice theory notation. Similarly we have

$$a_6 = (a_2a_3) \wedge (a_1a_4), \quad a_7 = (a_1a_2) \wedge (a_5a_6),$$

$$a_8 = (a_1a_2) \wedge (a_3a_4), \quad a_9 = (a_3a_4) \wedge (a_5a_6).$$

Similarly one can prove the rigidity in A_3 case. In both these cases the space of realisations modulo projective equivalence consists of only one point.

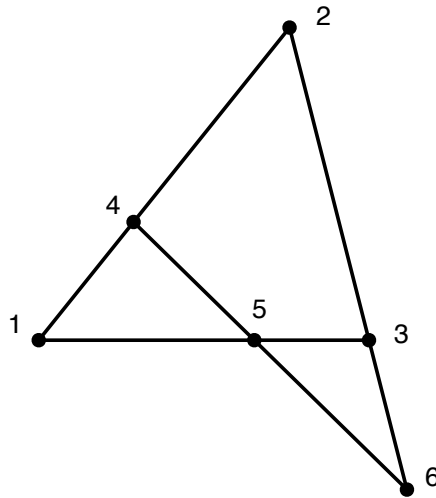


FIGURE 2.3: Graphical representation of A_3 -matroid

The H_3 case is more interesting. Fig. 2.4 shows the graphic representation of the system H_3 in the real projective plane $\mathbb{R}P^2$.

Recall that on the projective line $\mathbb{R}P^1$ any three points can be mapped into any other three via the action of the group $PGL(2, \mathbb{R})$. For four distinct points p_1, p_2, p_3, p_4 on the projective line $\mathbb{R}P^1$ with homogeneous coordinates $[x_i, y_i]$ there is a projective invariant, namely *cross-ratio* defined as

$$(p_1, p_2; p_3, p_4) = \frac{(x_1 y_3 - x_3 y_1)(x_1 y_4 - x_4 y_1)}{(x_2 y_4 - x_4 y_2)(x_2 y_3 - x_3 y_2)}.$$

If none of the y_i is zero the cross-ratio can be expressed in terms of the ratios $z_i = \frac{x_i}{y_i}$ as follows:

$$(z_1, z_2; z_3, z_4) = \frac{(z_1 - z_3)(z_1 - z_4)}{(z_2 - z_4)(z_2 - z_3)}.$$

Since any projection from a point in the projective plane preserves the cross-ratio of four points we have the equalities

$$(a_6, a_5; a_9, a_3) = (a_4, a_7; a_{10}, a_3) = (a_5, a_6; a_8, a_3),$$

$$(a_6, a_5; a_9, a_3) = (a_7, a_{11}; a_{10}, a_3) = (a_5, a_8; a_9, a_3).$$

One can check that they imply that $x = (a_6, a_5; a_9, a_3)$ satisfies the equation

$$x^2 - x - 1 = 0$$

with two solutions $x_1 = \frac{1+\sqrt{5}}{2}$ and $x_2 = \frac{1-\sqrt{5}}{2}$.

If we fix the positions of the four points a_4, a_5, a_6, a_7 forming a projective basis in $\mathbb{R}P^2$ the knowledge of $x = (a_6, a_5; a_9, a_3)$ allows us to reconstruct a_9 .

After this all the remaining points a_i can be reconstructed as

$$\begin{aligned} a_1 &= (a_5 a_4) \wedge (a_6 a_7), & a_3 &= (a_5 a_6) \wedge (a_7 a_4), \\ a_2 &= (a_5 a_7) \wedge (a_6 a_4), & a_{14} &= (a_2 a_9) \wedge (a_5 a_4), \\ a_{12} &= (a_7 a_6) \wedge (a_2 a_9), & a_{10} &= (a_2 a_9) \wedge (a_3 a_4), \\ a_{13} &= (a_9 a_4) \wedge (a_6 a_7), & a_8 &= (a_2 a_{13}) \wedge (a_3 a_6), \\ a_{15} &= (a_2 a_{13}) \wedge (a_5 a_4), & a_{11} &= (a_2 a_8) \wedge (a_3 a_4). \end{aligned}$$

Thus we have shown that modulo projective group we have only two different vector realisations of matroid H_3 . □

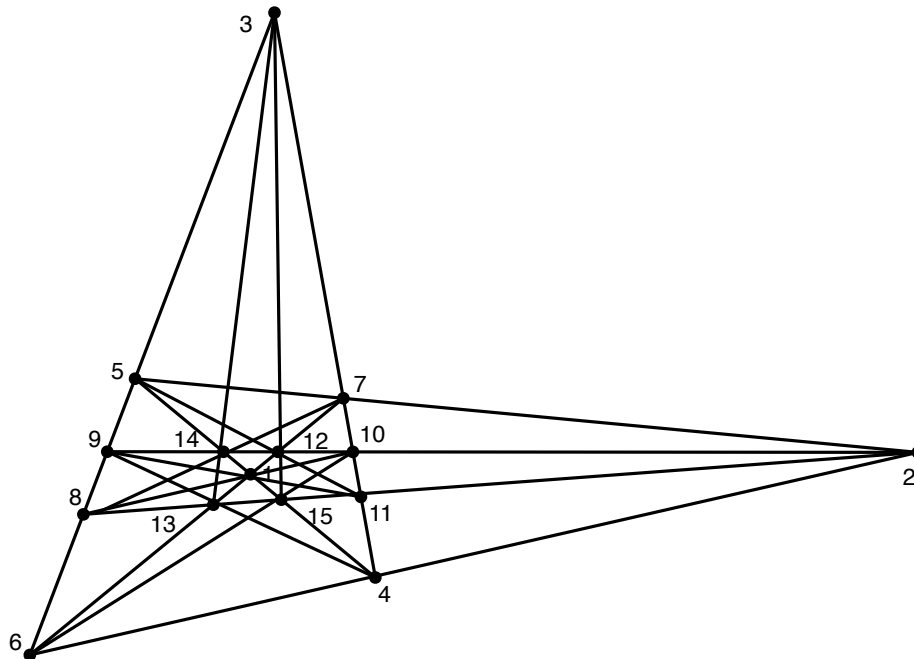


FIGURE 2.4: Graphical representation of H_3 -matroid

Remark. The existence of two projectively non-equivalent realisations is related to the existence of a symmetry of matroid $M(H_3)$, which can not be realised geometrically, see [12]. These two realisations are related by re-ordering of the vectors and thus give rise to equivalent \vee -systems.

Chapter 3

Deformations and classification

3.1 Classification of \vee -systems of A_3 and B_3 types

For any \vee -system $\mathcal{A} \subset V^*$ one can consider the corresponding matroid $M(\mathcal{A})$, which encodes a combinatorial structure of \mathcal{A} . Conversely, having a matroid M one can look for \vee -system realisations \mathcal{A} of M with given combinatorial structure $M(\mathcal{A}) = M$.

Let $\mathcal{R}^\vee(M)$ be the set of all such realisations modulo group $G = GL(V^*)$ of linear automorphisms of V^* .

If vector matroid $M = M(A)$ is strongly projectively rigid then all its vector realisations modulo G have the form $A' = AD$, or in terms of the columns a_i , $i = 1, \dots, n$ of A ,

$$a'_i = x_i a_i, \quad i = 1, \dots, n$$

with arbitrary non-zero parameters x_i . The \vee -conditions form an overdetermined system of nonlinear algebraic relations on the parameters $x_i \in \mathbb{R} \setminus 0$ and define $\mathcal{R}^\vee(M)$ as an open set of a real algebraic variety.

For a generic vector matroid this set is actually empty. For example, for n vectors a_i in \mathbb{R}^3 in general position the \vee -conditions imply that these vectors must be pairwise orthogonal, which is impossible if $n > 3$.

In the case when the space $\mathcal{R}^\vee(M)$ is known to be non-empty (for example, for all vector matroids M of Coxeter type) we have the question of how to describe this space effectively.

For the case of matroid of Coxeter type A_3 the answer is known [5]. The positive roots of A_3 system are $e_i - e_j$, $1 \leq i < j \leq 4$, where e_i , $i = 1, \dots, 4$ is an orthonormal basis in \mathbb{R}^4 .

Theorem 3.1. [5] *The system*

$$\mathcal{A} = \{\mu_{ij}(e_i - e_j), 1 \leq i < j \leq 4\} \quad (3.1)$$

satisfies the \vee -conditions if and only if the parameters satisfy the relations

$$\mu_{12}\mu_{34} = \mu_{13}\mu_{24} = \mu_{14}\mu_{23}.$$

All the corresponding \vee -systems can be parametrized as

$$A_3(c) = \{\sqrt{c_i c_j}(e_i - e_j), 1 \leq i < j \leq 4\},$$

with arbitrary positive real c_1, \dots, c_4 .

Without loss of generality, we may choose $c_4 = 1$ and consider the restriction of the system onto the hyperplane $x_4 = 0$. This gives the following parametrisation of the space $\mathcal{R}^\vee(M(A_3))$ by positive real c_1, c_2, c_3 as

$$A_3(c) = \begin{cases} \sqrt{c_i c_j}(e_i - e_j), & 1 \leq i < j \leq 3 \\ \sqrt{c_i}e_i, & i = 1, 2, 3. \end{cases}$$

Consider now the case B_3 , corresponding to the following configuration of vectors in \mathbb{R}^3

$$B_3 = \begin{cases} e_i \pm e_j, & 1 \leq i < j \leq 3, \\ e_i & i = 1, \dots, 3. \end{cases}$$

The following the 4-parametric family of \vee -systems of B_3 -type was found in [5]:

$$\mathcal{B}(\gamma, c) = \begin{cases} \sqrt{c_i c_j}(e_i \pm e_j), & 1 \leq j < i \leq 3 \\ \sqrt{2c_i(c_i + \gamma)}e_i, & 1 \leq i \leq 3 \end{cases} \quad (3.2)$$

with arbitrary positive c_1, c_2, c_3 and γ such that $c_i + \gamma > 0$ for all $i = 1, 2, 3$.

Theorem 3.2. *Formula (3.2) gives all \vee -systems realisations of matroid type B_3 .*

Proof. Since B_3 matroid is strongly projectively rigid, we can assume that the corresponding \vee -system realisation has the form

$$\mathcal{B}(\alpha, \tilde{\alpha}, \beta) = \begin{cases} \alpha_{ij}(e_i + e_j), & 1 \leq i < j \leq 3 \\ \tilde{\alpha}_{ij}(e_i - e_j), & 1 \leq j < i \leq 3 \\ \beta_i e_i, & 1 \leq i \leq 3. \end{cases}$$

where all the parameters can be assumed without loss of generality to be positive.

To write down all \vee -conditions consider all two-dimensional planes containing at least two vectors $v_1, v_2 \in \mathcal{B}(\alpha, \tilde{\alpha}, \beta)$.

There are 3 different types of such planes Π :

1. $\langle e_1, e_2 \pm e_3 \rangle, \langle e_2, e_1 \pm e_3 \rangle, \langle e_3, e_1 \pm e_2 \rangle,$
2. $\langle e_1, e_2, e_1 \pm e_2 \rangle, \langle e_1, e_3, e_1 \pm e_3 \rangle, \langle e_2, e_3, e_2 \pm e_3 \rangle,$
3. $\langle e_1 - e_2, e_2 - e_3, e_1 - e_3 \rangle, \langle e_1 - e_2, e_2 + e_3, e_1 + e_3 \rangle,$
 $\langle e_2 - e_3, e_1 + e_3, e_1 + e_2 \rangle, \langle e_1 - e_3, e_2 + e_3, e_1 + e_2 \rangle.$

The corresponding form G has the matrix

$$G = \begin{pmatrix} \alpha_{13}^2 + \alpha_{12}^2 + \tilde{\alpha}_{13}^2 + \tilde{\alpha}_{12}^2 + \beta_1^2 & \alpha_{12}^2 - \tilde{\alpha}_{12}^2 & \alpha_{13}^2 - \tilde{\alpha}_{13}^2 \\ \alpha_{12}^2 - \tilde{\alpha}_{12}^2 & \alpha_{23}^2 + \alpha_{12}^2 + \tilde{\alpha}_{23}^2 + \tilde{\alpha}_{12}^2 + \beta_2^2 & \alpha_{23}^2 - \tilde{\alpha}_{23}^2 \\ \alpha_{13}^2 - \tilde{\alpha}_{13}^2 & \alpha_{23}^2 - \tilde{\alpha}_{23}^2 & \alpha_{23}^2 + \alpha_{13}^2 + \tilde{\alpha}_{23}^2 + \tilde{\alpha}_{13}^2 + \beta_3^2 \end{pmatrix}$$

In case (1) the \vee -conditions are just the orthogonality conditions

$$G(\alpha^\vee, \beta^\vee) = 0$$

for the corresponding two covectors α and β in the plane Π . We obtain the system

$$\begin{cases} 2(\tilde{\alpha}_{23}^2 \tilde{\alpha}_{13}^2 + \tilde{\alpha}_{23}^2 \tilde{\alpha}_{12}^2 + \tilde{\alpha}_{13}^2 \tilde{\alpha}_{12}^2 - \alpha_{13}^2 \alpha_{12}^2 - \alpha_{13}^2 \tilde{\alpha}_{23}^2 - \alpha_{12}^2 \tilde{\alpha}_{23}^2) - \alpha_{13}^2 \beta_2^2 + \tilde{\alpha}_{13}^2 \beta_2^2 - \alpha_{12}^2 \beta_3^2 + \tilde{\alpha}_{12}^2 \beta_3^2 = 0 \\ 2(\tilde{\alpha}_{23}^2 \tilde{\alpha}_{13}^2 + \tilde{\alpha}_{23}^2 \tilde{\alpha}_{12}^2 + \tilde{\alpha}_{13}^2 \tilde{\alpha}_{12}^2 - \alpha_{23}^2 \alpha_{12}^2 - \alpha_{23}^2 \tilde{\alpha}_{13}^2 - \alpha_{12}^2 \tilde{\alpha}_{13}^2) - \alpha_{23}^2 \beta_1^2 + \tilde{\alpha}_{23}^2 \beta_1^2 - \alpha_{12}^2 \beta_3^2 + \tilde{\alpha}_{12}^2 \beta_3^2 = 0 \\ 2(\tilde{\alpha}_{23}^2 \tilde{\alpha}_{13}^2 - \alpha_{23}^2 \alpha_{13}^2 - \alpha_{23}^2 \tilde{\alpha}_{12}^2 - \alpha_{13}^2 \tilde{\alpha}_{12}^2 + \tilde{\alpha}_{23}^2 \tilde{\alpha}_{12}^2 + \tilde{\alpha}_{13}^2 \tilde{\alpha}_{12}^2) - \alpha_{23}^2 \beta_1^2 + \tilde{\alpha}_{23}^2 \beta_1^2 - \alpha_{13}^2 \beta_2^2 + \tilde{\alpha}_{13}^2 \beta_2^2 = 0 \\ 2(\alpha_{23}^2 \alpha_{12}^2 + \alpha_{23}^2 \tilde{\alpha}_{13}^2 + \alpha_{12}^2 \tilde{\alpha}_{13}^2 - \alpha_{23}^2 \alpha_{13}^2 - \alpha_{23}^2 \tilde{\alpha}_{12}^2 - \alpha_{13}^2 \tilde{\alpha}_{12}^2) - \alpha_{13}^2 \beta_2^2 + \tilde{\alpha}_{13}^2 \beta_2^2 + \alpha_{12}^2 \beta_3^2 - \tilde{\alpha}_{12}^2 \beta_3^2 = 0 \\ 2(\alpha_{13}^2 \alpha_{12}^2 + \alpha_{13}^2 \tilde{\alpha}_{23}^2 + \alpha_{12}^2 \tilde{\alpha}_{23}^2 - \alpha_{23}^2 \tilde{\alpha}_{12}^2 - \alpha_{13}^2 \tilde{\alpha}_{12}^2 - \alpha_{23}^2 \alpha_{13}^2) - \alpha_{23}^2 \beta_1^2 + \tilde{\alpha}_{23}^2 \beta_1^2 + \alpha_{12}^2 \beta_3^2 - \tilde{\alpha}_{12}^2 \beta_3^2 = 0 \\ 2(\alpha_{13}^2 \alpha_{12}^2 + \alpha_{13}^2 \tilde{\alpha}_{23}^2 + \alpha_{12}^2 \tilde{\alpha}_{23}^2 - \alpha_{23}^2 \tilde{\alpha}_{13}^2 - \alpha_{12}^2 \tilde{\alpha}_{13}^2 - \alpha_{23}^2 \alpha_{12}^2) - \alpha_{23}^2 \beta_1^2 + \tilde{\alpha}_{23}^2 \beta_1^2 + \alpha_{13}^2 \beta_2^2 - \tilde{\alpha}_{13}^2 \beta_2^2 = 0, \end{cases}$$

which can be reduced to

$$\begin{cases} (-\alpha_{12}^2 + \tilde{\alpha}_{12}^2)(\alpha_{23}^2 + \alpha_{13}^2 + \tilde{\alpha}_{23}^2 + \tilde{\alpha}_{13}^2 + \beta_3^2 - \frac{(\alpha_{13}^2 - \tilde{\alpha}_{13}^2)^2}{(\alpha_{13}^2 + \alpha_{12}^2 + \tilde{\alpha}_{13}^2 + \tilde{\alpha}_{12}^2 + \beta_1^2)}) = 0 \\ (-\alpha_{13}^2 + \tilde{\alpha}_{13}^2)(\alpha_{23}^2 + \alpha_{12}^2 + \tilde{\alpha}_{23}^2 + \tilde{\alpha}_{12}^2 + \beta_2^2 - \frac{(\alpha_{12}^2 - \tilde{\alpha}_{12}^2)^2}{(\alpha_{13}^2 + \alpha_{12}^2 + \tilde{\alpha}_{13}^2 + \tilde{\alpha}_{12}^2 + \beta_1^2)}) = 0 \\ (-\alpha_{23}^2 + \tilde{\alpha}_{23}^2)(\alpha_{12}^2 + \alpha_{13}^2 + \tilde{\alpha}_{12}^2 + \tilde{\alpha}_{13}^2 + \beta_1^2 - \frac{(\alpha_{13}^2 - \tilde{\alpha}_{13}^2)^2}{(\alpha_{13}^2 + \alpha_{23}^2 + \tilde{\alpha}_{13}^2 + \tilde{\alpha}_{23}^2 + \beta_3^2)}) = 0. \end{cases}$$

Note that the second factors in all equations are ratios of principal minors of matrix G and thus must be positive, since the form G is positive definite. This implies that $\alpha_{ij} = \tilde{\alpha}_{ij}$, which reduces the matrix G to

$$G = \begin{pmatrix} 2(\alpha_{13}^2 + \alpha_{12}^2) + \beta_1^2 & 0 & 0 \\ 0 & 2(\alpha_{23}^2 + \alpha_{12}^2) + \beta_2^2 & 0 \\ 0 & 0 & 2(\alpha_{23}^2 + \alpha_{13}^2) + \beta_3^2 \end{pmatrix}.$$

In cases (2) and (3) we fix for each plane Π a basis $v_1, v_2 \in \mathcal{A} \cap \Pi$. The corresponding dual plane Π^\vee is spanned by v_1^\vee and v_2^\vee and the \vee -condition implies the proportionality of the restrictions of the forms G and G_Π onto Π^\vee . In our case this proportionality turns out to be equivalent to the following system of equations:

$$\begin{cases} \frac{2\alpha_{12}^2}{2(\alpha_{23}^2 + \alpha_{12}^2) + \beta_2^2} - \frac{2\alpha_{13}^2}{2(\alpha_{23}^2 + \alpha_{13}^2) + \beta_3^2} = 0 \\ \frac{2\alpha_{12}^2}{2(\alpha_{13}^2 + \alpha_{12}^2) + \beta_1^2} - \frac{2\alpha_{23}^2}{2(\alpha_{23}^2 + \alpha_{13}^2) + \beta_3^2} = 0 \\ \frac{2\alpha_{13}^2}{2(\alpha_{13}^2 + \alpha_{12}^2) + \beta_1^2} - \frac{2\alpha_{23}^2}{2(\alpha_{23}^2 + \alpha_{12}^2) + \beta_2^2} = 0 \end{cases}$$

Introducing new parameters $c_i, i = 1, 2, 3$ and γ by

$$c_i := \frac{\alpha_{ij}\alpha_{ik}}{\alpha_{jk}}, \quad \gamma := \frac{\beta_3^2 - 2c_3^2}{2c_3}.$$

we can see that these relations imply

$$\alpha_{ij}^2 = c_i c_j, \quad \beta_i^2 = 2c_i(c_i + \gamma),$$

which leads to the parametrisation (3.2). \square

For larger matroids (like Coxeter one of type H_3 with 15 elements) the direct analysis of the \vee -conditions is very difficult, so we consider a simpler problem about infinitesimal deformations of \vee -systems.

3.2 Deformations of \vee -systems

Let $\mathcal{A} = \{\alpha\} \subset V^*$ be a \vee -system realisation of matroid M . Consider its smooth *scaling deformation* $\mathcal{A}(t)$ of the form

$$\mathcal{A}(t) = \{\alpha_t\}, \quad \alpha_t = \mu_\alpha(t)\alpha, \quad \mu_\alpha(0) = 1. \quad (3.3)$$

For projectively rigid matroids M one can always reduce any deformation to such a form.

Let $\xi_\alpha = \dot{x}_\alpha(0)$. We are going to derive the conditions on ξ_α , which can be considered as *linearised \vee -conditions* for such deformations.

Let

$$G_t(x, y) := G_{\mathcal{A}(t)}(x, y) = \sum_{\alpha \in \mathcal{A}} \alpha_t(x)\alpha_t(y)$$

with $G_0 = G = G_{\mathcal{A}(0)}$ and consider its derivative

$$\dot{G}_t(x, y) = \sum_{\alpha \in \mathcal{A}} \dot{\alpha}_t(x)\alpha_t(y) + \sum_{\alpha \in \mathcal{A}} \alpha_t(x)\dot{\alpha}_t(y),$$

which at $t = 0$ gives $\dot{G}_0(x, y) = 2X$, where

$$X = \sum_{\alpha \in \mathcal{A}} \xi_\alpha \alpha(x)\alpha(y).$$

Consider now the \vee -conditions.

For any two-dimensional plane containing only 2 covectors we have

$$G_t(\alpha_t^\vee, \beta_t^\vee) = 0.$$

Differentiating it in t we have

$$\dot{G}_t(\alpha_t^\vee, \beta_t^\vee) + G_t(\dot{\alpha}_t^\vee, \beta_t^\vee) + G_t(\alpha_t^\vee, \dot{\beta}_t^\vee) = 0, \quad (3.4)$$

where here and below by $\dot{\alpha}_t^\vee$ we mean $\frac{d}{dt}(\alpha_t^\vee)$.

To find $G(\dot{\alpha}_t^\vee, \beta_t^\vee)$ note that by definition of α_t^\vee $G_t(\alpha_t^\vee, v) = \alpha_t(v)$ for any fixed vector $v \in V$. Differentiating this with respect to t we have

$$\dot{G}_t(\alpha_t^\vee, v) + G_t(\dot{\alpha}_t^\vee, v) = \dot{\alpha}(v)$$

which for $t = 0$ gives

$$2X(\alpha_0^\vee, v) + G(\dot{\alpha}_0^\vee, v) = \xi_\alpha \alpha(v).$$

Thus we have

$$G(\dot{\alpha}_0^\vee, v) = \xi_\alpha \alpha(v) - 2X(\alpha_0^\vee, v).$$

and thus

$$G(\dot{\alpha}_0^\vee, \beta^\vee) = \xi_\alpha \alpha(\beta^\vee) - 2X(\alpha_0^\vee, \beta^\vee) = -2X(\alpha_0^\vee, \beta^\vee)$$

since $\alpha(\beta^\vee) = G(\alpha_0^\vee, \beta^\vee) = 0$ by the \vee -conditions.

Substituting this into (3.4) we have the first linearised \vee -condition: for α, β be the only two covectors in a plane Π we have

$$X(\alpha^\vee, \beta^\vee) = 0. \tag{3.5}$$

Let now Π be a two-dimensional plane containing more than two covectors from \mathcal{A} (and hence from \mathcal{A}_t). Then from the \vee -conditions there exists $\nu = \nu(\Pi) \in \mathbb{R}$ such that for any $\alpha \in \Pi \cap \mathcal{A}, v \in V$ we have

$$G^\Pi(\alpha^\vee, v) = \nu G(\alpha^\vee, v), \tag{3.6}$$

where $G^\Pi(x, y) = G_{\mathcal{A}}^\Pi(x, y) = \sum_{\alpha \in \Pi \cap \mathcal{A}} \alpha(x)\alpha(y)$ (see [15]). Now assuming that \mathcal{A} depends on t as above and differentiating with respect to t at $t = 0$ we have as before

$$\begin{aligned} \dot{G}^\Pi(\alpha^\vee, \beta^\vee) + G^\Pi(\dot{\alpha}^\vee, \beta^\vee) + G^\Pi(\alpha^\vee, \dot{\beta}^\vee) &= \dot{\nu}G(\alpha^\vee, \beta^\vee) \\ + \nu \dot{G}(\alpha^\vee, \beta^\vee) + \nu G(\dot{\alpha}^\vee, \beta^\vee) + \nu G(\alpha^\vee, \dot{\beta}^\vee). \end{aligned}$$

But from \vee -conditions we have

$$G^{\Pi}(\dot{\alpha}^{\vee}, \beta^{\vee}) = \nu G(\dot{\alpha}^{\vee}, \beta^{\vee})$$

and

$$G^{\Pi}(\alpha^{\vee}, \dot{\beta}^{\vee}) = \nu G(\alpha^{\vee}, \dot{\beta}^{\vee}).$$

Since $\dot{G}^{\Pi} = 2X^{\Pi}$, where

$$X^{\Pi}(x, y) = \sum_{\alpha \in \Pi \cap \mathcal{A}} \xi_{\alpha} \alpha(x) \alpha(y),$$

we have

$$2X^{\Pi}(\alpha^{\vee}, \beta^{\vee}) = \dot{\nu} G(\alpha^{\vee}, \beta^{\vee}) + 2\nu X(\alpha^{\vee}, \beta^{\vee}),$$

or, eventually

$$2(X^{\Pi} - \nu X)(\alpha^{\vee}, \beta^{\vee}) = \dot{\nu} G(\alpha^{\vee}, \beta^{\vee}). \quad (3.7)$$

Since this is true for all $\alpha, \beta \in \Pi \cap \mathcal{A}$ we have the second linearised \vee -condition: for any plane Π containing more than 2 covectors from \mathcal{A} we have

$$X^{\Pi} - \nu X \sim G|_{\Pi^{\vee}}, \quad (3.8)$$

where the sign \sim means proportionality.

Thus we have proved

Theorem 3.3. *The deformations of \vee -systems of the form (3.3) are described by the linear \vee -conditions (3.5), (3.8).*

Case by case check of the \vee -systems from the Appendix leads to the following

Theorem 3.4. *All rank 3 vector matroids corresponding to known irreducible 3D \vee -systems are projectively rigid. The H_3 matroid is the only one, which is not strongly projectively rigid.*

A direct computation shows that in case of the classical systems A_3 and B_3 the linear system (3.4), (3.7) has corank 4 in agreement with the results of the previous section.

The analysis of the linearised \vee -conditions for the families $D_3(t, s)$, $F_3(t)$, $G_3(t)$ and $(AB_4(t), A_1)_{1,2}$ shows that these families of \vee -systems can not be extended.

Consider, for example, the family of \vee -systems $D_3(t, s)$ from [15] with

$$A = \begin{pmatrix} 1 & 1 & 1 & 1 & 0 & 0 & \sqrt{2}\sqrt{s+t-1} \\ 1 & -1 & -1 & 1 & \sqrt{2}\sqrt{\frac{s-t+1}{t}} & 0 & 0 \\ 1 & -1 & 1 & -1 & 0 & \sqrt{2}\sqrt{\frac{-s+t+1}{s}} & 0 \end{pmatrix}$$

with real parameters s, t such that $|s - t| < 1$, $s + t > 1$. Matrices G and X have the form

$$G = \begin{pmatrix} 2(s+t+1) & 0 & 0 \\ 0 & \frac{2(s+t+1)}{t} & 0 \\ 0 & 0 & \frac{2(s+t+1)}{s} \end{pmatrix}$$

$$X = \begin{pmatrix} \xi_1 + \xi_2 + \xi_3 + \xi_4 + 2\xi_7(s+t-1) & \xi_1 - \xi_2 - \xi_3 + \xi_4 & \xi_1 - \xi_2 + \xi_3 - \xi_4 \\ \xi_1 - \xi_2 - \xi_3 + \xi_4 & \xi_1 + \xi_2 + \xi_3 + \xi_4 + \frac{2(s+1)}{t}\xi_5 - 2\xi_5 & \xi_1 + \xi_2 - \xi_3 - \xi_4 \\ \xi_1 - \xi_2 + \xi_3 - \xi_4 & \xi_1 + \xi_2 - \xi_3 - \xi_4 & \xi_1 + \xi_2 + \xi_3 + \xi_4 + \frac{2(-s+t+1)}{s}\xi_6 \end{pmatrix}$$

For the three covectors $\alpha_5, \alpha_6, \alpha_7$ the first linearised \vee -conditions

$$\vee\text{-conditions } X(\alpha_i^\vee, \alpha_j^\vee) = 0, \quad i, j = 5, 6, 7$$

are equivalent to

$$\xi_1 + \xi_2 - \xi_3 - \xi_4 = 0,$$

$$\xi_1 - \xi_2 - \xi_3 + \xi_4 = 0,$$

$$\xi_1 - \xi_2 + \xi_3 - \xi_4 = 0,$$

which imply that $\xi_1 = \xi_2 = \xi_3 = \xi_4$.

For the planes with more than two covectors we have the linear system

$$(s+t)(\xi_1(s+t+1) + \xi_2(s+t-3) + t(\xi_3(2s+3) + \xi_4(2s-1) - 2(s(\xi_5 + \xi_6) + \xi_5 + \xi_7)) + t^2(-(\xi_3 + \xi_4 - 2\xi_5)) - s(s(\xi_3 + \xi_4 - 2\xi_6) + \xi_3 - 3\xi_4 + 2(\xi_6 + \xi_7)) + 2\xi_7) = 0,$$

$$(s+t)((s-1)(\xi_2 - \xi_7 + s(\xi_6 - \xi_4)) + t(\xi_2 + \xi_3 - \xi_5 - \xi_7 + s(\xi_3 + \xi_4 - \xi_5 - \xi_6)) + t^2(-\xi_3 + \xi_5)) = 0,$$

$$(s+1)t(s(\xi_1 - \xi_2 + \xi_3 + 3\xi_4 - 2(\xi_5 + \xi_6)) + \xi_1 + 3\xi_2 + \xi_3 - \xi_4 - 2(\xi_5 + \xi_7)) + (s+1)t^2(\xi_1 - 3\xi_3 + 2\xi_5) + (s^2 - 1)(-\xi_2(s-1) - \xi_4(s-1) + 2\xi_6s - 2\xi_7) = 0,$$

$$(s+1)t(\xi_2 + s(\xi_3 + \xi_4 - \xi_5 - \xi_6) + \xi_3 - \xi_5 - \xi_7) + (s^2 - 1)(\xi_2 + s(\xi_6 - \xi_4) - \xi_7) + (s+1)t^2(-(\xi_3 - \xi_5)) = 0,$$

$$(t+1)(-t(s(\xi_1 + \xi_4 - 2(\xi_5 + \xi_6)) + \xi_3(3s+2) - 2(\xi_5 + \xi_7)) + s(-s(\xi_1 + 2\xi_6) + \xi_3 + \xi_4(3s-1) + 2(\xi_6 + \xi_7)) - \xi_1s + \xi_2s(t-3) + (t-1)^2) + t^2(\xi_3 - 2\xi_5) + \xi_3 - 2\xi_7 = 0,$$

$$(t+1)(t(\xi_2 + s(\xi_3 + \xi_4 - \xi_5 - \xi_6) + \xi_3 - \xi_5 - \xi_7) + (s-1)(\xi_2 + s(\xi_6 - \xi_4) - \xi_7) + t^2(\xi_5 - \xi_3)) = 0,$$

$$(t+1)(\xi_1(s(t-3) + (t-1)^2) - t(s(\xi_2 + \xi_3 - 2(\xi_5 + \xi_6)) + \xi_4(3s+2) - 2(\xi_5 + \xi_7)) - s(s(\xi_2 - 3\xi_3 + 2\xi_6) + \xi_2 + \xi_3 - \xi_4 - 2(\xi_6 + \xi_7)) + t^2(\xi_4 - 2\xi_5) + \xi_4 - 2\xi_7) = 0,$$

$$(t+1)(t(\xi_1 + s(\xi_3 + \xi_4 - \xi_5 - \xi_6) + \xi_4 - \xi_5 - \xi_7) + (s-1)(\xi_1 + s(\xi_6 - \xi_3) - \xi_7) + t^2(\xi_5 - \xi_4)) = 0,$$

$$(s+1)t(\xi_1(s-3) - s(\xi_2 + 3\xi_3 + \xi_4 - 2(\xi_5 + \xi_6)) - \xi_2 + \xi_3 - \xi_4 + 2(\xi_5 + \xi_7)) + (s^2 - 1)(\xi_1(s-1) + \xi_3(s-1) - 2\xi_6s + 2\xi_7) + (s+1)t^2(-(\xi_2 - 3\xi_4 + 2\xi_5)) = 0,$$

$$(s+1)t(\xi_1 + s(\xi_3 + \xi_4 - \xi_5 - \xi_6) + \xi_4 - \xi_5 - \xi_7) + (s^2 - 1)(\xi_1 + s(\xi_6 - \xi_3) - \xi_7) + (s+1)t^2(-(\xi_4 - \xi_5)) = 0,$$

$$(s+t)(t(\xi_1(2s+3) + \xi_2(2s-1) + \xi_4 - 2(s(\xi_5 + \xi_6) + \xi_5 + \xi_7)) + s(-s(\xi_1 + \xi_2 - 2\xi_6) + \xi_4 - 2(\xi_6 + \xi_7)) + t^2(-(\xi_1 + \xi_2 - 2\xi_5)) - \xi_1s + 3\xi_2s + \xi_3(s+t+1) - 3\xi_4 + 2\xi_7) = 0,$$

$$(s+t)(t(s(\xi_1 + \xi_2 - \xi_5 - \xi_6) + \xi_1 + \xi_4 - \xi_5 - \xi_7) + t^2(\xi_5 - \xi_1) + (s-1)(s(\xi_6 - \xi_2) + \xi_4 - \xi_7)) = 0.$$

A check with Mathematica shows that the co-rank of the total system is 3 for every admissible values of s and t . The free parameters correspond to the two deformation parameters s and t and the uniform scaling of the system.

This approach with the use of Mathematica allows us to prove that the isolated examples of \vee -systems from the list [15] are indeed isolated.

Theorem 3.5. [39] *There are no non-trivial deformations of the \vee -systems $(E_7, A_1^2 \times A_2)$, $(E_8, A_2 \times A_3)$, $(E_8, A_2^2 \times A_1)$, $(E_8, A_1^3 \times A_2)$, $(E_8, A_1^2 \times A_3)$, $(E_8, A_1 \times A_4)$, (H_4, A_1) and H_3 .*

3.3 ν -function, uniqueness and rigidity conjectures

Let M be a matroid and \mathcal{A} be its \vee -system realisation. Such realisation defines the ν -function on the 2-flats of M , where ν is the coefficient in the \vee -conditions (3.6) corresponding to the plane Π representing the flat.

Conjecture 3.6. (Uniqueness Conjecture) *An irreducible \vee -system \mathcal{A} is uniquely determined by its matroid M and the corresponding ν -function on its flats modulo linear group $GL(V^*)$.*

A weaker version of the conjecture is

Conjecture 3.7. (Rigidity Conjecture) *An irreducible \vee -system \mathcal{A} is locally uniquely determined by its matroid M and the corresponding ν -function on its flats.*

If the function ν is fixed under deformation then $\dot{\nu} = 0$ and the corresponding \vee -conditions are

$$X(\alpha^\vee, \beta^\vee) = 0 \tag{3.9}$$

for α, β be the only two covectors in the plane, and

$$X^\Pi - \nu X = 0 \big|_{\Pi^\vee} \tag{3.10}$$

for any plane Π containing more than 2 covectors from \mathcal{A} .

Conjecturally this should imply that $X = cG$ corresponding to the global scaling of the system.

Case by case check from the list in the Appendix leads to the following

Theorem 3.8. *Both conjectures are true for all known \vee -systems in dimension 3.*

Now we present some results about ν -functions for \vee -systems.

First we give the following, more direct geometric way to compute $\nu(\Pi)$. The form $G_{\mathcal{A}}$ on V defines the scalar product on V^* and thus the norm $|\alpha|$, $\alpha \in V^*$.

Theorem 3.9. *For every plane $\Pi \subset V^*$ containing more than two covectors α from a \vee -system \mathcal{A}*

$$\nu(\Pi) = \frac{1}{2} \sum_{\alpha \in \Pi \cap \mathcal{A}} |\alpha|^2. \quad (3.11)$$

Proof. From the \vee -conditions (1) we have

$$\sum_{\alpha \in \Pi \cap \mathcal{A}} \alpha^{\vee} \otimes \alpha \Big|_{\Pi^{\vee}} = \nu(\Pi) I \Big|_{\Pi^{\vee}}.$$

Taking the trace of both sides gives (3.11). □

Let $\mathcal{A} \subset V^*$ be a \vee -system generating V^* and consider the set $\mathcal{F}_{\mathcal{A}}$ of 2-flats in the corresponding matroid, which the same as the set of 2D planes $\Pi \subset V^*$ containing more than 2 covectors from \mathcal{A} .

We say that the set of weights x_{Π} , $\Pi \in \mathcal{F}_{\mathcal{A}}$ is *admissible* if for each $\alpha \in \mathcal{A}$

$$\sum_{\Pi \in \mathcal{F}_{\mathcal{A}}: \alpha \in \Pi} x_{\Pi} = 1. \quad (3.12)$$

Theorem 3.10. *For every admissible set of weights we have*

$$\sum_{\Pi \in \mathcal{F}_{\mathcal{A}}} x_{\Pi} \nu(\Pi) = \frac{n}{2}, \quad (3.13)$$

where n is the dimension of V .

Proof. We have

$$\sum_{\beta \in \mathcal{A}} \beta^\vee \otimes \beta = \sum_{\beta \in \mathcal{A}} \left(\sum_{\Pi \in \mathcal{F}_{\mathcal{A}}: \beta \in \Pi} x_{\Pi} \right) \beta^\vee \otimes \beta = \sum_{\Pi \in \mathcal{F}_{\mathcal{A}}} x_{\Pi} \sum_{\beta \in \Pi \cap \mathcal{A}} \beta^\vee \otimes \beta.$$

From the \vee -condition

$$\sum_{\beta \in \Pi \cap \mathcal{A}} \beta^\vee \otimes \beta = \nu(\Pi) P_{\Pi},$$

where P_{Π} is the orthogonal projector onto Π^\vee . Taking trace and using the fact that $\sum_{\beta \in \mathcal{A}} \beta^\vee \otimes \beta = Id$ we obtain (3.13). \square

We call (3.13) the *universal relation* for values of function ν .

For the \vee -system of type A_3 the universal relation completely describes the set of all possible functions ν . Indeed, one can easily see from Fig. 2 that $x_{\Pi} = 1/2$ is the only admissible weight system, which leads to the universal relation

$$\sum_{\Pi \in \mathcal{F}_{\mathcal{A}}} \nu(\Pi) = 3.$$

This gives us 3 free parameters, which are exactly 3 parameters of deformation.

However, in general universal relations are not strong enough to describe possible ν -functions. Moreover, a \vee -system \mathcal{A} may not have admissible weights x_{Π} at all. For instance, this is the case for the \vee -system of $D_3(t)$ -type (this is however the only case among known 3D \vee -systems).

In the Appendix we give the list of all known 3D \vee -systems together with the corresponding matroids and ν -functions.

3.4 Matroidal structure of \vee -systems

The main part of the classification problem is to characterise the corresponding class of possible matroids. This question was addressed by Lechtenfeld et al in [26]. One of the authors of [26] (K. Schwertfeger) had developed a Mathematica program [41], which generates simple and connected matroids of a given size of the ground set X . If a generated matroid has a vector representation they have checked first if the orthogonality \vee -conditions are possible to satisfy before verification of the \vee -conditions for the non-trivial planes (all 2-flats).

For matroids with $n < 10$ elements the orthogonality conditions turned out to be strong enough to identify all matroids corresponding to \vee -systems in dimensions 3. All the corresponding \vee -systems appeared in the Feigin-Veselov list [14].

However, for $n = 10$ the program generated a simple, connected matroid which is realisable with respect to the orthogonality \vee -conditions, but does not give rise to a \vee -system. This result shows that a more conceptual approach is needed. In this section we collect some observations which could be useful in this context.

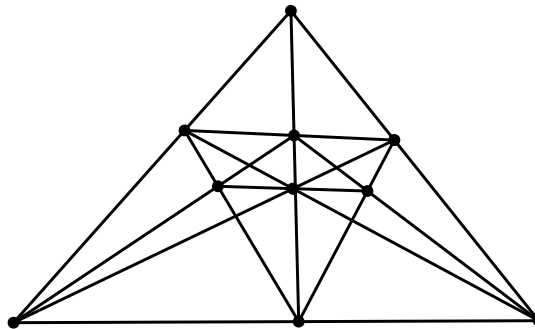


FIGURE 3.1: An example (given in [26]) of a 10-element matroid admitting a covector representation with respect to the orthogonality \vee -conditions, which is not \vee -realisable. The matroid has an (additional) orthogonality inside the plane spanned by 4 covectors.

3.4.1 Extensions and degenerations of \vee -systems

Let $\mathcal{A}_1, \mathcal{A}_2 \subset \mathbf{V}^*$ be two \vee -systems. If $\mathcal{A}_2 \subset \mathcal{A}_1$ we call \mathcal{A}_1 an *extension* of \mathcal{A}_2 .

Let \vee -system $\mathcal{A} = \mathcal{A}(t)$ depend on the parameter t . Assume that for some $t = t_0$ one or a set of the covectors $\alpha \in \mathcal{A}_{t_0}$ vanishes. In that case the system $\tilde{\mathcal{A}} = \lim_{t \rightarrow t_0} \mathcal{A}(t)$ is called a *degeneration* of $\mathcal{A}(t)$. A reverse process we will call a *regeneration*.

By the regeneration and extension we can get many \vee -systems starting from \mathcal{A}_3 .

In the tables below we give the list of all degenerations and extensions for known 3-dimensional \vee -systems. In the language of the theory of matroids both operations generate a *minor* of a given matroid [36]. Many families of matroids have been proved to be closed under taking minors. The purpose of the lists below is to provide some information for further investigations in favour of related results for the class of \vee -realisable matroids.

V-system	Degeneration	The vanishing covectors
$(F_3(t))_1$	$\lim_{t \rightarrow 0} (F_3(t))_1 \sim B_3(\sqrt{2})$	$\{11, 12, 13, 14\}$
$(F_3(t))_2$	$\lim_{t \rightarrow 0} (F_3(t))_2 \sim P$	$\{8, 9, 10, 11, 12, 13\}$
$B_3(c, c, c; \gamma)$	$\lim_{\gamma \rightarrow c} B_3(c, c, c; \gamma) \sim A_3$	$\{1, 2, 3\}$
$(AB_4(t), A_1)_2$	$\lim_{t \rightarrow \infty} (AB_4(t), A_1)_2 \sim P$	$\{5, 7, 9\}$
$(AB_4(t), A_1)_2$	$\lim_{t \rightarrow 0} (AB_4(t), A_1)_2 \sim B_3(\sqrt{2})$	$\{10\}$
$(AB_4(t), A_1)_1$	$\lim_{t \rightarrow \frac{1}{\sqrt{2}}} (AB_4(t), A_1)_1 \sim (E_6, A_1^3)$	$\{3\}$
$\frac{1}{t}(AB_4(t), A_1)_1$	$\lim_{t \rightarrow \infty} (AB_4(t), A_1)_1 \sim B_3(\sqrt{2})$	$\{5, 6\}$
$G_3(t)$	$\lim_{t \rightarrow \frac{1}{2}} G_3(t) \sim (E_6, A_1^3)$	$\{4, 5, 6\}$
$D_3(t, s)$	$\lim_{t \rightarrow (s+1)} D_3(t, s) \sim A_3$	$\{5\}$
$B_3(c_1, c_2, c_3, \gamma)$	$\lim_{c_1 \rightarrow (-\gamma)} B_3(c_1, c_2, c_3, \gamma) \sim (E_6, A_3)$	$\{1\}$
$B_3(c_1, c_2, c_3, \gamma)$	$\lim_{c_1, c_2 \rightarrow (-\gamma)} B_3(c_1, c_2, c_3, \gamma) \sim P$	$\{1, 2\}$

The case of the matroid of the V-system F_3 is particularly interesting. Due to the existence of two different realisations, the underlying matroid admits a decomposition into two smaller matroids of D_3 (or, equivalently, of P -type) and B_3 type.

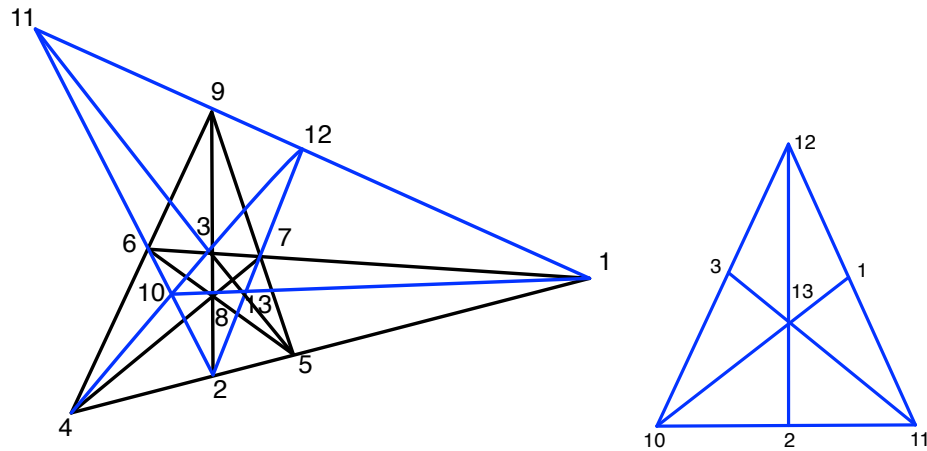


FIGURE 3.2: Decomposition of the matroid F_3 into the B_3 matroid (black) and the matroid P (blue). The graphic on the right shows the matroid P contained in F_3 in a more symmetrical form.

Removing a suitable set of covectors leads to another V-system in the following cases.

V-system	Extension	The added covectors
A_3	$(F_3(t))_1$	$\{1, 2, 3, 10, 11, 12, 13\}$
A_3	$(AB_4(t), A_1)_2$	$\{1, 2, 3, 10\}$
(E_6, A_1^3)	$(E_8, A_1^3 \times A_2)$	$\{3, 4, 5, 6, 9, 14, 15, 16, 17\}$
$G_3(\frac{3}{2})$	$(E_8, A_1^3 \times A_2)$	$\{1, 2, 10, 11, 12, 13\}$
H_3	(H_4, A_1)	$\{4, 5, 6, 7, 20, 21, 22, 23, 24, 25, 26, 27, 28, 29, 30\}$

Analysis of the list of extensions of V-systems from the previous section leads to the following

Conjecture 3.11. (Extension Conjecture) *For any irreducible V-system and its extension the values of the ν -functions on the corresponding flats are proportional.*

One can check that this is true for all known cases. For example, for the extension $H_3 \subset (H_4, A_1)$ we have the set of values

$$\{3/10, 1/2\} = 3 \times \{1/10, 1/6\}.$$

3.4.2 V-systems and harmonic bundles with two orthogonals

It is natural to study vector matroids using the corresponding cross-ratios of their projective realisation. A particular case of this approach is demonstrated in [54], where projective types of a certain class of matroids were studied in relation to a generalised version of the cross ratio defined for quadruples of subspaces of a given matroid. Here we consider the simplest case, namely the usual cross-ratio for the 2-flats with precisely 4 covectors.

Recall that 4 points A, B, C, D on a projective line form a *harmonic range* if the cross-ratio $(A, B; C, D) = -1$. The corresponding pencil of 4 lines on a plane is called *harmonic bundle*. The B_3 configuration provides a geometric way to construct harmonic ranges: on Fig. 2.2 the points 3,4,9,8 always form a harmonic range. Note that the covectors 8 and 9 are orthogonal and determine the bisectors for the lines corresponding to covectors 3 and 4.

To verify this we consider a set of collinear points $\{A, B, C, D\} \subset \mathbb{R}^3$ such that the line bundle $\{OA, OB, OC, OD\}$ is harmonic:

$$\frac{CA}{CB} = -\frac{DA}{DB}.$$

Let α denote the angle between the lines OB and OC , let α^* be the angle between the lines OA and OC , β - the angle between OD and OB and let β^* be the angle between OA and OD respectively (See Fig. 3.3).

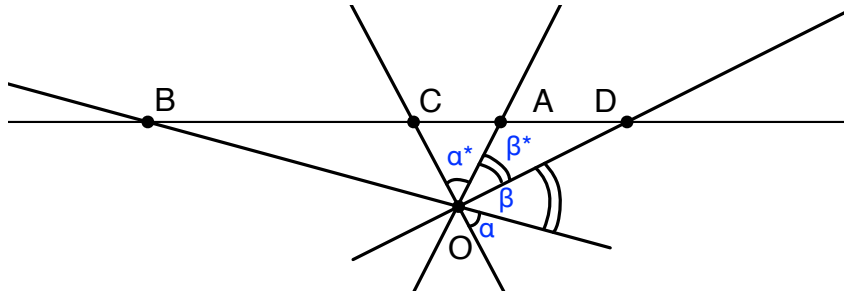


FIGURE 3.3: A harmonic bundle of lines with two orthogonals.

The cross-ratio (A, B, C, D) is the ratio of the sines of the angles between the lines as the following calculation shows.

$$\frac{DA}{DB} : \frac{CA}{CB} = \frac{DA \cdot CB}{CA \cdot DB} = \frac{DO \cdot \sin(\beta^*)}{OC \cdot \sin(\alpha^*)} \cdot \frac{OC \cdot \sin(\alpha)}{DO \cdot \sin(\beta)} = \frac{\sin(\alpha)}{\sin(\alpha^*)} : \frac{\sin(\beta)}{\sin(\beta^*)}.$$

Assume that the lines DO and CO are orthogonal. Then we have

$$\alpha + \beta = \alpha^* + \beta^* = \frac{\pi}{2}$$

It follows that $\sin(\alpha) = \cos(\beta)$ and also $\sin(\alpha^*) = \cos(\beta^*)$. Hence we obtain

$$\frac{\sin(\alpha)}{\sin(\alpha^*)} : \frac{\sin(\beta)}{\sin(\beta^*)} = \frac{\cos(\beta)}{\cos(\beta^*)} : \frac{\sin(\beta)}{\sin(\beta^*)}.$$

But this means that

$$\cot(\beta) = -\cot(\beta^*).$$

Therefore, $\cos(\beta - \beta^*) = 0$ and $\beta = \tilde{\beta}$. The lines DO and CO are indeed bisectors of the lines AO and BO .

Case by case check of the known 3D \vee -systems suggests that the same is true in general.

Conjecture 3.12. *Let \mathcal{A} be a \vee -system and $\Pi_{\mathcal{A}} \subset V^*$ be two-dimensional plane containing exactly four covectors $\alpha_i \in \mathcal{A}$, $i = 1, \dots, 4$, then the corresponding lines form a harmonic bundle with a pair of orthogonal covectors.*

3.4.3 \vee -systems and matroid duality

An important and powerful concept in projective geometry is the duality principle. In particular, all theorems occur in dual pairs. The cases involving self-dual configurations build an exception giving rise to identical statements. In this subsection we demonstrate that the duality between points and lines on the projective plane can be used to produce new \vee -realisable matroids.

We start with the smallest configuration $(6_2 4_3)$ corresponding to the \vee -system type A_3 . This is a complete quadrilateral. It consists of 4 lines, no 3 of which pass through the same point and 6 points of intersection. Its projective dual is a complete quadrangle $(4_3 6_2)$ consisting of 4 points, no three of which are collinear and 6 lines connecting each pair of points (see Fig. 3.4). In the next step we extend the dual configuration $(4_3 6_2)$ by adding the remaining three points of intersections of lines (the points marked white in the graphic).

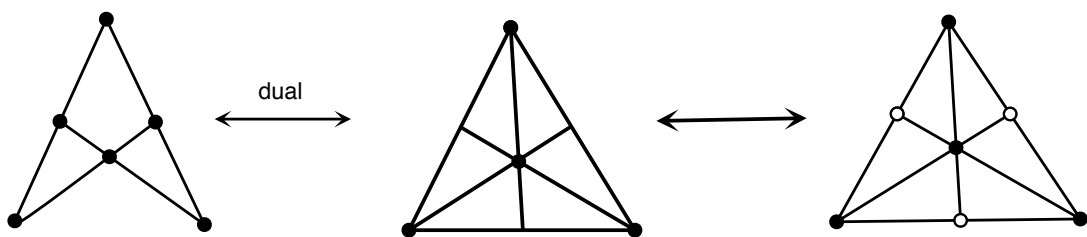


FIGURE 3.4: The projective configuration $(6_2 4_3)$, its dual $(4_3 6_2)$ and the extended configuration containing points of intersection of each pair of lines.

Recall that the configuration $(6_2 4_3)$ corresponds to a \vee -realisable matroid. For any \vee -system A_3 the three orthogonal pairs of vector correspond to the three pairs of points in $(6_2 4_3)$, which are not connected by a line. In the dual picture they correspond to the pairs of lines with no common point. Adding exactly those

points is therefore equivalent to adding three lines connecting the three pairs of "orthogonal" vectors (points) in the first picture (left).

The resulting matroid on 7 points and 6 lines is a \vee -realisable matroid of $D_3(t, s)$ -type.

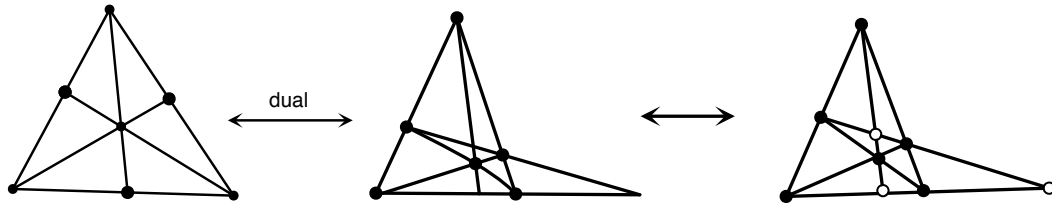


FIGURE 3.5: Graphical representation of the D_3 matroid, its projective dual on 7 lines and 6 points and the extended configuration containing all points of intersection of lines.

We proceed the construction by taking the dual of the new obtained configuration and extending it by adding the missing points of intersections of lines. The result is the configuration on 9 points and 7 lines realisable as B_3 \vee -system (see Fig. 3.5).

The next step of the construction is demonstrated in Fig. 3.6. The dual configuration was obtained from the configuration D_3 by adding all missing lines passing through any pair of points. Consider the red and the blue triangles. Taking the point 1 as the center of perspectivity it follows from Desargue's theorem that the white marked points of the extended configuration are collinear. The obtained configuration is realisable as the \vee -system $(AB_4(t), A_1)_2$.

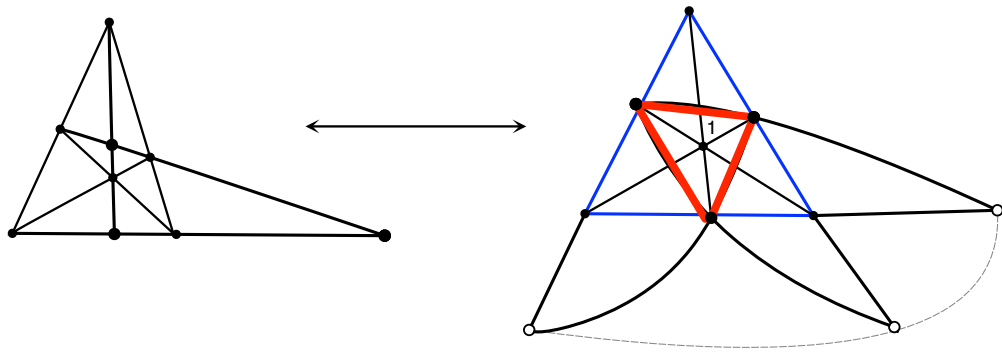


FIGURE 3.6: Graphical representation of the B_3 -matroid and its projective dual on 9 lines and 7 points. The extended configuration contains three additional (white) points. Due to Desargue's theorem of the projective geometry the three white points are collinear.

The list [14] contains a second \vee -system consisting of 10 covectors, which we don't obtain from our construction method, namely the system (E_6, A_1^3) . As a projective configuration (E_6, A_1^3) is self-dual and contains a special case of the Pappus configuration (9_3) (see Fig. 3.7).

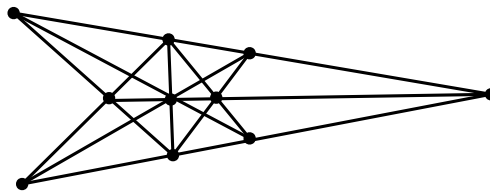


FIGURE 3.7: Graphical representation of the self-dual configuration corresponding to the \vee -system (E_6, A_1^3) .

We can conclude that projective duality can be used in order to generate suitable candidates for \vee -realisable matroids. However, not all \vee -realisable matroids can be build up by the described method starting from the matroid of type A_3 .

Part II

BUFFON TRANSFORMATION FOR POLYHEDRA

Chapter 4

Buffon transformation

4.1 Buffon transformation for polygons.

The following construction, to which we will refer to as the *Buffon procedure*, was previously studied, for example, in [50, 51, 52]. Consider an arbitrary n -gon P with vertices described by the column vector

$$r = [r_1, r_2, \dots, r_n], \quad r_i \in \mathbb{R}^3$$

(and an integer $n \geq 3$) and generate a second polygon P' by joining the centres of the consecutive edges of P . The corresponding transformation acts on the vertices of P as follows:

$$r'_i = \frac{1}{2}(r_i + r_{i+1}).$$

In the matrix form this can be described as

$$r' = Br$$

where

$$B = \begin{bmatrix} \frac{1}{2} & \frac{1}{2} & 0 & \dots & 0 \\ 0 & \frac{1}{2} & \frac{1}{2} & \dots & 0 \\ \vdots & \vdots & \vdots & \vdots & \vdots \\ \frac{1}{2} & 0 & 0 & \dots & \frac{1}{2} \end{bmatrix}$$

After k transformations we obtain a polygon with the vertices

$$r^k = B^k r.$$

Recall that a polygon is *affine regular* if it is affine equivalent to a regular polygon. For example, all triangles are affine-regular. Parallelograms are the only affine images of a square are. But not all $2N$ -sided polygons with pairwise equal and parallel sides are affine regular. This follows from the fact that an affine transformation in the plane (modulo translation) is defined by four parameters. In forming such polygons, however, there are more degrees of freedom. On the other hand, an $2N$ -sided affine-regular polygon has necessarily parallel and equal opposite sides.

Following Buffon we claim that for generic initial polygons P the limiting shape of the polygons P^k as k increases becomes affine regular.

To prove this we will use the following result from Linear Algebra (see e.g. Theorems 5.1.1, 5.1.2 in [53]).

Theorem 4.1. (Subspace Iteration Theorem) *Let A be a real $n \times n$ matrix and let $\text{Spec}(A) = \{\lambda_1, \lambda_2, \dots, \lambda_n\}$ be the set of its eigenvalues (in general, complex and with multiplicities) ordered in such a way that*

$$|\lambda_1| = |\lambda_2| = \dots = |\lambda_k| > |\lambda_{k+1}| \geq \dots \geq |\lambda_n|.$$

Let W and W' be the dominant and complementary invariant subspaces associated with $\lambda_1, \dots, \lambda_k$ and $\lambda_{k+1}, \dots, \lambda_n$ respectively and $m = \dim W$. Then for any m -dimensional subspace $U \subset \mathbb{R}^n$ such that $U \cap W' = \{0\}$ the image of U under the iterations of A

$$A^n(U) \xrightarrow{n \rightarrow \infty} W$$

turns to the dominant subspace in the Grassmannian $G_m(\mathbb{R}^n)$.

To apply this to our case first note that

$$B = \frac{1}{2}(I + T),$$

where the $n \times n$ matrix

$$T = \begin{bmatrix} 0 & 1 & 0 & \dots & 0 \\ 0 & 0 & 1 & \dots & 0 \\ \vdots & \vdots & \vdots & \ddots & \vdots \\ 1 & 0 & 0 & \dots & 0 \end{bmatrix}$$

has the property $T^n = I$ and the eigenvalues being n -th roots of unity. The spectrum of B is therefore

$$\text{Spec}(B) = \left\{ \frac{1}{2} + \frac{1}{2}\varepsilon_j, \varepsilon_j = e^{\frac{2\pi i}{n}j}, j = 0, 1, \dots, n-1 \right\}.$$

The eigenvalues of maximum modulus, other than $\lambda_0 = 1$, are $\lambda_1 = \frac{1}{2} + \frac{1}{2}e^{\frac{2\pi i}{n}}$ and its complex conjugate $\lambda_2 = \frac{1}{2} + \frac{1}{2}e^{-\frac{2\pi i}{n}} = \overline{\lambda_1}$.

The dominant subspace W in this case corresponds to $\lambda_0 = 1$ and is generated by the corresponding eigenvector $v_0 = (1, 1, \dots, 1)$:

$$W = \{(r, r, \dots, r)\}.$$

The previous result can be interpreted that as n increases $B^n(P)$ converges to a point. To see the limiting shape we should look at the *subdominant invariant* subspace corresponding to λ_1 and λ_2 .

Geometrically one can do this by assuming that the centroid of the vertices is at the origin (*centre of mass condition*). This means that we restrict the action of B on the invariant subspace

$$V_C = \{(r_1, \dots, r_n) : r_1 + \dots + r_n = 0\}$$

This eliminates the eigenvalue $\lambda_0 = 1$ and the new dominant subspace W corresponding to $\lambda_1 = \frac{1}{2} + \frac{1}{2}\varepsilon$, $\lambda_2 = \overline{\lambda_1}$ is precisely the one describing the limiting shape. One can easily check that

$$W = \left\langle \begin{pmatrix} 1 \\ \varepsilon \\ \varepsilon^2 \\ \cdot \\ \cdot \\ \varepsilon^{n-1} \end{pmatrix}, \begin{pmatrix} 1 \\ \bar{\varepsilon} \\ \bar{\varepsilon}^2 \\ \cdot \\ \cdot \\ \bar{\varepsilon}^{n-1} \end{pmatrix} \right\rangle = \left\{ a \begin{pmatrix} 1 \\ \cos \frac{2\pi}{n} \\ \cos \frac{4\pi}{n} \\ \cdot \\ \cdot \\ \cdot \end{pmatrix} + b \begin{pmatrix} 0 \\ \sin \frac{2\pi}{n} \\ \sin \frac{4\pi}{n} \\ \cdot \\ \cdot \\ \cdot \end{pmatrix} \right\}$$

Choosing a and b to be orthogonal unit vectors we see that the corresponding vertices form a regular polygon. In general, the dominant subspace W describe all affine regular polygons. The other eigenspaces correspond to the affine regular "polygrams".

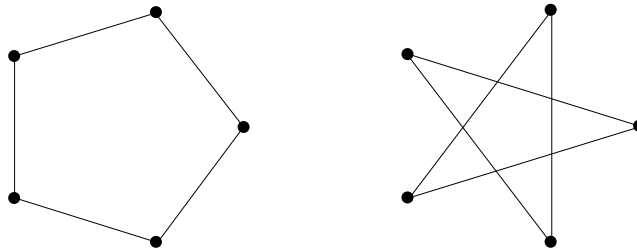
For example, when $n = 5$ we have the eigenvalues

$$\lambda_1 = \frac{1}{2} + \frac{1}{2}e^{\frac{2\pi i}{n}}, \lambda_2 = \overline{\lambda_1}, \lambda_3 = \frac{1}{2} + \frac{1}{2}e^{\frac{4\pi i}{5}}, \lambda_4 = \overline{\lambda_3}$$

and the corresponding eigenspaces

$$W = \left\{ a \begin{pmatrix} 1 \\ \cos\frac{2\pi}{5} \\ \cos\frac{4\pi}{5} \\ \cos\frac{6\pi}{5} \\ \cos\frac{8\pi}{5} \end{pmatrix} + b \begin{pmatrix} 0 \\ \sin\frac{2\pi}{5} \\ \sin\frac{4\pi}{5} \\ \sin\frac{6\pi}{5} \\ \sin\frac{8\pi}{5} \end{pmatrix} \right\}, \quad W' = \left\{ a \begin{pmatrix} 1 \\ \cos\frac{4\pi}{5} \\ \cos\frac{8\pi}{5} \\ \cos\frac{2\pi}{5} \\ \cos\frac{6\pi}{5} \end{pmatrix} + b \begin{pmatrix} 0 \\ \sin\frac{4\pi}{5} \\ \sin\frac{8\pi}{5} \\ \sin\frac{2\pi}{5} \\ \sin\frac{6\pi}{5} \end{pmatrix} \right\}$$

describing the affine regular pentagons and pentagrams respectively:



In the next section we will introduce the generalisation of the Buffon procedure for polyhedra. It will be important for us to distinguish between a geometric representation and the purely combinatorial structure of a given object. In case of polygons this translates as follows [see e.g. [18]]:

A *combinatorial (or abstract) n -gon* is a (simple) circuit C of n (distinct) vertices and n edges.

A *geometric n -gon* (or polygon for short) is an image of an abstract n -gon in a plane, such that the vertices of C are mapped onto points and edges of C onto segments with appropriate points as endpoints.

Our result can therefore be reformulated as follows:

Theorem 4.2. *The Buffon procedure gives a unique affine regular representative for each abstract n -gon.*

Note that one can modify the described procedure by choosing the centroid of centroids of the incident edges as the vertices of the new polygon, which will lead to the same result.

4.2 Buffon transformation for polyhedra

Motivated by the regularisation effect of the Buffon procedure observed for polygons we study its natural analogon for 3-dimensional polytopes and introduce representatives of simplicial convex polyhedra of a given simplicial combinatorial type. We will refer to these representatives as *affine B -regular polyhedra*.

A polytope can be defined as a subset $P \subseteq \mathbb{R}^d$ admitting a presentation as the convex hull of a finite set $X = \{x^1, \dots, x^n\}$ of points in \mathbb{R}^d :

$$P = \text{conv}(X) := \left\{ \sum_{i=1}^n \lambda_i x^i \mid \lambda_i \geq 0, \sum_{i=1}^n \lambda_i = 1 \right\}.$$

Equivalently, $P \subseteq \mathbb{R}^d$ is a polytope if it is a bounded solution set of a finite system of linear inequalities:

$$P = P(A, b) := \{x \in \mathbb{R}^d \mid a_i^T x \leq b_i \text{ for } 1 \leq i \leq m\},$$

where $A \in \mathbb{R}^{m \times d}$ is a real matrix with rows a_i^T , and $b \in \mathbb{R}^m$ is a real vector with entries b_i . A solution is said to be bounded if there is a constant N such that $\|x\| \leq N$ holds for all $x \in P$ [56].

The equivalence of both definitions is sometimes referred to as the *Main Theorem of Polytope Theory* [56]. A d -polytope is a d -dimensional polytope, referring to the dimension of its affine hull. 3-polytopes are also called polyhedra.

For our purpose it will be convenient to approach the theory of polyhedra from the graph-theoretical point of view. In this section we will recall some basic notions of graphs and their relation with polyhedra (for details, we refer to [8, 18]).

A *graph* $\Gamma = (\mathcal{V}, \mathcal{E})$ consists of a finite set V (vertices), together with a subset $\mathcal{E} \subseteq \mathcal{V} \times \mathcal{V}$ (edges). A *geometric realisation* of Γ is the image of Γ under a mapping in which the vertices are mapped to points in the Euclidean space, and the edges are mapped to segments with appropriate endpoints. We will call a geometric realisation P of Γ *polyhedral* if P is a realisation of Γ in Euclidean 3-space, and all simple circuits (circuits with no repeated vertices) of Γ are mapped to polygons.

For every polyhedron P one can consider the *1-skeleton* $\Gamma(P)$, which is the graph formed by the vertices and edges of P . More general, the *k-skeleton* of a d -polytope P is the polyhedral complex generated by all k -faces of P . The *d-skeleton* is just P itself. This terminology is useful in order to distinguish between the combinatorial structure of a polytope, and the geometric realisations of this combinatorial structure.

In general, a graph realisation problem is concerned with determining positions of the nodes of a given graph in \mathbb{R}^d under consideration of some additional constraints. Combinatorial types of polytopes are defined as their equivalence classes under combinatorial equivalence. Two polytopes P and P' are *combinatorially isomorphic* if their sets of all faces (face lattices) are isomorphic as abstract (un-labeled) partially ordered sets. The set of all realisations of a *combinatorial polyhedral type* is formalised by the concept of the *realisation space* of a polytope.

The question of construction of geometric representations of graphs goes back to Paul Erdős. For an extensive investigation on a variety of geometric realisations of graphs, such as metric embeddings, unit distance graphs and orthogonal representations, we refer to [8] and also [28].

We will assume that the graph Γ has no loops $[i, i]$, $i \in \mathcal{V}$ and is *undirected*, which means that for each edge $[i, j] \in \mathcal{E}$ we also have $[j, i] \in \mathcal{E}$.

We say that the vertices i and j are *adjacent* and write $i \sim j$ if there is an edge $[i, j] \in \mathcal{E}$ connecting them. The *degree* d_i of a vertex i is the number of the adjacent vertices. A graph is called *regular* when every graph vertex has the same degree.

A graph is *connected* when there is a path between any two vertices. A graph is called *3-connected* if for every pair of vertices i and j there are at least three paths from i to j , whose only vertices in common are i and j .

A graph is called *planar* if an isomorphic copy of the graph can be drawn in a plane, such that the edges which join the vertices only meet (intersect) at vertices.

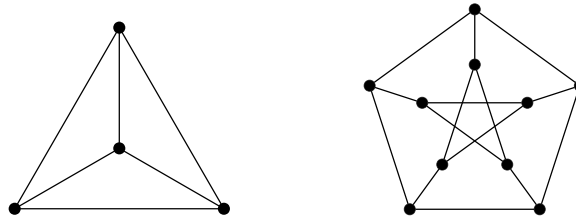


FIGURE 4.1: the planar tetrahedral graph K_4 and the non-planar Petersen graph.

One of the oldest results in polytope theory is a remarkable theorem by Ernst Steinitz. It is often referred to as the Steinitz' *fundamental theorem of convex types* and gives a completely combinatorial characterization of the graphs Γ , which can be realised as 1-skeletons of 3-dimensional polytopes (see [18]).

Theorem 4.3. (Steinitz, 1922) *A graph Γ is isomorphic to the 1-skeleton of a 3-dimensional convex polyhedron P if and only if Γ is planar and 3-connected.*

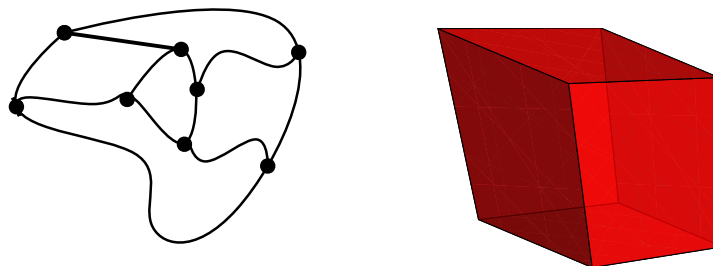


FIGURE 4.2: The graph on the left is isomorphic to the 1-skeleton of the cube. According to Steinitz' Theorem there is a bijection between planar 3-connected graphs and 3-polytopes.

For any 3-polytope one can consider the abstract graph whose nodes are the vertices of the polytope, and whose arcs are given by the edges of the polytope. A radial projection of the polytope boundary (and thus of the vertices and edges) onto a sphere that contains the polytope, and a stereographic projection to the plane produces a straight-edge drawing of this graph in the plane demonstrating its planarity. From Mengers characterization of a d -connected graph as a graph that cannot be disconnected by removing or blocking less than d of its vertices follows that the graph of any 3-polytope is 3-connected [56].

The non-trivial part of Steinitz' theorem is the problem of producing a convex 3-polytope with a prescribed 1-skeleton starting from combinatorial data of an abstract planar graph.

The proof given by Steinitz has an inductive character. It uses a combinatorial local reduction technique. For instance, removing an edge $[i, j] \in \mathcal{E}$ from the graph Γ , such that if an endpoint of $[i, j]$ is 3-valent, the remaining two edges "collapse" into a single edge, reduces Γ into a simpler graph. That this reduction operation is admissible follows from the following fact (see [18]).

Lemma 4.4. *Every 3-connected planar graph Γ with more than six edges has an edge $[i, j] \in \mathcal{E}$ such that if $[i, j]$ is deleted from the graph, the resulting smaller graph Γ' is still 3-connected (and planar).*

Repeated reductions yield a sequence of transformations of Γ into simpler graphs leading to the tetrahedral graph K_4 .

Reversing the order of these operations starting with the graph K_4 (and its polyhedral realisation as a simplex) and building up a sequence of polytopes one obtains a polyhedral realisation of the original graph Γ . The reversed procedure is based on the following result (see [18]).

Lemma 4.5. *Given a 3-connected planar graph Γ and any edge $[i, j] \in \mathcal{E}(\Gamma)$, it is possible to arrange the elements of the set which consists of all vertices and all faces of Γ into such a list that the two vertices and two faces of Γ incident with $[i, j]$ are the first four elements, and that each element in the list is incident with at most three elements that precede it in the list.*

It follows from the lemma that starting with a polyhedral realisation P' of a reduced graph Γ' an edge $[i, j] \in \mathcal{E}(\Gamma')$ can be drawn as a chord on a face of P' . Suitable choices for other vertices and faces will then allow to construct a polyhedral realisation P of Γ in which $[i, j]$ will become an edge of P .

There exist different proofs of Steinitz' theorem. The so-called Koebe-Thurston type proof leads to the famous Koebe-Andreev-Thurston circle packing theorem and the existence result of geometric realisations of 3-polytopes with all edges tangent to the sphere. Another interesting result motivated by Steinitz' theorem is Peter Mani's theorem dealing with the relationship between the automorphism groups of planar 3-connected graphs and the symmetry of their polyhedral realisations [30].

Let P be a polyhedron in \mathbb{R}^3 with vertices r_1, \dots, r_n . There are two natural ways to introduce the *Buffon transformation* $B(P)$. The first one is to define $B(P)$ as

a new polyhedron with the vertices being the centroids of midpoints of all edges, which meet at a vertex [50, 52]:

$$B(r_i) = \sum_{j \sim i} \frac{1}{2d_i} (r_i + r_j), \tag{4.1}$$

where d_i is the degree of the vertex r_i . For simplicial P the polyhedron $B(P)$ is well-defined, even if P is not convex.

The linear *Buffon operator* $B : \mathcal{F}(\mathcal{V}) \rightarrow \mathcal{F}(\mathcal{V})$, where $\mathcal{F}(\mathcal{V})$ is the vector space of functions on the vertices of the graph $\Gamma = \Gamma(P)$ is defined by the same formula:

$$B(f)(i) = \sum_{j \sim i} \frac{1}{2d_i} (f(i) + f(j)), \quad f \in \mathcal{F}(\mathcal{V}). \tag{4.2}$$

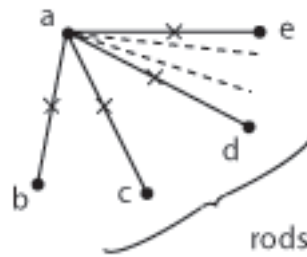


FIGURE 4.3: The vertex a connects together d_a edges. Thus the row B_a of the Buffon transformation matrix has the form $[B]_a = [\dots, \frac{1}{2d_a}, 0, 0, \dots, \frac{1}{2}, 0, \dots, \frac{1}{2d_a}, \dots]$.

Alternatively, one can define the Buffon transformation by taking the centroids of the centroids of all the faces meeting at a vertex [50],[52]. We denote this transformation by B_F .

Recall that the polyhedron P is called *simplicial* if it contains only triangular faces. Via Steinitz’s theorem simplicial polyhedra correspond to maximal planar graphs. A graph is called *maximal planar* if it is planar and if adding any edge on the given vertex set destroys the planarity property. For simplicial polyhedra P we have the following simple relation for the corresponding Buffon operators

$$B_F = \frac{4}{3}B - \frac{1}{3}I,$$

which means that the result of the Buffon procedure will be the same.

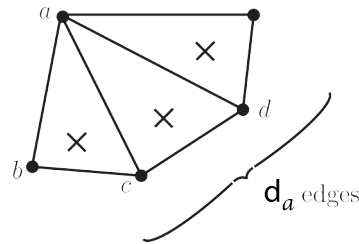


FIGURE 4.4: The geometry of polyhedra with triangular faces is the same using faces or edges generated Buffon transformation.

In general, the operator B is not symmetric. It can, however, as we will see later, be symmetrised.

We ask the same question as in case of polygons: What is the limiting shape of $B^n(P)$ when n goes to infinity? Figure 4.5 shows the effect of applying the Buffon transformation B to a polyhedron P whose vertex-edge-structure is isomorphic to the 1-skeleton of a cube. As we can observe the Buffon transformation breaks the faces of P already at the first step.

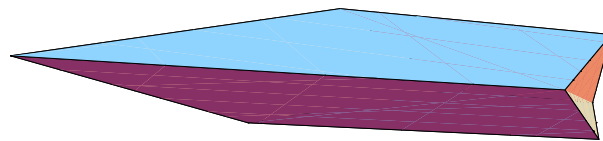


FIGURE 4.5: The effect of the Buffon transformation on a polyhedron with combinatorial structure isomorphic to the cubical graph. $B(P)$ has non-planar faces.

By the same arguments using the Subspace Iteration Theorem the limiting shape of $B^n(P)$ is given by the subdominant eigenspace of the corresponding Buffon operator B . In general it is one-dimensional, which means that the limiting shape is one-dimensional. However, as we will see, under the additional assumption of symmetry and simpliciality the limiting shape is three-dimensional. More precisely we obtain the following result.

Let G be one of the symmetry groups $G = T, O, I$ of the Platonic solids: tetrahedron, octahedron/cube, icosahedron/dodecahedron respectively. Assume that the combinatorial structure of the initial polyhedron P is G -invariant, which means that G faithfully acts on the graph $\Gamma(P)$. Then the following theorem holds.

Theorem 4.6. *Let P be a simplicial polyhedron in \mathbb{R}^3 with G -invariant combinatorial structure. Then for a generic P the limiting shape obtained by repeatedly applying Buffon procedure to P is a star-shaped polyhedron P_B . The vertices of P_B are explicitly determined by the subdominant eigenspace of the Buffon operator, which in this case has dimension 3.*

Recall that the polyhedron P is called *star-shaped* (not to be mixed with star polyhedra like Kepler-Poinsot) if there is a point inside it from which one can see the whole boundary of P , or equivalently, the central projection gives a homeomorphism of the boundary of P onto a sphere.

Note that polyhedra can be considered as solids or as surfaces. For convex polyhedra, there is a straightforward correspondence between these two interpretations. This is not the case for nonconvex polyhedra. For example, if interpreted as solids, the Kepler-Poinsot star polyhedra become star-shaped. However, this may change the combinatorial structure of the polyhedron.

The proof of the existence of star-shaped affine B -regular version of P is based on deep results from the spectral theory on graphs due to Colin de Verdière [6] and Lovasz et al [47, 27, 29] which we will discuss in the next chapter.

Chapter 5

Spectral graph theory and proof of theorem 4.6

5.1 Graphs and matrices

There are many ways to assign a matrix to a given graph. Connections between the eigenvalues of a matrix representation of a graph, discrete operators and combinatorial properties are subject of study of spectral graph theory - a branch of algebraic graph theory.

The purpose of this section is to investigate the connections between the Buffon operator and some well studied linear operators on graphs.

The types of matrices most commonly associated with graphs are the adjacency matrix, the graph Laplacian and the transition matrix of a random walk.

The *adjacency matrix* of Γ is the symmetric matrix $A = (A_{ij})$ of order n , defined as

$$A_{ij} = \begin{cases} 1, & ij \in E \\ 0, & ij \notin E. \end{cases}$$

For a regular graph Γ the adjacency matrix provides an understanding of a very natural operator - the discrete transition operator defined as the $n \times n$ matrix $P = (P_{ij})$ where

$$P_{ij} = \frac{1}{d_i} A_{ij}.$$

Here d_i denotes the degree of the vertex $v_i \in V$. The diagonal matrix D in which $D_{ii} = d_i$ is called the *degree matrix* of Γ . For a d -regular graph the transition matrix

$$P = D^{-1}A$$

is just a rescaling of the corresponding adjacency matrix. P describes the probability distribution of a random walk on a graph. A random walk is a process that starts at some vertex, and moves to a neighbor vertex at each time step. Let the vector $p^t \in \mathbb{R}^n$ denote the distribution at the time step t . The initial probability distribution, p^0 , is concentrated at one vertex and corresponds therefore to the vector

$$p^0(i) = \begin{cases} 1, & i = 1 \\ 0, & i \neq 1. \end{cases}$$

After moving to a neighbor of the starting vertex, the distribution at time step 1 corresponds to $p^1 = Pp^0$. The procedure leads to a sequence of vertices. At the time t the distribution can be expressed through the equation

$$p^t = Pp^{t-1} = P^t p^0.$$

Another prominent operator on a graph is the discrete Laplacian operator. The *Laplacian* of Γ is defined as the $n \times n$ matrix $L = (L_{ij})$ in which

$$L_{ij} = \begin{cases} d_i, & i = j \\ -A_{ij}, & i \neq j. \end{cases}$$

It follows

$$L = D - A.$$

Note that there are various definitions of the discrete Laplacian. They differ by sign and a scale factor. The graph Laplacian can be thought of as discrete analogue of the Laplace-Beltrami operator on Riemannian manifolds. Let $\phi \in \mathbb{R}^V$ be a function on the set of vertices of Γ . The *Laplacian quadratic form* is

$$\phi^T L \phi = \sum_{v_i \sim v_j} (\phi(v_i) - \phi(v_j))^2$$

The Laplacian matrix representation of a graph has the following properties:

- L is symmetric positive semi-definite.
- All eigenvalues of L are non-negative.
- The smallest eigenvalue is equal to 0.
- If Γ a connected graph, then the multiplicity of the eigenvalue 0 is 1.

The last property is a consequence of the Perron-Frobenius theorem for nonnegative matrices applied to $(cI - L)$ with a large $c \in \mathbb{R}$.

Theorem 5.1. (Perron-Frobenius, 1912) *If a real matrix has non-negative entries then it has a nonnegative real eigenvalue λ which has maximum absolute value among all eigenvalues. This eigenvalue λ has a nonnegative real eigenvector. If the matrix is irreducible, then λ has multiplicity 1 and the corresponding eigenvector can be chosen to be positive.*

In general case, the multiplicity of the eigenvalue 0 of the Laplacian matrix is equal to the number of connected components. An equivalent statement is not true for the adjacency matrix of Γ . The multiplicity of the largest eigenvalue of the matrix A remains 1 even when Γ has more than one connected component with different largest eigenvalues.

Another interesting spectral parameter is the gap between the smallest and the second smallest eigenvalues of the Laplacian (or, equivalently, the gap between the largest and the second largest eigenvalues of the adjacency matrix A of Γ) which is also related to some connectivity properties of Γ .

According to [25] the study of the connection between Laplacian spectra (particularly with respect to the smallest non-trivial eigenvalue) and properties of the associated graphs dates back to Fiedler's work in the 1970's. A graph Γ is *edge-weighted* if a real, non-zero weight w_{ij} is associated with each edge $(i,j) \in E(\Gamma)$. Fiedler extended the notion of the Laplacian [16] to graphs with positive edge weights defining a matrix representation as follows: the i -th diagonal entry l_{ii} is the sum of the weights of the edges incident to the vertex i . For $i \neq j, i \sim j$ set $l_{ij} = -w_{ij}$ and $l_{ij} = 0$ otherwise. Fiedler referred to this representation as the *generalised Laplacian*. Choosing each edge weight equal to one, the weighted Laplacian is the Laplacian of an unweighted graph.

Fiedler also used the eigenvectors of the weighted Laplacian as coordinate vectors for graph embeddings. The resulting embeddings, however, do not have very appealing geometric properties. In particular, the faces of such embeddings may overlap.

Buffon transformation matrix B and the described matrix representations are related in the following way. The matrix of the Buffon transformation in a natural basis in $\mathcal{F}(\mathcal{V})$ has the form

$$B = \frac{1}{2}(I + D^{-1}A) = \frac{1}{2}(I + P), \quad (5.1)$$

where A is the *adjacency matrix*, D the diagonal matrix with the degrees of vertices d_i on the diagonal, and P is the matrix of *transition probabilities* of the Markov chain describing the random walk on graph Γ .

Note that unless Γ is a regular graph, matrix B is not symmetric. In order to bring it to a symmetric form we introduce the *normalised adjacency matrix*

$$N = D^{-\frac{1}{2}}AD^{-\frac{1}{2}} \quad (5.2)$$

with matrix elements $N_{ij} = 1/\sqrt{d_i d_j}$ if i is adjacent to j and 0 otherwise. It is easy to see that

$$B = \frac{1}{2}(I + D^{-\frac{1}{2}}ND^{\frac{1}{2}}) = \frac{1}{2}D^{-\frac{1}{2}}(I + N)D^{\frac{1}{2}},$$

so B is conjugated to the symmetric matrix $\tilde{B} = 1/2(I + N)$.

In particular, this means that all the eigenvalues of B are real. The maximal eigenvalue is $\lambda_1 = 1$ and the corresponding eigenvector is $(1, \dots, 1)^T$.

5.2 Colin de Verdière number and null space representation

In this section we discuss the geometrical realisation of graphs following [46], [27], [24].

Let $\Gamma(\mathcal{V}, \mathcal{E})$ be a finite, connected, undirected graph with no self-loops or multiple edges (i.e. simple), and M a matrix whose rows and columns are indexed by the

vertex set V of Γ . Let $\sigma(M)$ be the spectrum and $\lambda \in \sigma(M)$ an eigenvalue of M with multiplicity k . A matrix with rows forming a basis of the eigenspace of M corresponding to λ has columns that serve as coordinate vectors of the vertices of a geometric realisation of Γ . The obtained system of vectors is called an *eigenspace realisation* of Γ .

The resulting geometric realisation is not unique. Moreover, as we know from the Subspace Iteration Theorem, different vertices do not necessarily correspond to distinct points and different edges are not necessarily non-degenerate line segments. We are interested in non-degenerate realisations, that is when the segments do not collapse.

A spectral representation $\Phi : V \rightarrow \mathbb{R}^n$ is *faithful* if Φ is injective. A particularly strong faithfulness result for 3-connected planar graphs was obtained in [29]. It is connected with the graph parameter known as the *Colin de Verdière number* which we will introduce in this section.

In 1990 Yves Colin de Verdière [6] introduced a new spectral graph invariant $\mu(\Gamma)$. Roughly speaking, $\mu(\Gamma)$ is the maximal multiplicity of the second largest eigenvalue of the matrices C with the property $C_{ij} = C_{ji} > 0$ for adjacent i and j , $C_{ij} = 0$ for non-adjacent i and j and arbitrary diagonal elements C_{ii} . The precise definition is as follows.

Let Γ be a connected undirected graph with the vertex set $\{1, \dots, n\}$. Let \mathcal{M}_Γ denote the set of symmetric matrices $M = (M_{ij}) \in \mathbb{R}^{V \times V}$ associated with Γ satisfying

1. $M_{ij} \begin{cases} < 0, & ij \in E \\ = 0, & ij \notin E \end{cases}$;
2. M has exactly one (simple) negative eigenvalue.

M is said to satisfy the *Strong Arnold Property* if the relation $MX = 0$ with a symmetric $n \times n$ matrix X such that $X_{ij} = 0$ for any adjacent i and j and for $i = j$ implies that $X = 0$. This property is a restriction, which excludes some degenerate choices of the edge weights and the diagonal entries.

The *Colin de Verdière invariant* $\mu(\Gamma)$ is the largest corank of matrices from the set \mathcal{M}_Γ satisfying the Strong Arnold Property. A matrix $M \in \mathcal{M}_\Gamma$ with corank $\mu(\Gamma)$ is called a *Colin de Verdière matrix* of Γ .

After the change of sign and shift by a scalar matrix $C = cI - M$ the corank, which is the dimension of the null space of M becomes the multiplicity of the second largest eigenvalue of C .

Colin de Verdière characterised all the graphs with parameter $\mu(\Gamma) \leq 3$.

A graph is called *outerplanar* if it can be drawn in the plane without crossings in such a way that all of the vertices belong to the unbounded face of the drawing.

Theorem 5.2. (Colin de Verdière, 1990)

- $\mu(\Gamma) \leq 1$ if and only if Γ is a path;
- $\mu(\Gamma) \leq 2$ if and only if Γ is outerplanar;
- $\mu(\Gamma) \leq 3$ if and only if Γ is planar.

A graph is *linkless embeddable* if it can be embedded in \mathbb{R}^3 so that any two disjoint circuits in Γ form unlinked closed curves in \mathbb{R}^3 . Graphs satisfying $\mu(\Gamma) \leq 4$ are exactly the linkless embeddable graphs [28].

Colin de Verdière's planarity characterisation of graphs is a remarkable result, which will be important for us. The "only if" part is relatively simple and follows from Kuratowski's characterisation of the planar graphs [19]. The original proof of the "if" part was quite involved. Van der Holst [46] substantially simplified it and showed that for 3-connected planar graphs the Strong Arnold property does not play any role.

Theorem 5.3. (Van der Holst, 1995 [46]) *For any matrix M from \mathcal{M}_Γ the corank of M can not be larger than 3.*

Before we come to the proof we recall some necessary definitions and concepts.

A subgraph H is a *minor* of a graph Γ (denoted by $H \leq \Gamma$) if H can be obtained by removing and contracting edges from Γ .

Y. Colin de Verdière showed that the graph parameter $\mu(\Gamma)$ is *minor-monotone*. In fact, it is the minor-monotonicity that makes these parameters very useful. A good overview of the results on different graph-theoretic properties of $\mu(\Gamma)$ can be found in [47].

A graph Γ is said to be *bipartite* if its vertices can be partitioned into two subsets such that each edge of Γ connects a vertex from one subset with a vertex from the second subset. Γ is *complete bipartite* if each vertex from one subset is adjacent to each vertex of the second subset. The common notation for such type of graphs is $K_{m,n}$ where m and n are the number of vertices in the two subsets.

A graph Γ is said to be *complete* if every pair of distinct vertices of Γ is connected by a unique edge.

Let from now on Γ be a (3-connected) planar graph and $M_{CdV} \in \mathcal{M}_\Gamma$ a corresponding Colin de Verdière matrix. Note that Γ remains planar after removing an edge from it. It also remains planar if we contract an edge $(i, j) \in \mathcal{E}(\Gamma)$ to one vertex. It follows that every minor of a planar graph is again planar. A characterisation of the class of planar graphs in terms of *excluded minors* was given by Kuratowski.

Theorem 5.4. (Kuratowski) *A graph Γ is embeddable in the plane if and only if it does not contain a subgraph homeomorphic to the complete graph K_5 or the complete bipartite graph $K_{3,3}$.*

For any vector $x \in \mathbb{R}^n$ the set $\text{supp}(x) = \{i \in \mathcal{V} \mid x_i \neq 0\}$ is called *the support* of x . The subsets $\text{supp}^+(x) = \{i \in \mathcal{V} \mid x_i > 0\}$ and $\text{supp}^-(x) = \{i \in \mathcal{V} \mid x_i < 0\}$ are the so-called *positive* and the *negative support* of x , respectively. Consider a matrix $M \in \mathcal{M}_\Gamma$ and a null space vector $x \in \ker(M)$. Up to scaling, the eigenvector π belonging to the negative eigenvalue of M is positive and orthogonal to x . This implies that both subsets $\text{supp}^+(x)$ and $\text{supp}^-(x)$ are non-empty.

Let $x \in \ker(M)$, $x \neq 0$ be a null space vector such that for each $y \in \ker(M)$, $y \neq 0$ with $\text{supp}(y) \subseteq \text{supp}(x)$ the equality $\text{supp}(y) = \text{supp}(x)$ holds. Then x is said to have *minimal support*.

Let further for any subset $\mathcal{U} \subseteq \mathcal{V}$ the subset of all vertices $i \in \mathcal{V} \setminus \mathcal{U}$ adjacent to at least one of the vertices $i \in \mathcal{U}$ be denoted by $N(\mathcal{U})$. Then each node in $N(\text{supp}(x))$ belongs to both, the negative and the positive support of x .

We are now ready to present the lemma used by Van der Holst in his proof of the planarity characterisation [46].

Lemma 5.5. (Van der Holst) [46] *Let Γ be connected, let $M \in \mathcal{M}_\Gamma$ and let $x \in \ker(M)$ have minimal support. Then both $\text{supp}^+(x)$ and $\text{supp}^-(x)$ are nonempty and induce connected subgraphs of Γ .*

The following is the reproduced version of the proof of Colin de Verdière's planarity characterisation given by Van der Holst.

The parameter $\mu(\Gamma)$ does not increase after deleting edges from Γ . Therefore, we may assume that Γ is maximally planar. Then Γ has at least one triangular face f . Let a, b and c denote the vertices of f . Assume that the corank of a matrix $M_{CdV} \in \mathcal{M}_\Gamma$ is greater than or equal to 4. Let $v \in \text{Ker}(M_{CdV})$ be a nonzero null space vector with minimal support such that $v_a = v_b = v_c$. Then $\Gamma|_{\text{supp}^+(v)}$ and $\Gamma|_{\text{supp}^-(v)}$ are nonempty and connected.

Let d be any vertex for which $v_d > 0$. From the three-connectivity of Γ follows that it contains three vertex-disjoint paths from d to each of the vertices a, b , and c . Now, as $v_d > 0$ and $v_a = 0$, there is a vertex a' on the path from d to a for which $v_{a'} = 0$. Moreover a' has a neighbor a^+ for which $v_{a^+} > 0$ is true. a' also has a neighbor a^- for which $v_{a^-} < 0$ holds. Similar vertices exist for b and c .

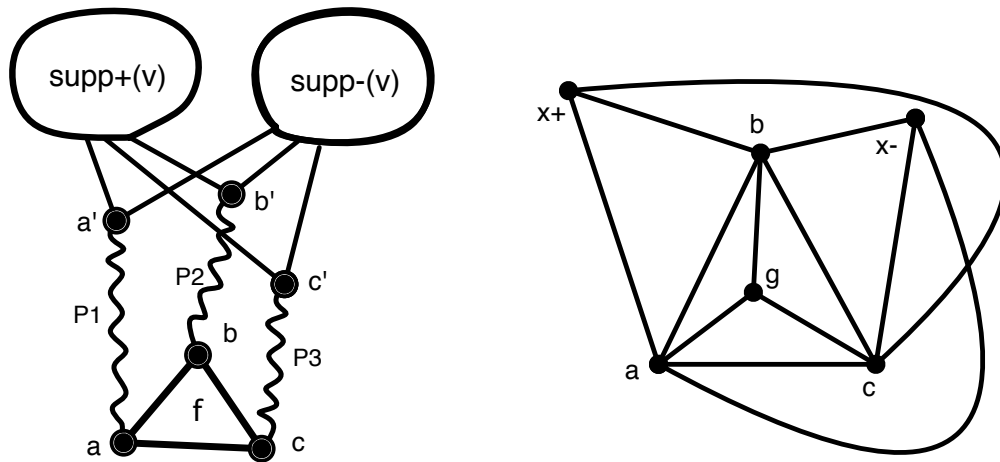


FIGURE 5.1: Holst planarity

A subgraph of Γ can be constructed through contraction of every edge on the path from a to a' , as well as on the path from b to b' and on the path from c to c' . Moreover, all the vertices for which v is positive and all the vertices for which v is negative can be contracted. This is possible due to the fact that both sets are connected. Contract then every edge in the face f not involving vertices a, b , or c . In this way the graph we obtain has a triangular face (a, b, c) such that each of the vertices a, b , and c have an edge to one positive and one negative vertex.

The graph obtained in such way is not planar. To see this, add one vertex g inside the face and connect it to each of a, b , and c . This does not effect planarity. But

the obtained graph contains $K_{3,3}$ as subgraph. Hence Γ cannot be planar and we have a contradiction. The corank of M_{CdV} is therefore 3. This proves Theorem 5.3.

The "only if" part of Colin de Verdière's planarity characterisation follows from the fact that $\mu(K_5) = \mu(K_{3,3}) = 4$ and from minor monotonicity of μ .

In [27] Lovász found an explicit way of constructing Colin de Verdière matrix for any 3-connected planar graph Γ using the Steinitz' realisation of Γ as 1-skeleton of a convex polyhedron P . This result will be crucial for us, so we will sketch here the main steps of his construction following [27].

Recall first the notion of polarity for polyhedra in \mathbb{R}^3 , see e.g. [56]. Let P be any convex polytope in \mathbb{R}^3 , containing the origin in its interior. The *polar polyhedron* P^* is defined as

$$P^* = \{y \in \mathbb{R}^3 : (y, x) \leq 1 \text{ for all } x \in P\},$$

where $(,)$ denote the scalar product in \mathbb{R}^3 . It is known that P^* is also a convex polyhedron and the 1-skeleton of P^* is the planar dual graph $\Gamma^* = (\mathcal{V}^*, \mathcal{E}^*)$ with vertices corresponding to the faces of P and edges corresponding to edges of P [56].

Now let $P \subset \mathbb{R}^3$ be Steinitz' realisation of graph Γ , so that Γ is isomorphic to 1-skeleton $\Gamma(P)$. We can always assume that P contains the origin inside it. Consider its polar polyhedron P^* .

Let u_i and u_j be two adjacent vertices of P , and w_f and w_g be the endpoints of the corresponding edge of P^* . Then by the definition of polarity we have

$$(w_f, u_i) = (w_g, u_i) = 1.$$

This implies that $w_f - w_g$ is perpendicular to u_i , and similarly to u_j . Hence the vectors $w_f - w_g$ and the cross-product $u_i \times u_j$ are parallel and we can find the coefficients M_{ij} such that

$$w_f - w_g = M_{ij}(u_i \times u_j).$$

We can always choose the labelling of w_f and w_g in such a way that $M_{ij} < 0$.

This defines M_{ij} for adjacent $i \neq j$. For non-adjacent i and j we define M_{ij} to be zero. To define M_{ii} consider the vector

$$u'_i = \sum_{j \sim i} M_{ij} u_j.$$

Then

$$u_i \times u'_i = \sum_{j \sim i} M_{ij} u_i \times u_j = \sum (w_f - w_g),$$

where the last sum is taken over all edges fg of the face of P^* corresponding to i , oriented counterclockwise. Since this sum is zero we have

$$u_i \times u'_i = 0,$$

which means that u_i and u'_i are parallel. Therefore we can define M_{ii} by the relation

$$u'_i = -M_{ii} u_i.$$

Theorem 5.6. (Lovász, 2000) *The matrix M described above is a Colin de Verdière matrix for the graph Γ .*

Proof. Indeed by construction M has the right pattern of zeros and negative elements. The condition $u'_i = -M_{ii} u_i$ can be written in the following form

$$\sum_j M_{ij} u_j = 0.$$

This means that each coordinate of the u_i defines a vector in the kernel of M and hence M has corank at least 3. But by 5.3 it can not be larger than 3, so the corank is 3 and thus maximal.

To prove that M has exactly one negative eigenvalue one can use the classical Perron-Frobenius theorem: Choosing sufficiently large $c > 0$ we have the matrix $cI - M$, which has non-negative entries and is irreducible, so we can apply the Perron-Frobenius Theorem to conclude that the smallest eigenvalue of M has multiplicity 1. It must be negative since we know that 0 has multiplicity at least 3. The fact that there are no more negative multiplicities requires a bit of work using the connectivity of the space of Steinitz' realisations, see [27]. \square

Conversely, having a Colin de Verdière matrix $M \in \mathcal{M}_\Gamma$ one can consider the following *null space representation* $\nu : \mathcal{V} = \{1, 2, \dots, n\} \rightarrow \mathbb{R}^3$ (see [29]).

Choose a basis a_1, a_2, a_3 in the kernel of M and consider $3 \times n$ matrix X with rows being the coordinates of a_1, a_2, a_3 . Then the columns $u_i, i = 1, \dots, n$ of this matrix give the set of 3-vectors, defining the map ν . The problem is that in general they will not be vertices of a convex polyhedron, but Lovász [27] showed that after some scaling $u_i \rightarrow \mu_i u_i$ this is the case (such a scaling he called *proper*). At the level of the Colin de Verdière matrices this corresponds to the change $M \rightarrow DMD$, where $D = \text{diag}(\mu_1, \dots, \mu_n)$ is a non-degenerate diagonal matrix, which obviously preserves the properties of \mathcal{M}_Γ .

Theorem 5.7. (Lovász, 2000) *For a 3-connected planar graph Γ any Colin de Verdière matrix $M \in \mathcal{M}_\Gamma$ can be properly scaled, so that null space representation gives a convex polyhedron with 1-skeleton isomorphic to Γ .*

Note that the change of basis in the kernel of M corresponds to a linear transformation of \mathbb{R}^3 , so the corresponding polyhedron is defined only modulo affine transformation.

The eigenspace realisation offers an interesting interpretation of an eigenvalue problem as a graph realisation problem. Realisations derived from the spectrum of the generalised Laplacian M are closely related to the structural properties of the graph. The multiplicities of the eigenvalues of a matrix representation of a graph usually correspond to graph's symmetries. An interesting result in this direction was obtained by Mowshowitz [35], who showed that if all eigenvalues of the adjacency matrix A of a graph are different, then every automorphism of A has order 1 or 2. In general, higher multiplicities serve as indication for degree of symmetry in the underlying graph.

Note that there are plenty of polyhedra P with G -invariant combinatorial structures, which can be constructed from the Platonic solids using Conway operations [7]. In particular, one will have a simplicial polyhedron by applying to any such P the operation, which Conway called *kis* and denoted k , consisting of building the pyramids on all the faces.

Now we are ready to prove our main result.

5.3 Proof of Theorem 4.6

Let G be a Platonic group and Γ a G -invariant planar 3-connected graph.

We know after Steinitz that Γ can be realised by a 3-dimensional convex polyhedron P . There exist several modifications of Steinitz's original proof differing in the used reduction methods. One of those modifications has been used to show that a graph Γ with certain automorphisms has a geometric realisation P in Steinitz's sense which admits isometric symmetries that correspond to the automorphisms of Γ . For the full group of automorphisms of Γ this is the following result by Mani [30].

Theorem 5.8. (Mani, 1971) *There exists a convex polyhedron $P_G \subset \mathbb{R}^3$ with the group of isometries isomorphic to G and with 1-skeleton isomorphic to Γ .*

Since Γ is planar and 3-connected, its Colin de Verdière invariant $\mu(\Gamma)$ must be 3. Let M be the Colin de Verdière matrix given by Lovasz construction applied to Mani's version of Steinitz realisation P_G .

Let N be the normalised adjacency matrix (5.2). We know that the matrix of the Buffon transformation B is related to N by

$$B = \frac{1}{2}D^{-\frac{1}{2}}(I + N)D^{\frac{1}{2}}$$

and that its largest eigenvalue is $\lambda_0 = 1$. Let λ_1 be the second largest eigenvalue of B . We would like to show that it has multiplicity 3.

To do this consider the symmetric matrix

$$\widehat{B} = -\frac{1}{2}N + \left(\lambda_1 - \frac{1}{2}\right)I.$$

It is easy to see that $\widehat{B} \in \mathcal{M}_\Gamma$ and that the corank of \widehat{B} is precisely the multiplicity of λ_1 .

Define a parameter family of matrices

$$M_t = (1 - t)M - t\widehat{B}, \quad t \in [0, 1] \tag{5.3}$$

where M is the Colin de Verdière matrix defined above.

Since M_t is G -invariant, the group G acts on the kernel of M_t . When $t = 0$ we know that the kernel of $M(0) = M$ has dimension 3 and by Lovasz result [27] the corresponding representation of G is standard geometric by the isometries of P_G .

Since this representation is irreducible and the set of 3-dimensional representations of G is discrete, by continuity arguments the kernel will remain 3-dimensional geometric representation for all $t \in [0, 1]$, in particular for $t = 1$.

These arguments will not work only if 0 collides with another eigenvalue. But this could not happen with the negative eigenvalue because of Perron-Frobenius theorem. In particular, all matrices M_t belong to \mathcal{M}_Γ . If this happens with a positive eigenvalue we will have the corank of the corresponding M_t to be at least 4, which contradicts the Colin de Verdière result.

Thus we have proved that the kernel of $M_1 = -\widehat{B}$ is 3-dimensional, and hence the same is true for the subdominant eigenspace of the Buffon operator B . The limiting shape is given essentially by the null space representation construction, but the proper scaling may not hold. However, the very existence of a proper scaling [27, 29] and the assumption of simplicity imply that the corresponding vectors u_i are the vertices of a certain star-shaped polyhedron with 1-skeleton isomorphic to Γ . The triakis example on Fig.1 shows that the proper scaling is indeed not automatic, so the convexity property is not necessary holds. This completes the proof of Theorem 4.6.

5.4 On the symmetry assumption

In [50] the effect of the Buffon procedure applied to prisms and anti-prisms was studied. Taking a general prism with upper and lower faces having n nodes the analysis the spectrum of the corresponding Buffon matrix B gives following results.

The eigenvalues of B split into two groups:

$$\lambda_r - \frac{1}{6} \quad \lambda_r + \frac{1}{6} \quad r = 1, 2, \dots, n$$

Writing these in order of magnitude (with multiplicities) gives for the $\lambda_r - \frac{1}{6}$:

$$\left[\frac{4}{6}^{(1)}, (\lambda_1 - \frac{1}{6})^{(2)}, \dots, (\lambda_{(n-1)/2} - \frac{1}{6})^{(2)} \right] \quad n \text{ odd}$$

$$\left[\frac{4}{6}^{(1)}, (\lambda_1 - \frac{1}{6})^{(2)}, \dots, (\lambda_{(n/2-1)} - \frac{1}{6})^{(2)}, 0^{(1)} \right] \quad n \text{ even}$$

And for the $\lambda_r + \frac{1}{6}$ set follows:

$$[1^{(1)}, (\lambda_1 + \frac{1}{6})^{(2)}, \dots, (\lambda_{(n-1)/2} + \frac{1}{6})^{(2)}] \quad n \text{ odd}$$

$$[1^{(1)}, (\lambda_1 + \frac{1}{6})^{(2)}, \dots, (\lambda_{(n/2-1)} + \frac{1}{6})^{(2)}, \frac{1}{6}^{(1)}] \quad n \text{ even}$$

If an eigenvalue has multiplicity 3 it may occur in both sets. An eigenvalue of multiplicity 3 with maximum modulus (other than 1) will only occur if the first eigenvalue from the first set matches with the second eigenvalue of the second set. This gives

$$\cos \frac{2\pi}{n} = 0 \quad \text{implying } n = 4$$

This corresponds to the cube which is one of the regular polyhedra.

For an eigenvalue of less than maximum modulus a match will occur if

$$\cos \frac{2\pi k}{n} = 0 \quad k = 2, 3, \dots, n \text{ implying } n = 4, 8, 12, \dots$$

This again corresponds to the cube (obtained by coalescing nodes). [50] conclude from this that apart from the cube, a prism is not naturally interpreted by the Buffon matrix as a three dimensional object.

The same approach was used for anti-prisms. The eigenvalues of the Buffon matrix B are of the form

$$\frac{1}{2} + \frac{1}{4} \left(\cos \frac{\pi r}{n} + \cos \frac{2\pi r}{n} \right) \quad r = 1, 2, \dots, 2n$$

The eigenvalues $r = k$ and $r = 2n - k$ for $k = 1, 2, \dots, n - 1$ have the same magnitude giving multiplicity 2. However the eigenvalue $r = n$ may have magnitude equal to one of these pairs. In this case the multiplicity will be 3. This will occur if

$$\cos \frac{\pi r}{n} + \cos \frac{2\pi r}{n} = 0$$

If $c = \cos \frac{\pi r}{n}$ then we require

$$2c^2 + c - 1 = 0 \quad \text{giving} \quad c = \frac{1}{2}$$

This implies n is divisible by 3. The remaining eigenvalue $r = 2n$ has value 1.

The authors conclude that of all the anti-prisms only those for which n is divisible by 3 gives rise to a three-dimensional object. This is the octahedron.

The eigenvalues of largest magnitude, other than 1, are

$$\lambda_1 = \lambda_{2n-1} = \frac{1}{2} + \frac{1}{4}(\cos \frac{\pi}{n} + \cos \frac{2\pi}{n})$$

The corresponding eigenvectors are complex conjugate. As the number of Buffon transformations increases the *shape* of the iterated figure tends to an affine regular $2n$ th order polygon.

We conclude that the dihedral symmetry is not enough. The assumption of Platonic symmetry is essential.

Chapter 6

Representation theory and affine B-regular polyhedra

An interesting question is about the decomposition of $\mathcal{F}(\mathcal{V})$ into the irreducible G -modules with respect to the Buffon spectrum. We saw that the geometric representation always appears at the subdominant level, but we do not know much about higher level.

6.1 The symmetry groups of Platonic solids and their characters

The symmetry group of a regular tetrahedron is S_4 and is isomorphic to the permutation group of the vertices.

The full symmetry group of the octahedron is the same as for the cube: $G = S_4 \times \mathbb{Z}_2$. S_4 is the rotation subgroup, which is isomorphic to the permutation group of the 4 long diagonals, and \mathbb{Z}_2 corresponds to the central symmetry of cube.

For the icosahedron and dodecahedron the full symmetry group is known to be $A_5 \times \mathbb{Z}_2$, where $A_5 \subset S_5$ is the alternating subgroup of S_5 describing the rotational symmetry and \mathbb{Z}_2 is again the central symmetry of the solids.

24	1	6	8	6	3
S_4	1	(12)	(123)	(1234)	(12)(34)
U	1	1	1	1	1
U'	1	-1	1	-1	1
V	3	1	0	-1	-1
V'	3	-1	0	1	-1
W	2	0	-1	0	2

TABLE 6.1: The character table of S_4 .

60	1	20	15	12	12
A_5	1	(123)	(12)(34)	(12345)	(21345)
U	1	1	1	1	1
V	4	1	0	-1	-1
W	5	-1	1	0	0
Y	3	0	-1	$\frac{1+\sqrt{5}}{2}$	$\frac{1-\sqrt{5}}{2}$
Z	3	0	-1	$\frac{1-\sqrt{5}}{2}$	$\frac{1+\sqrt{5}}{2}$

TABLE 6.2: The character table of A_5 .

The irreducible representations of the group $G = H \times \mathbb{Z}_2$ have the form $V_1 \otimes V_2$, where V_1 and V_2 are irreducible representations of H and \mathbb{Z}_2 respectively. Note that V_2 is either trivial or sign representation of \mathbb{Z}_2 , which we will denote respectively by 1 and ε . Thus we need only the character tables of the groups S_4 and A_5 , which in the notations of Fulton and Harris [17] are given below in Tables 6.1 and 6.2.

With these notations the geometric representations are: V for tetrahedral group $G = S_4$, $\varepsilon V' = V' \otimes \varepsilon$ for cube/octahedral group $G = S_4 \times \mathbb{Z}_2$ and $\varepsilon Y = Y \otimes \varepsilon$ for icosahedral/dodecahedral group $G = A_5 \times \mathbb{Z}_2$.

The corresponding decompositions of the space of functions on the vertices into irreducible G -modules are

$$\mathcal{F}(T) = U \oplus V \tag{6.1}$$

for tetrahedron,

$$\mathcal{F}(O) = U \oplus \varepsilon V' \oplus W \tag{6.2}$$

for octahedron,

$$\mathcal{F}(C) = U \oplus \varepsilon V' \oplus V \oplus \varepsilon U' \tag{6.3}$$

for cube,

$$\mathcal{F}(I) = U \oplus \varepsilon Y \oplus W \oplus \varepsilon Z \tag{6.4}$$

for icosahedron,

$$\mathcal{F}(D) = U \oplus \varepsilon Y \oplus W \oplus \varepsilon V \oplus V \oplus \varepsilon Z \quad (6.5)$$

for dodecahedron.

We have ordered them according to the appearance in the spectrum of the Buffon operator. It turns out that in all these cases the spectral decomposition coincides with G -decomposition (see the examples below). Note that the first two are always trivial and geometric representations in agreement with our result.

6.2 Examples of Buffon realizations of polyhedra

For the polyhedra P with combinatorial structure of Platonic solids the Buffon procedure leads to the polyhedron P_B , which is affine equivalent to the regular realisation of P .

Since in the regular case the Buffon matrix B can be replaced by the adjacency matrix A the calculations are essentially the same as in [33], where one can find also the corresponding shapes. The calculation of spectra of regular polytopes can be found in [38].

We have used Mathematica to do all the calculations and pictures.

Platonic Solids

In this case we consider also the higher dimensional embeddings corresponding to other multiplicities to show the relation with G -decomposition.

The Tetrahedron

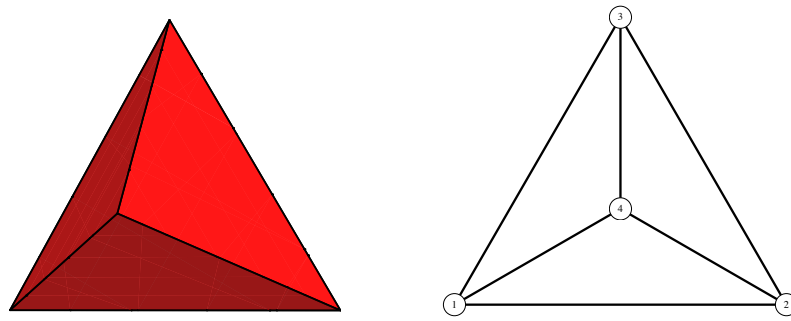


FIGURE 6.1: The tetrahedron and the corresponding 1-skeleton graph.

The corresponding Buffon eigenvalues denoted with multiplicities are:

$$\left\{ 1^{(1)}, \frac{1}{9}^{(3)} \right\}$$

in agreement with the decomposition (6.1).

The eigenspace corresponding to $\frac{1}{9}$ is

$$X = \begin{pmatrix} -\alpha - \beta - \gamma \\ \gamma \\ \beta \\ \alpha \end{pmatrix}$$

This corresponds to geometric representation V describing a general tetrahedron.

The Octahedron

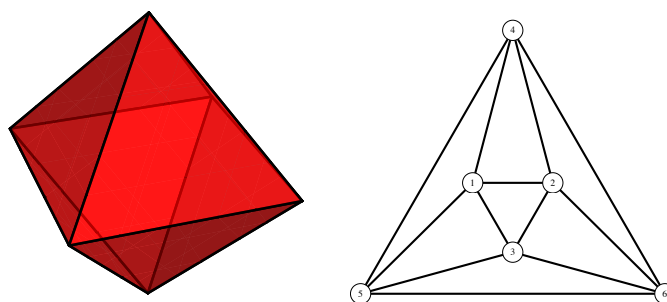


FIGURE 6.2: The octahedron and the corresponding 1-skeleton graph.

The Buffon spectrum denoted with multiplicities is:

$$\left\{ 1^{(1)}, \frac{1}{2}^{(3)}, \frac{1}{4}^{(2)} \right\}$$

in agreement with the decomposition (6.2).

The eigenspace corresponding to the second highest eigenvalue is

$$X = \begin{pmatrix} -\alpha \\ -\beta \\ -\gamma \\ \gamma \\ \beta \\ \alpha \end{pmatrix}$$

Geometrically this describes an affine regular octahedron.

The Cube

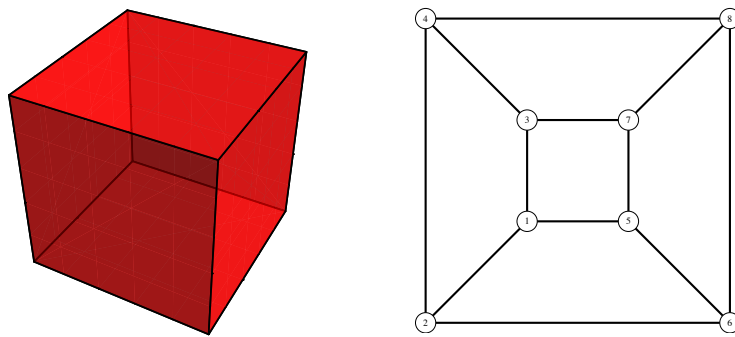


FIGURE 6.3: The cube and the corresponding 1-skeleton graph.

The corresponding Buffon eigenvalues denoted with multiplicities are:

$$\left\{ 1^{(1)}, \frac{2}{3}^{(3)}, \frac{1}{3}^{(3)}, 0^{(1)} \right\}$$

in agreement with the decomposition (6.3).

The eigenspaces corresponding to $\lambda_2 = \frac{2}{3}$ and $\lambda_3 = \frac{1}{3}$ are:

$$X_2 = \begin{pmatrix} -\alpha \\ -\beta \\ -\gamma \\ \alpha - \beta - \gamma \\ -\alpha + \beta + \gamma \\ \gamma \\ \beta \\ \alpha \end{pmatrix} \quad X_3 = \begin{pmatrix} \alpha \\ \beta \\ \gamma \\ -\alpha - \beta - \gamma \\ -\alpha - \beta - \gamma \\ \gamma \\ \beta \\ \alpha \end{pmatrix}$$

They correspond to geometric $\varepsilon V'$ and V representations respectively. Geometrically, X_2 describes an affine regular cube while in X_3 the opposite vertices coalesce together giving an affine tetrahedron. Note that in the second case the faces of cube are "broken", but in the first case they are not, which is a kind of miracle since the Buffon transformation breaks them generically already at the first step.

The Icosahedron

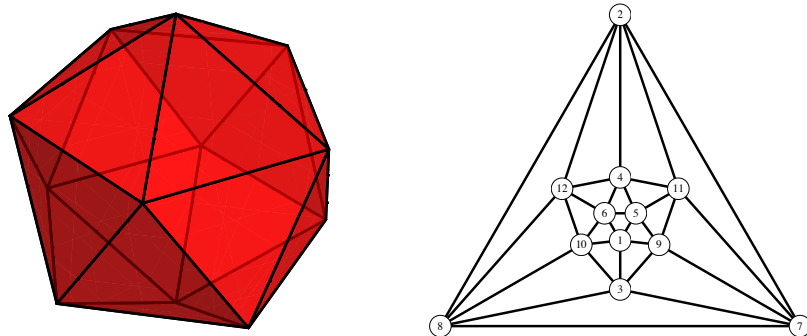


FIGURE 6.4: The icosahedron and the corresponding 1-skeleton graph.

The corresponding Buffon spectrum is:

$$\left\{ 1^{(1)}, \frac{1}{10} (5 + \sqrt{5})^{(3)}, \frac{2}{5}^{(5)}, \frac{1}{10} (5 - \sqrt{5})^{(3)} \right\}$$

in agreement with (6.4).

The eigenspaces corresponding to the second highest eigenvalue and its conjugate eigenvalue $\frac{1}{10}(5 - \sqrt{5})$ are:

$$X_2 = \begin{pmatrix} a(\alpha + \gamma) - \beta \\ \beta - a(\alpha + \gamma) \\ a(\beta - \gamma) - \alpha \\ a(\gamma - \beta) + \alpha \\ -\gamma \\ a(\beta - \alpha) - \gamma \\ a(\alpha - \beta) + \gamma \\ \gamma \\ -\alpha \\ -\beta \\ \beta \\ \alpha \end{pmatrix} \quad X_4 = \begin{pmatrix} b(\alpha + \gamma) - \beta \\ \beta - b(\alpha + \gamma) \\ b(\beta - \gamma) - \alpha \\ \alpha + b(\gamma - \beta) \\ -\gamma \\ b(\beta - \alpha) - \gamma \\ b(\alpha - \beta) + \gamma \\ \gamma \\ -\alpha \\ -\beta \\ \beta \\ \alpha \end{pmatrix},$$

where $a = \frac{1}{2}(1 - \sqrt{5})$ and $b = \frac{1}{2}(1 + \sqrt{5})$.

Geometrically, X_2 describes an affine regular icosahedron, while X_4 corresponds to an affine great icosahedron, which is one of four Kepler-Poinsot regular star polyhedra.

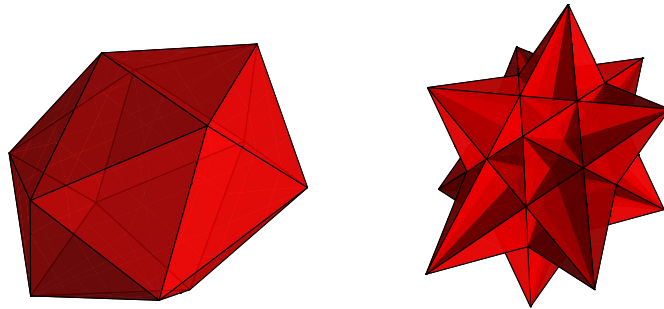


FIGURE 6.5: Affine B -regular icosahedron and great icosahedron.

The eigenspace X_3

$$X_3 = \begin{pmatrix} -\alpha - \beta - \gamma - \delta - \rho \\ -\alpha - \beta - \gamma - \delta - \rho \\ \rho \\ \rho \\ \gamma \\ \delta \\ \delta \\ \gamma \\ \alpha \\ \beta \\ \beta \\ \alpha \end{pmatrix}$$

describes the 5-dimensional realisation of an icosahedron as a 5-simplex: 6 pairs of opposite vertices identified with 6 vertices of the simplex.

The Dodecahedron

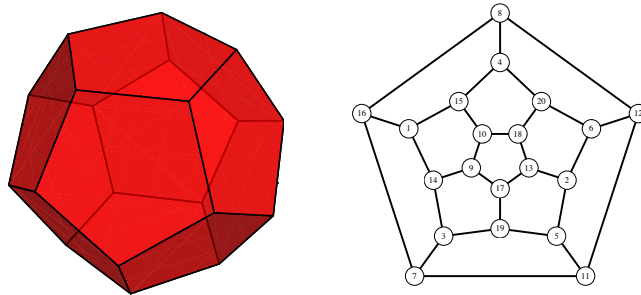


FIGURE 6.6: The dodecahedron and the dodecahedral 1-skeleton graph.

The corresponding Buffon spectrum is

$$\left\{ 1^{(1)}, \frac{1}{6} (3 + \sqrt{5})^{(3)}, \frac{2}{3}^{(5)}, \frac{1}{2}^{(4)}, \frac{1}{6}^{(4)}, \frac{1}{6} (3 - \sqrt{5})^{(3)} \right\}$$

in agreement with (6.5).

The eigenspaces corresponding to the second highest eigenvalue $\lambda_2 = \frac{1}{6} (3 + \sqrt{5})$ and to its conjugate $\lambda_6 = \frac{1}{6} (3 - \sqrt{5})$ are:

$$X_2 = \begin{pmatrix} -a\gamma - 2\alpha - b\beta \\ a\gamma + 2\alpha + b\beta \\ -\alpha \\ -\beta \\ b(\alpha + \beta) - \gamma \\ \sqrt{5}\alpha + \beta - \gamma \\ -\gamma \\ a(\beta - \alpha) - \gamma \\ a\beta - 2\alpha + b\gamma \\ b(\gamma - \alpha) - \beta \\ b(\alpha - \gamma) + \beta \\ -a\beta + 2\alpha - b\gamma \\ \beta - a(\alpha + \gamma) \\ -\sqrt{5}\alpha - \beta + \gamma \\ \gamma - b(\alpha + \beta) \\ a(\alpha + \gamma) - \beta \\ a(\alpha - \beta) + \gamma \\ \gamma \\ \beta \\ \alpha \end{pmatrix}, \quad X_6 = \begin{pmatrix} -a\beta - 2\alpha - b\gamma \\ a\beta + 2\alpha + b\gamma \\ -\alpha \\ -\beta \\ a(\alpha + \beta) - \gamma \\ -\sqrt{5}\alpha + \beta - \gamma \\ -\gamma \\ b(\beta - \alpha) - \gamma \\ a\gamma - 2\alpha + b\beta \\ a(\gamma - \alpha) - \beta \\ a(\alpha - \gamma) + \beta \\ -a\gamma + 2\alpha - b\beta \\ \beta - b(\alpha + \gamma) \\ \sqrt{5}\alpha - \beta + \gamma \\ \gamma - a(\alpha + \beta) \\ b(\alpha + \gamma) - \beta \\ b(\alpha - \beta) + \gamma \\ \gamma \\ \beta \\ \alpha \end{pmatrix},$$

where $a = \frac{1}{2}(1 - \sqrt{5})$ and $b = \frac{1}{2}(1 + \sqrt{5})$.

Geometrically, X_2 describes an affine regular dodecahedron, while X_6 corresponds to an affine version of the great stellated dodecahedron, which is another Kepler-Poinsot polyhedron (see Fig. 7).

It is interesting that the remaining two Kepler-Poinsot polyhedra (small stellated dodecahedron and great dodecahedron) do not appear in this way.

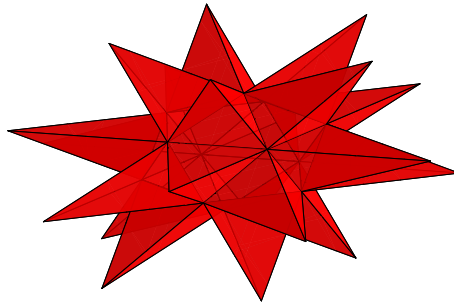


FIGURE 6.7: Affine great stellated dodecahedron.

The eigenspace X_3 corresponds to the 5-dimensional embedding of dodecahedron with "broken faces" given by

$$X_3 = \begin{pmatrix} -\gamma - \delta + \rho \\ -\gamma - \delta + \rho \\ \alpha \\ \beta \\ -\alpha + \beta - \delta \\ \alpha - \beta - \gamma \\ \gamma \\ \delta \\ -\beta + \delta - \rho \\ -\alpha + \gamma - \rho \\ -\alpha + \gamma - \rho \\ -\beta + \delta - \rho \\ \rho \\ \alpha - \beta - \gamma \\ -\alpha + \beta - \delta \\ \rho \\ \delta \\ \gamma \\ \beta \\ \alpha \end{pmatrix} .$$

The 4-dimensional eigenspaces X_4 and X_5 are respectively:

$$X_4 = \begin{pmatrix} \gamma + \delta \\ -\gamma - \delta \\ -\alpha \\ -\beta \\ \alpha - \delta \\ \beta - \gamma \\ -\gamma \\ -\delta \\ \alpha - \gamma - \delta \\ \beta - \gamma - \delta \\ -\beta + \gamma + \delta \\ -\alpha + \gamma + \delta \\ -\alpha - \beta + \gamma + \delta \\ \gamma - \beta \\ \delta - \alpha \\ \alpha + \beta - \gamma - \delta \\ \delta \\ \gamma \\ \beta \\ \alpha \end{pmatrix}, \quad X_5 = \begin{pmatrix} 2\alpha + 2\beta + \gamma + \delta \\ 2\alpha + 2\beta + \gamma + \delta \\ \alpha \\ \beta \\ -\alpha - 2\beta - \delta \\ -2\alpha - \beta - \gamma \\ \gamma \\ \delta \\ \alpha + \gamma - \delta \\ \beta - \gamma + \delta \\ \beta - \gamma + \delta \\ \alpha + \gamma - \delta \\ -\alpha - \beta - \gamma - \delta \\ -2\alpha - \beta - \gamma \\ -\alpha - 2\beta - \delta \\ -\alpha - \beta - \gamma - \delta \\ \delta \\ \gamma \\ \beta \\ \alpha \end{pmatrix}.$$

Since in the second case the opposite vertices are identified it corresponds to the representation V in agreement with (6.5).

Archimedean Solids

The Archimedean solids, also referred to as the semi-regular polyhedra, are the convex polyhedra which have a similar arrangement of nonintersecting regular convex polygons of two or more different types arranged in the same way about each vertex with all sides the same length. Solids with a dihedral group of symmetries (e.g., regular prisms and antiprisms) are not considered to be Archimedean solids. With this restriction there are 13 solids classified as Archimedean solids.

For Archimedean solids the affine B -regular version is in general different from the affine regular one as the following example shows.

The Truncated Cube

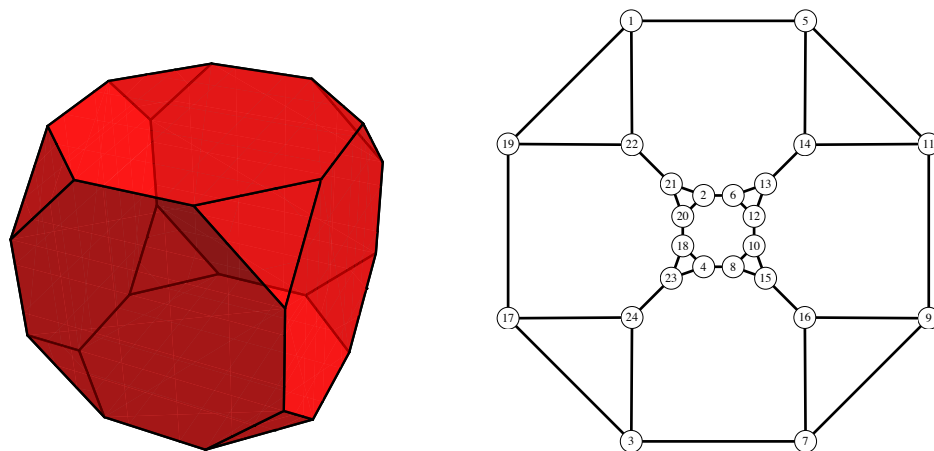


FIGURE 6.8: The truncated cube and the corresponding 1-skeleton graph.

The corresponding Buffon spectrum is:

$$\left\{ 1^{(1)}, \frac{1}{12} (7 + \sqrt{17})^{(3)}, \frac{5}{6}^{(3)}, \frac{2}{3}^{(1)}, \frac{1}{2}^{(5)}, \frac{1}{3}^{(3)}, \frac{1}{12} (7 - \sqrt{17})^{(3)}, \frac{1}{6}^{(5)} \right\}$$

The eigenspace corresponding to the second highest eigenvalue is:

$$X_2 = \begin{pmatrix} \frac{1}{8} ((\sqrt{17} - 1) (\alpha + 2\gamma) + (\sqrt{17} - 9) \beta) \\ \frac{1}{8} ((\sqrt{17} - 1) (3\beta + 2\gamma) - (7 + \sqrt{17}) \alpha) \\ \frac{1}{8} ((7 + \sqrt{17}) \alpha + (\sqrt{17} - 9) \beta + 2 (\sqrt{17} - 5) \gamma) \\ \frac{1}{8} (-\sqrt{17}\alpha + \alpha + 3 (\sqrt{17} - 1) \beta + 2 (\sqrt{17} - 5) \gamma) \\ \frac{1}{8} ((\sqrt{17} - 1) \alpha - 3 (\sqrt{17} - 1) \beta - 2 (\sqrt{17} - 5) \gamma) \\ \frac{1}{8} (-(7 + \sqrt{17}) \alpha - (\sqrt{17} - 9) \beta - 2 (\sqrt{17} - 5) \gamma) \\ \frac{1}{8} ((7 + \sqrt{17}) \alpha - (\sqrt{17} - 1) (3\beta + 2\gamma)) \\ \frac{1}{8} ((1 - \sqrt{17})\alpha - (\sqrt{17} - 9) \beta - 2 (\sqrt{17} - 1) \gamma) \\ \frac{1}{8} ((\sqrt{17} - 1) (3\alpha - 2\gamma) - (7 + \sqrt{17}) \beta) \\ \frac{1}{8} ((\sqrt{17} - 9) \alpha + (\sqrt{17} - 1) (\beta - 2\gamma)) \\ \frac{1}{8} (-(\sqrt{17} - 9) \alpha - (7 + \sqrt{17}) \beta + 2 (\sqrt{17} - 5) \gamma) \\ \frac{1}{8} ((\sqrt{17} - 1) (-3\alpha + \beta) + 2 (\sqrt{17} - 5) \gamma) \\ -\alpha \\ -\beta \\ -\gamma \\ \alpha - \beta - \gamma \\ \frac{1}{8} (3 (\sqrt{17} - 1) \alpha + (1 - \sqrt{17})\beta - 2 (\sqrt{17} - 5) \gamma) \\ \frac{1}{8} ((\sqrt{17} - 9) \alpha + (7 + \sqrt{17}) \beta - 2 (\sqrt{17} - 5) \gamma) \\ \frac{1}{8} (-(\sqrt{17} - 9) \alpha - (\sqrt{17} - 1) (\beta - 2\gamma)) \\ \frac{1}{8} ((\sqrt{17} - 1) (-3\alpha + 2\gamma) + (7 + \sqrt{17}) \beta) \\ -\alpha + \beta + \gamma \\ \gamma \\ \beta \\ \alpha \end{pmatrix},$$

The facing octagons of the geometric realisation of X_2 are not affine regular: one can check that $(x_{22} - x_{14}) = \frac{3+\sqrt{17}}{4}(x_1 - x_5)$ while for the regular octagon $(x_{22} - x_{14}) = (1 + \sqrt{2})(x_1 - x_5)$. Thus the affine B -regular truncated cube obtained by the Buffon procedure is not an affine version of the regular truncated cube.

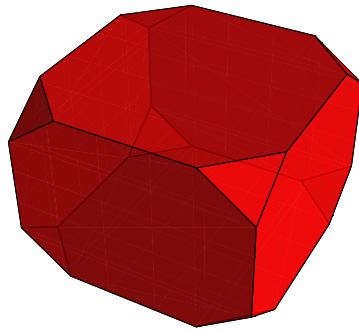
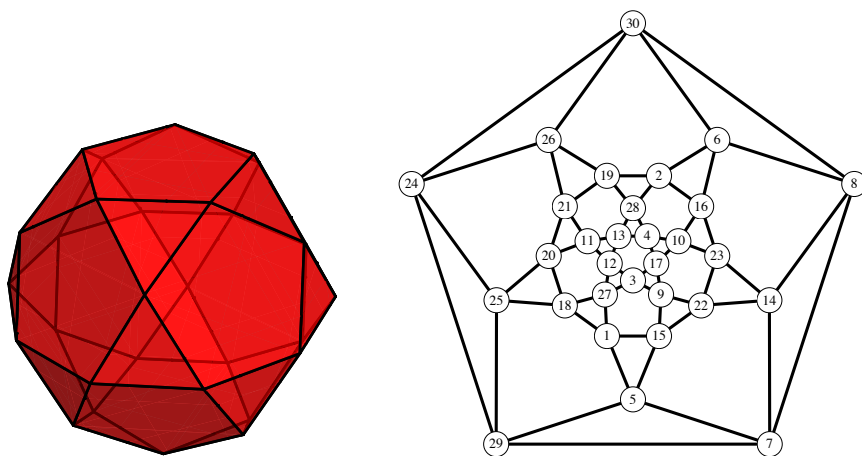
FIGURE 6.9: The affine B -regular truncated cube*The Icosidodecahedron*

FIGURE 6.10: The icosidodecahedron and the corresponding 1-skeleton graph.

Let A denote the adjacency matrix of the 1-skeleton graph and I_{30} the n -dimensional identity matrix. Then the Buffon transformation matrix for the icosidodecahedron has the form:

$$B = \frac{1}{8}A + \frac{1}{2}I_{30}$$

The corresponding eigenvalues are:

$$\left\{ 1^{(1)}, \frac{1}{8} \left(5 + \sqrt{5} \right)^{(3)}, \frac{3}{4}^{(5)}, \frac{5}{8}^{(4)}, \frac{3}{8}^{(4)}, \frac{1}{8} \left(5 - \sqrt{5} \right)^{(3)}, \frac{1}{4}^{(10)} \right\}$$

The eigenspace corresponding to the second highest eigenvalue is

$$X_2 = \begin{pmatrix} \beta - \alpha \\ \alpha - \beta \\ -\alpha \\ -\beta \\ -\gamma \\ a(\alpha - \beta) - \gamma \\ -a\gamma + \alpha - \beta \\ a(\alpha - \beta - \gamma) \\ -a(\beta + \gamma) \\ a(-\beta - \gamma) + \alpha - \beta \\ a(-\alpha + \beta + \gamma) + \beta + \gamma \\ a(-\alpha + \beta + \gamma) \\ a\gamma - \alpha + \beta \\ a(\alpha - \beta - \gamma) - \beta - \gamma \\ -a\gamma - \beta \\ a(\alpha - \beta - \gamma) - \beta \\ -a\beta - \gamma \\ a(-\alpha + \beta + \gamma) + \beta \\ a\gamma + \beta \\ a(-\alpha + 2\beta + \gamma) + \gamma \\ a(\beta + \gamma) - \alpha + \beta + \gamma \\ a(-\beta - \gamma) + \alpha - \beta - \gamma \\ a(\alpha - 2\beta - \gamma) - \gamma \\ a\beta + \gamma \\ a(\beta + \gamma) - \alpha + \beta \\ a(\beta + \gamma) \\ a(\beta - \alpha) + \gamma \\ \gamma \\ \beta \\ \alpha \end{pmatrix},$$

where $a = \frac{1}{2}(1 + \sqrt{5})$.

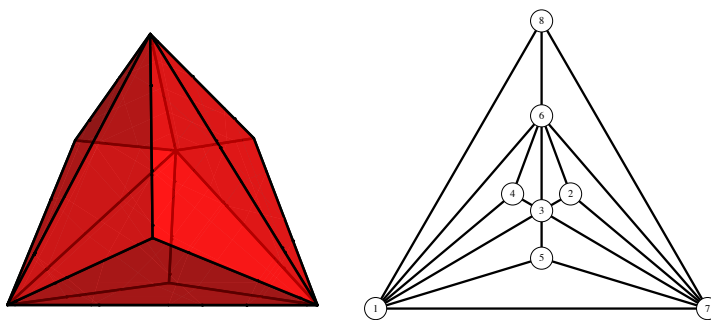
A direct computation shows that in this case the B -affine version coincides with the usual affine regular icosidodecahedron.

Catalan Solids

The 13 duals of the Archimedean solids are called the Catalan solids after the Belgian mathematician E. Catalan who described them first in 1865. The dual polyhedra is defined through polar reciprocation. The dual of an Archimedean solid can, for example, be obtained by connecting the points of the vertex figure, and constructing the polygon tangent to the circumcircle of the vertex figure. The Catalan solids are convex polyhedra with the following characteristics. The faces of a Catalan solid are not regular, but each vertex figure has only one type of face. The vertex figures are regular but not congruent. Each Catalan solid has one dihedral angle, but not the same number of edges meeting at each vertex.

For Catalan solids the affine B -regular versions may not be convex or, in non-simplicial case, may even not exist, as the following two examples show.

Triakis Tetrahedron



The corresponding Buffon eigenvalues are:

$$\left\{ 1^{(1)}, \frac{7}{12}^{(3)}, \frac{1}{3}^{(3)}, \frac{1}{4}^{(1)} \right\}$$

The eigenspaces corresponding to the eigenvalues $\lambda_2 = \frac{7}{12}$ and to $\lambda_3 = \frac{1}{3}$ are:

$$X_2 = \begin{pmatrix} \frac{\alpha}{2} - \beta - \gamma \\ -\alpha + 2\beta + 2\gamma \\ -\frac{\alpha}{2} \\ -2\beta \\ -2\gamma \\ \gamma \\ \beta \\ \alpha \end{pmatrix} \quad X_3 = \begin{pmatrix} -\alpha - \beta - \gamma \\ -\alpha - \beta - \gamma \\ \alpha \\ \beta \\ \gamma \\ \gamma \\ \beta \\ \alpha \end{pmatrix}$$

A particular geometric realisation derived from X_2 looks as follows:

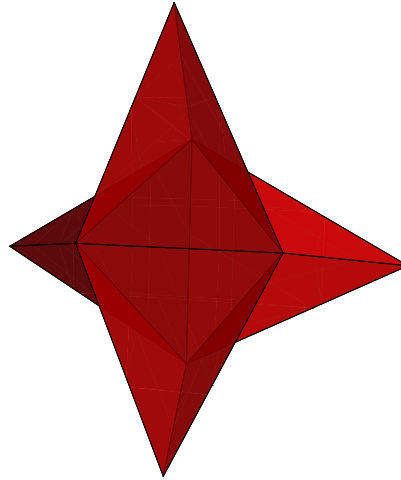


FIGURE 6.11: The affine B -regular version of the triakis tetrahedron is star-shaped but not convex.

As X_3 shows the vertices coalesce together pairwise. The corresponding geometrical realisation gives a general tetrahedron.

The Rhombic Dodecahedron

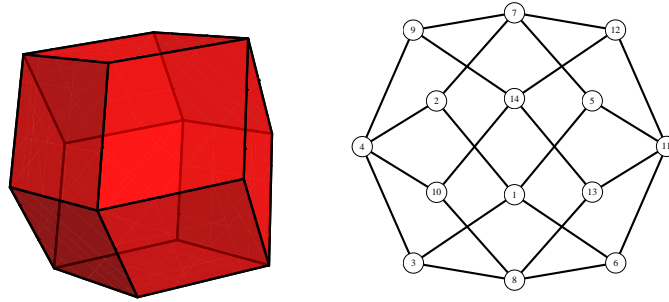


FIGURE 6.12: The rhombic dodecahedron and the corresponding 1-skeleton graph.

The corresponding eigenvalues are:

$$\left\{ 1^{(1)}, \frac{1}{6} (3 + \sqrt{3})^{(3)}, \frac{1}{2}^{(6)}, \frac{1}{6} (3 - \sqrt{3})^{(3)}, 0^{(1)} \right\}$$

The 3-dimensional eigenspaces corresponding to the eigenvalues $\lambda_2 = \frac{1}{6} (3 + \sqrt{3})$ and $\lambda_4 = \frac{1}{6} (3 - \sqrt{3})$ are:

$$X_2 = \begin{pmatrix} -\alpha \\ -\beta \\ -\gamma \\ \alpha - \frac{\sqrt{3}\beta}{2} - \frac{\sqrt{3}\gamma}{2} \\ \gamma - \frac{2\alpha}{\sqrt{3}} \\ \beta - \frac{2\alpha}{\sqrt{3}} \\ \frac{\sqrt{3}\gamma}{2} - \frac{\sqrt{3}\beta}{2} \\ \frac{\sqrt{3}\beta}{2} - \frac{\sqrt{3}\gamma}{2} \\ \frac{2\alpha}{\sqrt{3}} - \beta \\ \frac{2\alpha}{\sqrt{3}} - \gamma \\ -\alpha + \frac{\sqrt{3}\beta}{2} + \frac{\sqrt{3}\gamma}{2} \\ \gamma \\ \beta \\ \alpha \end{pmatrix} \quad X_4 = \begin{pmatrix} -\alpha \\ -\beta \\ -\gamma \\ \alpha + \frac{\sqrt{3}\beta}{2} + \frac{\sqrt{3}\gamma}{2} \\ \frac{2\alpha}{\sqrt{3}} + \gamma \\ \frac{2\alpha}{\sqrt{3}} + \beta \\ \frac{\sqrt{3}\beta}{2} - \frac{\sqrt{3}\gamma}{2} \\ \frac{\sqrt{3}\gamma}{2} - \frac{\sqrt{3}\beta}{2} \\ -\frac{2\alpha}{\sqrt{3}} - \beta \\ -\frac{2\alpha}{\sqrt{3}} - \gamma \\ -\alpha - \frac{\sqrt{3}\beta}{2} - \frac{\sqrt{3}\gamma}{2} \\ \gamma \\ \beta \\ \alpha \end{pmatrix}$$

Both eigenspaces, X_2 and X_4 , fail to correspond to a polyhedron with the combinatorial structure of the 1-skeleton of the rhombic dodecahedron. A particular graph realisation obtained from the eigenspace X_2 looks as follows:

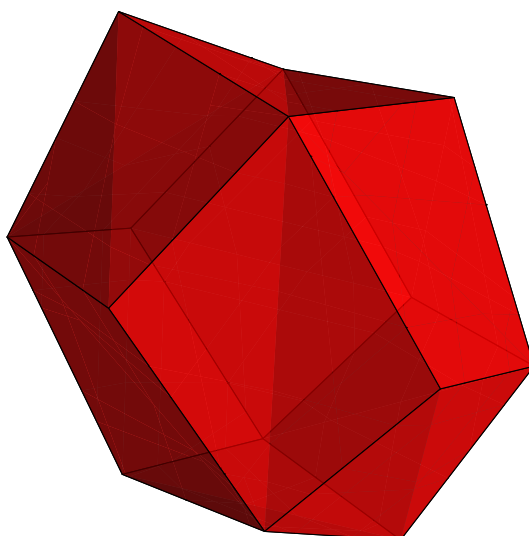


FIGURE 6.13: Eigenspace realisation of the rhombic dodecahedral graph derived from the eigenspace X_2 . All "faces" are non-planar.

The Triakis Octahedron

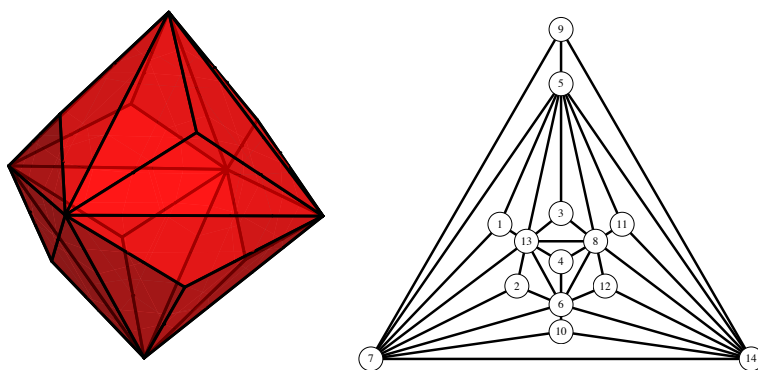


FIGURE 6.14: The triakis octahedron and the corresponding 1-skeleton graph.

The corresponding Buffon eigenvalues are:

$$\left\{ 1^{(1)}, \frac{1}{12} (6 + \sqrt{6})^{(3)}, \frac{1}{2}^{(4)}, \frac{3}{8}^{(2)}, \frac{1}{12} (6 - \sqrt{6})^{(3)}, \frac{1}{4}^{(1)} \right\}$$

The 3-dimensional eigenspaces corresponding to the eigenvalues λ_2 and λ_5 are:

$$X_2 = \begin{pmatrix} -\beta \\ -\gamma \\ \gamma - 2\sqrt{\frac{2}{3}}\alpha \\ \beta - 2\sqrt{\frac{2}{3}}\alpha \\ \frac{1}{2}\sqrt{\frac{3}{2}}(\gamma - \beta) \\ \frac{1}{2}\sqrt{\frac{3}{2}}(\beta - \gamma) \\ \alpha - \frac{1}{2}\sqrt{\frac{3}{2}}(\beta + \gamma) \\ \frac{1}{4}(\sqrt{6}(\beta + \gamma) - 4\alpha) \\ 2\sqrt{\frac{2}{3}}\alpha - \beta \\ 2\sqrt{\frac{2}{3}}\alpha - \gamma \\ \gamma \\ \beta \\ -\alpha \\ \alpha \end{pmatrix} \quad X_5 = \begin{pmatrix} -\beta \\ -\gamma \\ 2\sqrt{\frac{2}{3}}\alpha + \gamma \\ 2\sqrt{\frac{2}{3}}\alpha + \beta \\ \frac{1}{2}\sqrt{\frac{3}{2}}(\beta - \gamma) \\ \frac{1}{2}\sqrt{\frac{3}{2}}(\gamma - \beta) \\ \alpha + \frac{1}{2}\sqrt{\frac{3}{2}}(\beta + \gamma) \\ \frac{1}{4}(-4\alpha - \sqrt{6}(\beta + \gamma)) \\ -2\sqrt{\frac{2}{3}}\alpha - \beta \\ -2\sqrt{\frac{2}{3}}\alpha - \gamma \\ \gamma \\ \beta \\ -\alpha \\ \alpha \end{pmatrix}$$

Geometrically, X_2 corresponds to a non-convex star shaped polyhedron. The geometric realisation derived from the eigenspace X_5 is self-intersecting:

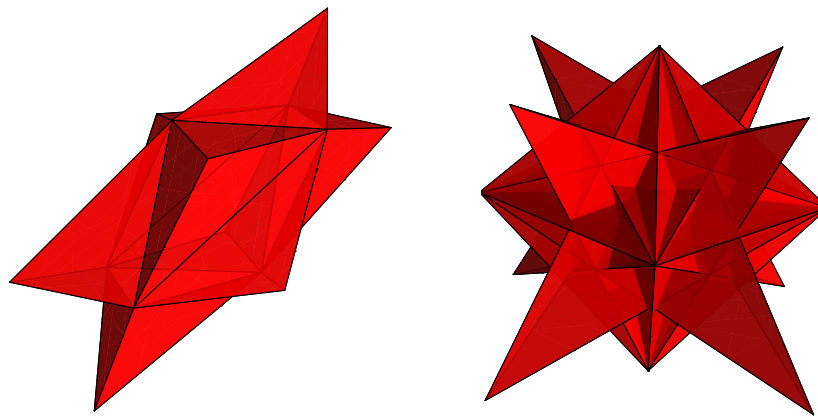


FIGURE 6.15: Affine B -regular triakis octahedron and the geometric realisation derived from the eigenspace X_5 .

Further examples

Small Rhombicuboctahedron

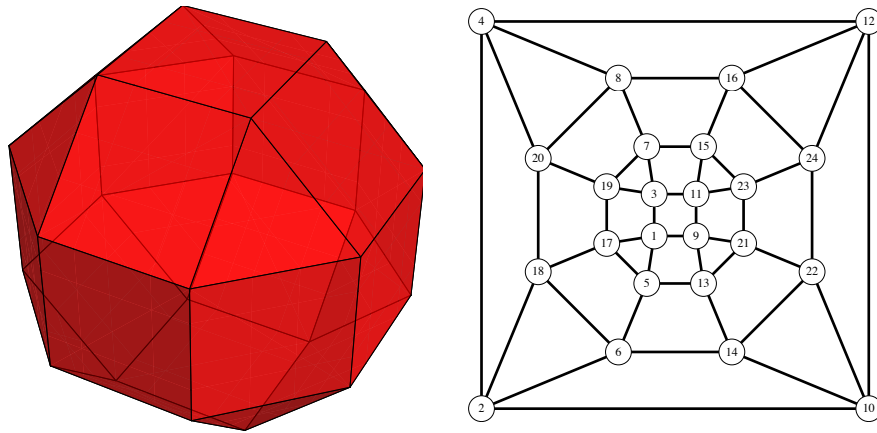


FIGURE 6.16: The small rhombicuboctahedron and the corresponding 1-skeleton graph.

The eigenvalues of the Buffon matrix (denoted with their multiplicities) are:

$$\left\{ 1^{(1)}, \frac{7}{8}^{(3)}, \frac{1}{16} \left(7 + \sqrt{17} \right)^{(3)}, \frac{5}{8}^{(2)}, \frac{1}{2}^{(4)}, \frac{1}{2}^{(3)}, \frac{3}{8}^{(6)}, \frac{1}{16} \left(7 - \sqrt{17} \right)^{(3)}, \frac{1}{8}^{(2)} \right\}$$

The eigenspace X_2 corresponding to the second highest eigenvalue is:

$$X_2 = \begin{pmatrix} -\frac{3\alpha}{2} + \frac{3\beta}{4} + \frac{\gamma}{4} \\ \frac{\alpha}{2} - \frac{5\beta}{4} + \frac{\gamma}{4} \\ -\frac{\alpha}{2} + \frac{3\beta}{4} - \frac{3\gamma}{4} \\ \frac{3\alpha}{2} - \frac{5\beta}{4} - \frac{3\gamma}{4} \\ -\frac{3\alpha}{2} + \frac{\beta}{4} + \frac{3\gamma}{4} \\ -\frac{\alpha}{2} - \frac{3\beta}{4} + \frac{3\gamma}{4} \\ \frac{\alpha}{2} + \frac{\beta}{4} - \frac{5\gamma}{4} \\ \frac{3\alpha}{2} - \frac{3\beta}{4} - \frac{5\gamma}{4} \\ -\frac{3\alpha}{2} + \frac{5\beta}{4} + \frac{3\gamma}{4} \\ \frac{\alpha}{2} - \frac{3\beta}{4} + \frac{3\gamma}{4} \\ -\frac{\alpha}{2} + \frac{5\beta}{4} - \frac{\gamma}{4} \\ \frac{3\alpha}{2} - \frac{3\beta}{4} - \frac{\gamma}{4} \\ -\frac{3\alpha}{2} + \frac{3\beta}{4} + \frac{5\gamma}{4} \\ -\frac{\alpha}{2} - \frac{\beta}{4} + \frac{5\gamma}{4} \\ \frac{\alpha}{2} + \frac{3\beta}{4} - \frac{3\gamma}{4} \\ \frac{3\alpha}{2} - \frac{\beta}{4} - \frac{3\gamma}{4} \\ -\alpha \\ -\beta \\ -\gamma \\ \alpha - \beta - \gamma \\ -\alpha + \beta + \gamma \\ \gamma \\ \beta \\ \alpha \end{pmatrix}$$

The affine B -regular small rhombicuboctahedron obtained by the Buffon procedure is not an affine version of the small rhombicuboctahedron.

Fig. 6.17 shows one particular realisation.

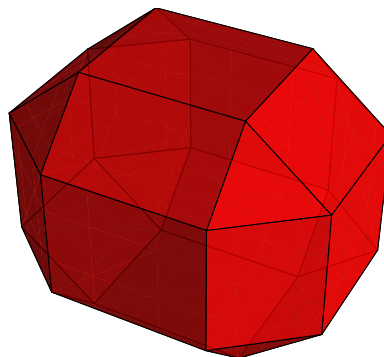
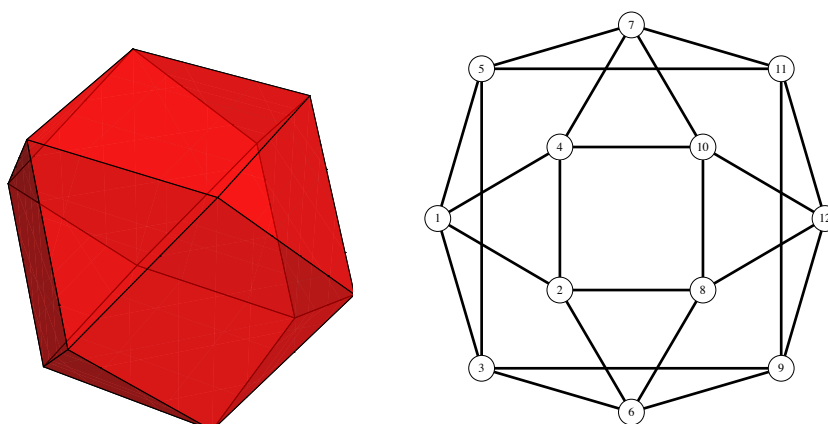
FIGURE 6.17: The affine B -regular small rhombicuboctahedron*The Cuboctahedron*

FIGURE 6.18: The cuboctahedron and the corresponding 1-skeleton graph.

The eigenvalues of the Buffon matrix (denoted with their multiplicities) are:

$$\left\{ 1^{(1)}, \frac{3}{4}^{(3)}, \frac{1}{2}^{(3)}, \frac{1}{4}^{(5)} \right\}$$

The eigenspace corresponding to the second highest eigenvalue is

$$X_2 = \begin{pmatrix} -\alpha \\ -\beta \\ -\gamma \\ \gamma - \alpha \\ \beta - \alpha \\ \alpha - \beta - \gamma \\ -\alpha + \beta + \gamma \\ \alpha - \beta \\ \alpha - \gamma \\ \gamma \\ \beta \\ \alpha \end{pmatrix}$$

A direct computation shows that geometrically, this corresponds to an affine cuboctahedron.

The Truncated Tetrahedron

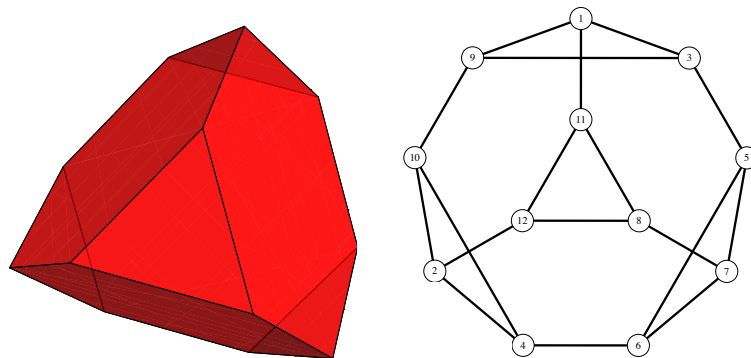


FIGURE 6.19: The truncated tetrahedron and the corresponding 1-skeleton graph.

The eigenvalues of the Buffon matrix (denoted with their multiplicities) are:

$$\left\{ 1^{(1)}, \frac{5}{6}^{(3)}, \frac{1}{2}^{(2)}, \frac{1}{3}^{(3)}, \frac{1}{6}^{(3)} \right\}$$

The eigenspaces corresponding to the eigenvalues second highest eigenvalue is

$$X_2 = \begin{pmatrix} -2\alpha + \frac{7\beta}{3} + \frac{2\gamma}{3} \\ \alpha - \frac{2\beta}{3} + \frac{2\gamma}{3} \\ -2\alpha + \frac{5\beta}{3} + \frac{\gamma}{3} \\ \alpha - \frac{4\beta}{3} + \frac{\gamma}{3} \\ -\beta - \gamma \\ \alpha - 2\beta - \gamma \\ \alpha - \frac{5\beta}{3} - \frac{4\gamma}{3} \\ \alpha - \frac{\beta}{3} - \frac{2\gamma}{3} \\ -2\alpha + 2\beta + \gamma \\ \gamma \\ \beta \\ \alpha \end{pmatrix}$$

A particular geometric realisation derived from X_2 looks as follows:

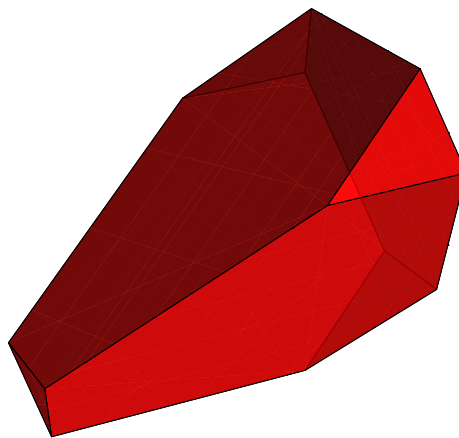


FIGURE 6.20: The affine B -regular version of the truncated tetrahedron. It is not affine regular.

The Truncated Octahedron

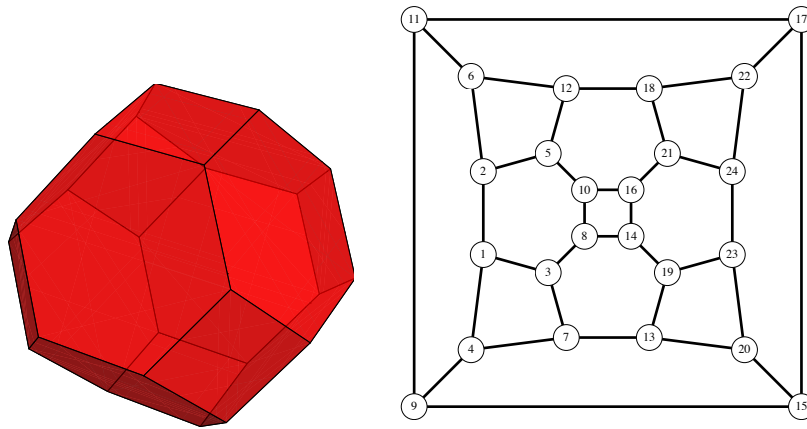


FIGURE 6.21: The truncated octahedron and the corresponding 1-skeleton graph.

The eigenvalues of the Buffon matrix (denoted with their multiplicities) are:

$$\left\{ 1^{(1)}, \frac{1}{6} (4 + \sqrt{2})^{(3)}, \frac{1}{6} (3 + \sqrt{3})^{(2)}, \frac{2}{3}^{(3)}, \frac{1}{6} (2 + \sqrt{2})^{(3)}, \frac{1}{6} (4 - \sqrt{2})^{(3)}, \frac{1}{3}^{(3)}, \frac{1}{6} (3 - \sqrt{3})^{(2)}, \frac{1}{6} (2 - \sqrt{2})^{(3)}, 0^{(1)} \right\}$$

The 3-dimensional eigenspace

$$X_2 = \begin{pmatrix} -\alpha \\ -\beta \\ -\gamma \\ (-1 - \sqrt{2})\alpha + \beta + \gamma \\ (\frac{1}{2}(4 + \sqrt{2}) - 1)\alpha + (1 + \frac{1}{2}(-4 - \sqrt{2}))\beta - \gamma \\ (2 + \frac{1}{2}(-4 - \sqrt{2}))\alpha + (2 + \frac{1}{2}(-4 - \sqrt{2}))\beta + \gamma \\ \beta - \sqrt{2}\alpha \\ (1 + \sqrt{2})\alpha - \beta + (-1 - \sqrt{2})\gamma \\ (-2 - \sqrt{2})\alpha + \sqrt{2}\beta + (1 + \sqrt{2})\gamma \\ (\frac{3}{2}(4 + \sqrt{2}) - 5)\alpha + (1 + \frac{1}{2}(-4 - \sqrt{2}))\beta + (-1 - \sqrt{2})\gamma \\ \frac{1}{2}(-4 - \sqrt{2})\alpha + (\frac{1}{2}(4 + \sqrt{2}) - 2)\beta + (1 + \sqrt{2})\gamma \\ \alpha - \sqrt{2}\beta \\ \sqrt{2}\beta - \alpha \\ \frac{1}{2}(4 + \sqrt{2})\alpha + (2 + \frac{1}{2}(-4 - \sqrt{2}))\beta + (-1 - \sqrt{2})\gamma \\ (5 - \frac{3}{2}(4 + \sqrt{2}))\alpha + (\frac{1}{2}(4 + \sqrt{2}) - 1)\beta + (1 + \sqrt{2})\gamma \\ (2 + \sqrt{2})\alpha - \sqrt{2}\beta + (-1 - \sqrt{2})\gamma \\ (-1 - \sqrt{2})\alpha + \beta + (1 + \sqrt{2})\gamma \\ \sqrt{2}\alpha - \beta \\ (\frac{1}{2}(4 + \sqrt{2}) - 2)\alpha + (\frac{1}{2}(4 + \sqrt{2}) - 2)\beta - \gamma \\ (1 + \frac{1}{2}(-4 - \sqrt{2}))\alpha + (\frac{1}{2}(4 + \sqrt{2}) - 1)\beta + \gamma \\ (1 + \sqrt{2})\alpha - \beta - \gamma \\ \gamma \\ \beta \\ \alpha \end{pmatrix}$$

A particular graph realisation obtained from the eigenspace X_2 look as follows:

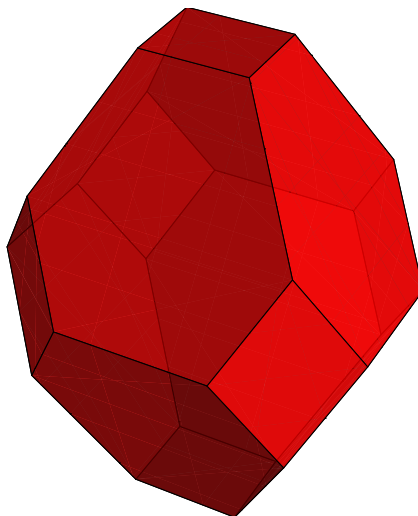


FIGURE 6.22: Eigenspace realisation of the truncated octahedron graph derived from the eigenspace X_2 .

The Great Rhombicosidodecahedron

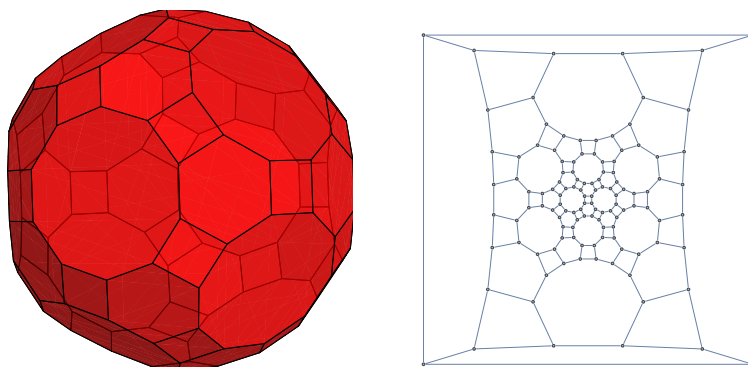


FIGURE 6.23: The great rhombicosidodecahedron and the corresponding 1-skeleton graph.

A particular geometric realisation derived from the eigenspace X_2 :

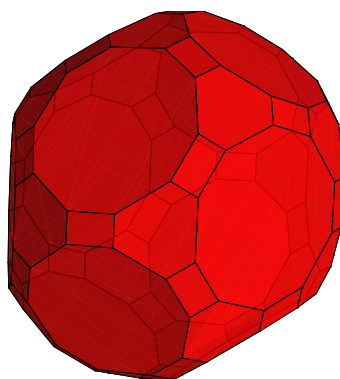


FIGURE 6.24: Affine B -regular great rhombicosidodecahedron.

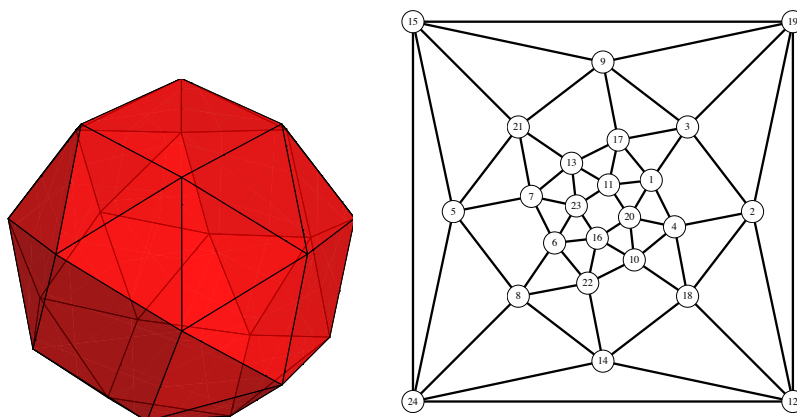
The Snub Cube

FIGURE 6.25: The small rhombicuboctahedron and the corresponding 1-skeleton graph.

The eigenspace X_2 corresponding to the second highest eigenvalue is:

$$X_2 = \left(\begin{array}{c}
\left(\frac{107}{111} - \frac{26}{111} (6 + \sqrt{7}) \right) \alpha + \left(\frac{209}{111} - \frac{29}{111} (6 + \sqrt{7}) \right) \beta + \left(\frac{6}{37} (6 + \sqrt{7}) - \frac{56}{37} \right) \gamma \\
\left(\frac{41}{111} - \frac{11}{111} (6 + \sqrt{7}) \right) \alpha + \left(-\frac{61}{111} - \frac{8}{111} (6 + \sqrt{7}) \right) \beta + \left(\frac{56}{37} - \frac{6}{37} (6 + \sqrt{7}) \right) \gamma \\
\left(\frac{209}{111} - \frac{29}{111} (6 + \sqrt{7}) \right) \alpha + \left(\frac{41}{111} - \frac{11}{111} (6 + \sqrt{7}) \right) \beta + \left(\frac{1}{37} (6 + \sqrt{7}) - \frac{34}{37} \right) \gamma \\
\left(-\frac{61}{111} - \frac{8}{111} (6 + \sqrt{7}) \right) \alpha + \left(\frac{107}{111} - \frac{26}{111} (6 + \sqrt{7}) \right) \beta + \left(\frac{34}{37} + \frac{1}{37} (-6 - \sqrt{7}) \right) \gamma \\
\left(\frac{47}{111} (6 + \sqrt{7}) - \frac{266}{111} \right) \alpha + \left(\frac{14}{111} (6 + \sqrt{7}) - \frac{32}{111} \right) \beta + \left(\frac{50}{37} - \frac{8}{37} (6 + \sqrt{7}) \right) \gamma \\
\left(\frac{118}{111} - \frac{10}{111} (6 + \sqrt{7}) \right) \alpha + \left(\frac{23}{111} (6 + \sqrt{7}) - \frac{116}{111} \right) \beta + \left(\frac{8}{37} (6 + \sqrt{7}) - \frac{50}{37} \right) \gamma \\
\left(\frac{23}{111} (6 + \sqrt{7}) - \frac{116}{111} \right) \alpha + \left(\frac{47}{111} (6 + \sqrt{7}) - \frac{266}{111} \right) \beta + \left(\frac{78}{37} - \frac{11}{37} (6 + \sqrt{7}) \right) \gamma \\
\left(\frac{14}{111} (6 + \sqrt{7}) - \frac{32}{111} \right) \alpha + \left(\frac{118}{111} - \frac{10}{111} (6 + \sqrt{7}) \right) \beta + \left(\frac{11}{37} (6 + \sqrt{7}) - \frac{78}{37} \right) \gamma \\
\left(\frac{7}{111} (6 + \sqrt{7}) - \frac{16}{111} \right) \alpha + \left(\frac{59}{111} - \frac{5}{111} (6 + \sqrt{7}) \right) \beta + \left(\frac{72}{37} - \frac{13}{37} (6 + \sqrt{7}) \right) \gamma \\
\left(\frac{275}{111} - \frac{44}{111} (6 + \sqrt{7}) \right) \alpha + \left(\frac{200}{111} - \frac{32}{111} (6 + \sqrt{7}) \right) \beta + \left(\frac{13}{37} (6 + \sqrt{7}) - \frac{72}{37} \right) \gamma \\
\left(\frac{200}{111} - \frac{32}{111} (6 + \sqrt{7}) \right) \alpha + \left(\frac{7}{111} (6 + \sqrt{7}) - \frac{16}{111} \right) \beta + \left(\frac{25}{37} - \frac{4}{37} (6 + \sqrt{7}) \right) \gamma \\
\left(\frac{59}{111} - \frac{5}{111} (6 + \sqrt{7}) \right) \alpha + \left(\frac{275}{111} - \frac{44}{111} (6 + \sqrt{7}) \right) \beta + \left(\frac{4}{37} (6 + \sqrt{7}) - \frac{25}{37} \right) \gamma \\
\left(\frac{8}{111} (6 + \sqrt{7}) - \frac{50}{111} \right) \alpha + \left(\frac{26}{111} (6 + \sqrt{7}) - \frac{107}{111} \right) \beta + \left(\frac{1}{37} (6 + \sqrt{7}) - \frac{34}{37} \right) \gamma \\
\left(\frac{29}{111} (6 + \sqrt{7}) - \frac{209}{111} \right) \alpha + \left(\frac{11}{111} (6 + \sqrt{7}) - \frac{152}{111} \right) \beta + \left(\frac{34}{37} + \frac{1}{37} (-6 - \sqrt{7}) \right) \gamma \\
\left(\frac{26}{111} (6 + \sqrt{7}) - \frac{107}{111} \right) \alpha + \left(\frac{29}{111} (6 + \sqrt{7}) - \frac{209}{111} \right) \beta + \left(\frac{19}{37} - \frac{6}{37} (6 + \sqrt{7}) \right) \gamma \\
\left(\frac{11}{111} (6 + \sqrt{7}) - \frac{152}{111} \right) \alpha + \left(\frac{8}{111} (6 + \sqrt{7}) - \frac{50}{111} \right) \beta + \left(\frac{6}{37} (6 + \sqrt{7}) - \frac{19}{37} \right) \gamma \\
\left(\frac{5}{37} (6 + \sqrt{7}) - \frac{59}{37} \right) \alpha + \left(\frac{7}{37} (6 + \sqrt{7}) - \frac{53}{37} \right) \beta + \left(\frac{75}{37} - \frac{12}{37} (6 + \sqrt{7}) \right) \gamma \\
\left(\frac{22}{37} - \frac{5}{37} (6 + \sqrt{7}) \right) \alpha + \left(\frac{16}{37} - \frac{7}{37} (6 + \sqrt{7}) \right) \beta + \left(\frac{12}{37} (6 + \sqrt{7}) - \frac{75}{37} \right) \gamma \\
\left(\frac{7}{37} (6 + \sqrt{7}) - \frac{53}{37} \right) \alpha + \left(\frac{22}{37} - \frac{5}{37} (6 + \sqrt{7}) \right) \beta + \left(-\frac{6}{37} - \frac{2}{37} (6 + \sqrt{7}) \right) \gamma \\
\left(\frac{16}{37} - \frac{7}{37} (6 + \sqrt{7}) \right) \alpha + \left(\frac{5}{37} (6 + \sqrt{7}) - \frac{59}{37} \right) \beta + \left(\frac{6}{37} + \frac{2}{37} (6 + \sqrt{7}) \right) \gamma \\
\alpha + \beta - \gamma \\
\gamma \\
\beta \\
\alpha
\end{array} \right)$$

The affine B -regular snub cube is not affine regular. A particular realisation looks as follows.

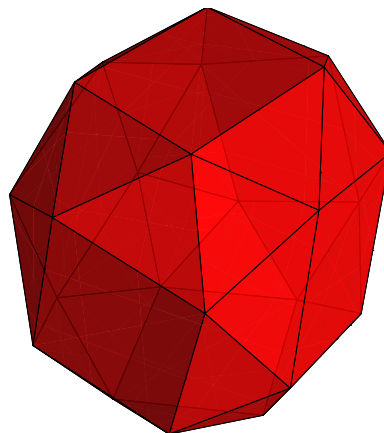


FIGURE 6.26: The affine B -regular snub cube

Chapter 7

Conclusion

In the thesis we studied

- classification of \mathcal{V} -systems
- limiting shapes of polyhedra under Buffon transformation

The main findings of the thesis are

- proof of the local completeness of Feigin-Veselov list of the 3-dimensional \mathcal{V} -systems
- proof of the existence of affine B -regular polyhedron of a given simplicial combinatorial type with Platonic symmetry.

Although the problem of classification of \mathcal{V} -systems seems to be very hard, in dimension 3 it does not look hopeless. As we have seen, matroids provide a natural framework for the problem of classification of \mathcal{V} -systems. Fixing the matroidal structure of a certain type the projective rigidity property allows to analyse the \mathcal{V} -conditions directly starting with one vector realisation of a given \mathcal{V} -system. All known irreducible \mathcal{V} -systems in dimensions 3 have a rigid underlying matroid. For small vector configurations this direct method leads to the full classification of \mathcal{V} -systems of a given matroid type.

A big step towards the full classification would be finding a procedure for generation of the class of \mathcal{V} -system type matroids. As we have seen [26] this is a highly

non-trivial task for several reasons. The number of simple rank 3-matroids grows rapidly with the number of elements. Moreover, the number of realisable (vector-) matroids on more than 8 elements is unknown. Further constraints are needed in order to restrict and characterise the class of suitable candidates.

An important result from the theory of matroids is Seymour's decomposition theorem [44]. A matroid is called regular if it is representable over all fields. Seymour's theorem states that all regular matroids can be built up in a simple way as sums of certain type of simpler well defined (graphic) matroids, their duals, and one special matroid on 10 elements. Examples of degenerations and extensions of \vee -system matroids indicate a possibility of the existence of a similar result for the \vee -system type matroids. In particular, we have seen that the matroid F_3 can be obtained as a sum of two simpler matroids.

Another possible direction is the problem of identification of forbidden minors. In analogy to the theory of matroids and the theory of graphs, where many families have been proved to be closed under taking minors, there is a possibility to reduce the problem of classification of \vee -systems to the task of the identification of the forbidden minors. The interesting example of the matroid on 10 elements [26], which does not permit a vector realisation with respect to the \vee -conditions would be a natural choice as a starting point in this direction.

Further investigation of the structural properties of the \vee -system type matroids listed in Chapter 2 could develop useful as tools for both directions, the question of characterisation of the class of admissible matroids and the identification of forbidden type matroids.

In the second part the main remaining problem is to describe all combinatorial structures of polyhedra admitting affine B -regular realisations. In Colin de Verdière approach this means that the corresponding symmetrised Buffon matrix has Colin de Verdière property. Again in full generality this seems to be a very hard question.

Note that the Buffon regularisation procedure can naturally be interpreted as the search of an ideal shape of a given polyhedron. In that sense it can be considered as one of the earliest examples of the trend, popular in modern differential geometry.

For manifolds this usually leads to the solutions of certain nonlinear PDEs like the mean curvature flow in the theory of minimal surfaces [20] or the celebrated

Ricci flow in Thurston's geometrisation programme [34]. Our case is conceptually closer to the description of the minimal submanifolds in the unit sphere using the eigenfunctions of the Laplace-Beltrami operator, see [23, 45].

The main difference with the differential case is that the generic graphs are much less regular objects than manifolds, even under our assumption of Platonic symmetry. The crucial thing here is a large multiplicity of the second eigenvalue of the Buffon operator. How to guarantee this is a good question.

The symmetry assumption seems to be natural. We already mentioned an interesting result of Mowshowitz [35], who showed that if all eigenvalues of the adjacency matrix A of a graph are different, then every automorphism of A has order 1 or 2. Some interesting related results for the graphs with vertex transitive group action can be found in [21]. Note that in our case the group action is far from being vertex transitive.

An interesting question concerns the decomposition of $\mathcal{F}(\mathcal{V})$ into the irreducible G -modules with respect to the Buffon spectrum. We saw that the geometric representation always appears at the subdominant level, but we do not know much about higher levels.

Finally, a natural question is what happens in higher dimension. We believe that for the simplicial polyhedra we should expect similar result if we assume the symmetry under an irreducible Coxeter group. Note that in dimension 4 we have 6 regular polyhedra with the symmetry groups $A_4 = S_5$, B_4 , F_4 and H_4 , while in dimension more than 4 we have only analogues of tetrahedron, cube and octahedron. A generalisation of Lovász construction to many dimensions can be found in [22].

Appendix A

Catalogue of all known real 3-dimensional ∇ -systems

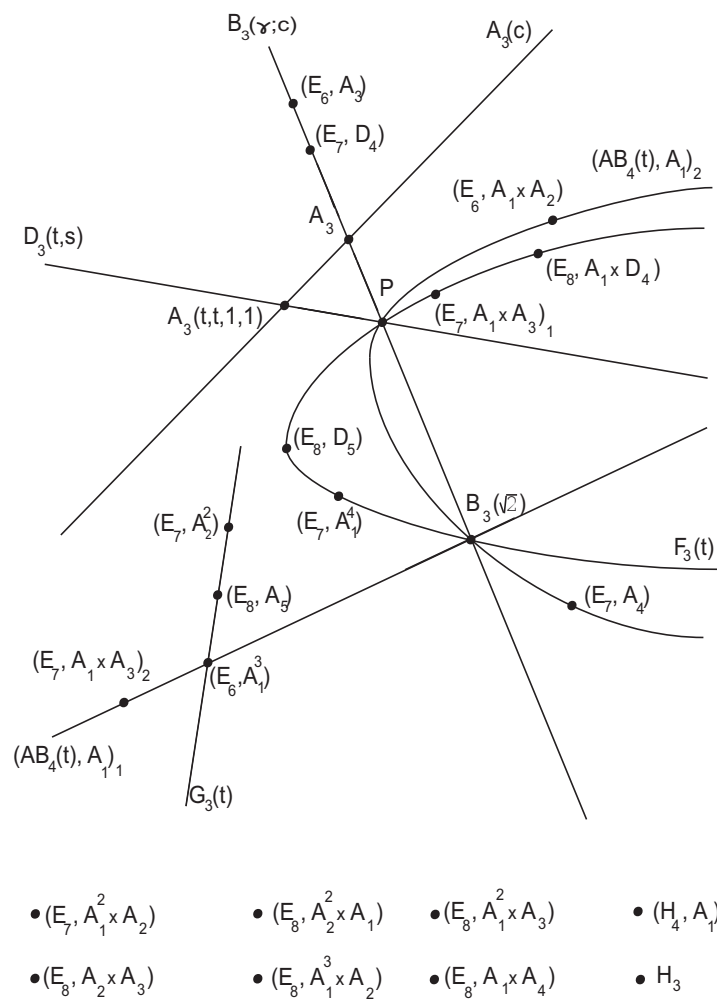


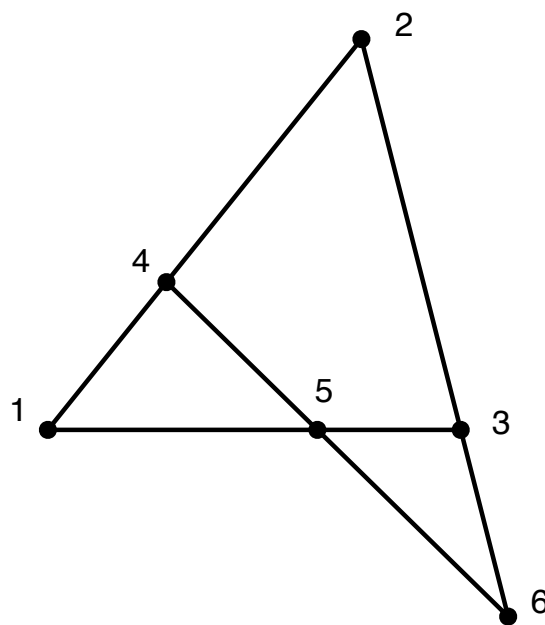
FIGURE A.1: The map of all known 3-dimensional ∇ -systems from [15]

We use here the notations from [14, 15]. In particular, for a Coxeter group G and its parabolic subgroup H (G, H) denotes the corresponding \vee -system given by the restriction procedure [14]. When the type of the subgroup does not fix the subgroup up to a conjugation the index 1 or 2 is used to distinguish them. A schematic way to present all known \vee -systems in dimension 3 taken from [15] is shown above.

Each 3D \vee -system \mathcal{A} is presented below by the matrix with columns giving the covectors of the system (the first row is simply the labelling of the covectors). We give the graphical representation of the corresponding matroid with the list of orthogonal pairs, 2-flats, the form G and the values of ν -function. The ordering of the list is according to the number of covectors in the system. The parameters are assumed to be chosen in such a way that all the covectors are real and non-zero.

\vee -systems $A_3(c_1, c_2, c_3)$

$$\mathcal{A} = \begin{bmatrix} 1 & 2 & 3 & 4 & 5 & 6 \\ \sqrt{c_1} & 0 & 0 & -\sqrt{c_1 c_2} & -\sqrt{c_1 c_3} & 0 \\ 0 & \sqrt{c_2} & 0 & \sqrt{c_1 c_2} & 0 & -\sqrt{c_2 c_3} \\ 0 & 0 & \sqrt{c_3} & 0 & \sqrt{c_1 c_3} & \sqrt{c_2 c_3} \end{bmatrix}$$



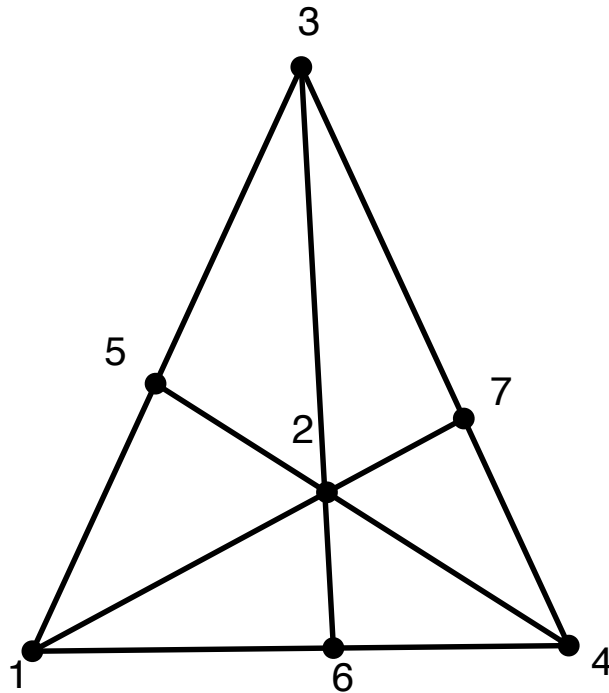
$$G = \begin{bmatrix} c_1(1 + c_2 + c_3) & -c_1c_2 & -c_1c_3 \\ -c_1c_2 & c_2(1 + c_1 + c_3) & -c_2c_3 \\ -c_1c_3 & -c_2c_3 & c_3(1 + c_1 + c_2) \end{bmatrix}$$

$$\mathcal{I}_2 = \{(1, 6), (2, 5), (3, 4)\}$$

$$\mathcal{I}_3 = \begin{cases} (1, 2, 4), (1, 3, 5), (2, 3, 6), & \nu_j = \frac{1 - c_j + \sum_{i=1}^3 c_i}{1 + \sum_{i=1}^3 c_i}, j = 1, 2, 3 \\ (4, 5, 6), & \nu = \frac{\sum_{i=1}^3 c_i}{1 + \sum_{i=1}^3 c_i} \end{cases}$$

\vee -system $D_3(t, s)$

$$\mathcal{A} = \begin{bmatrix} 1 & 2 & 3 & 4 & 5 & 6 & 7 \\ 1 & 1 & 1 & 1 & 0 & 0 & \sqrt{2(s+t-1)} \\ 1 & -1 & -1 & 1 & \sqrt{\frac{2(s-t+1)}{t}} & 0 & 0 \\ 1 & -1 & 1 & -1 & 0 & \sqrt{\frac{2(t-s+1)}{s}} & 0 \end{bmatrix}$$



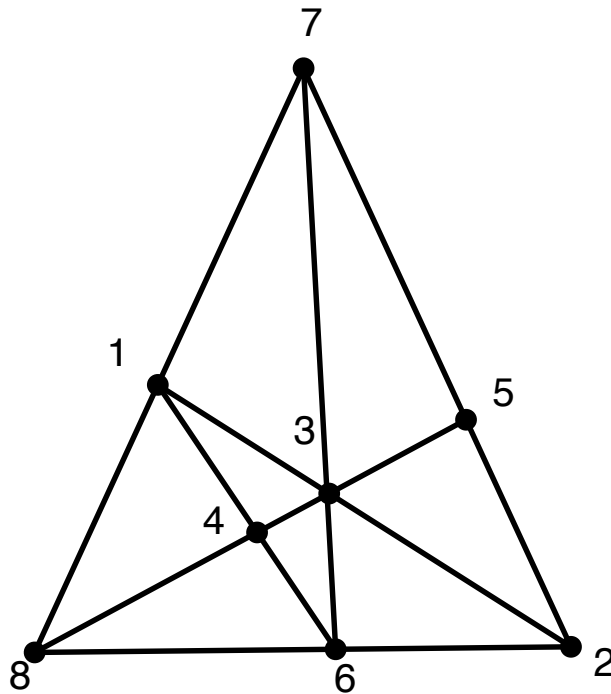
$$G = 2(1 + s + t) \begin{bmatrix} 1 & 0 & 0 \\ 0 & \frac{1}{t} & 0 \\ 0 & 0 & \frac{1}{s} \end{bmatrix}$$

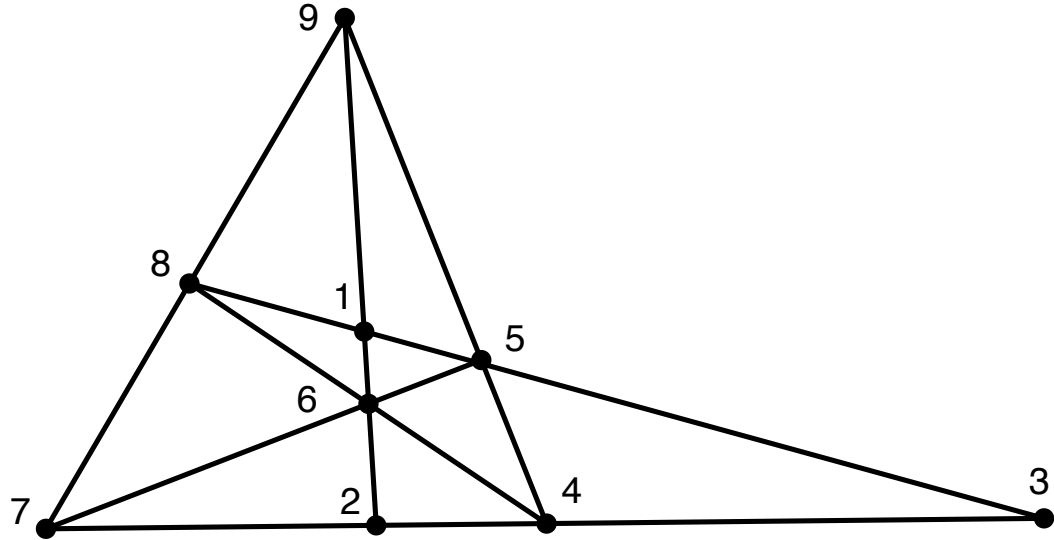
$$\mathcal{I}_2 = \{(5, 6), (5, 7), (6, 7)\}$$

$$\mathcal{I}_3 = \begin{cases} (1, 2, 7), (3, 4, 7) & \nu_{31} = \frac{s+t}{1+s+t} \\ (1, 3, 5), (2, 4, 5) & \nu_{32} = \frac{1+s}{1+s+t} \\ (1, 4, 6), (2, 3, 6) & \nu_{33} = \frac{1+t}{1+s+t} \end{cases}$$

\vee -system (E_6, A_3)

$$A = \begin{bmatrix} 1 & 2 & 3 & 4 & 5 & 6 & 7 & 8 \\ 2 & 2 & 2\sqrt{6} & 2 & -2 & 2 & -2 & 0 \\ 2 & -2 & 0 & \frac{1}{2} & \frac{1}{2} & -1 & -1 & \frac{\sqrt{6}}{2} \\ 0 & 0 & 0 & \frac{1}{2} & \frac{1}{2} & 1 & 1 & \frac{\sqrt{6}}{2} \end{bmatrix}$$





$$G = 2(c_1 + c_2 + c_3 + \gamma) \begin{bmatrix} c_1 & 0 & 0 \\ 0 & c_2 & 0 \\ 0 & 0 & c_3 \end{bmatrix}$$

$$\mathcal{I}_2 = \{(1, 4), (1, 7), (2, 5), (2, 8), (3, 6), (3, 9)\}$$

Four 3-point lines:

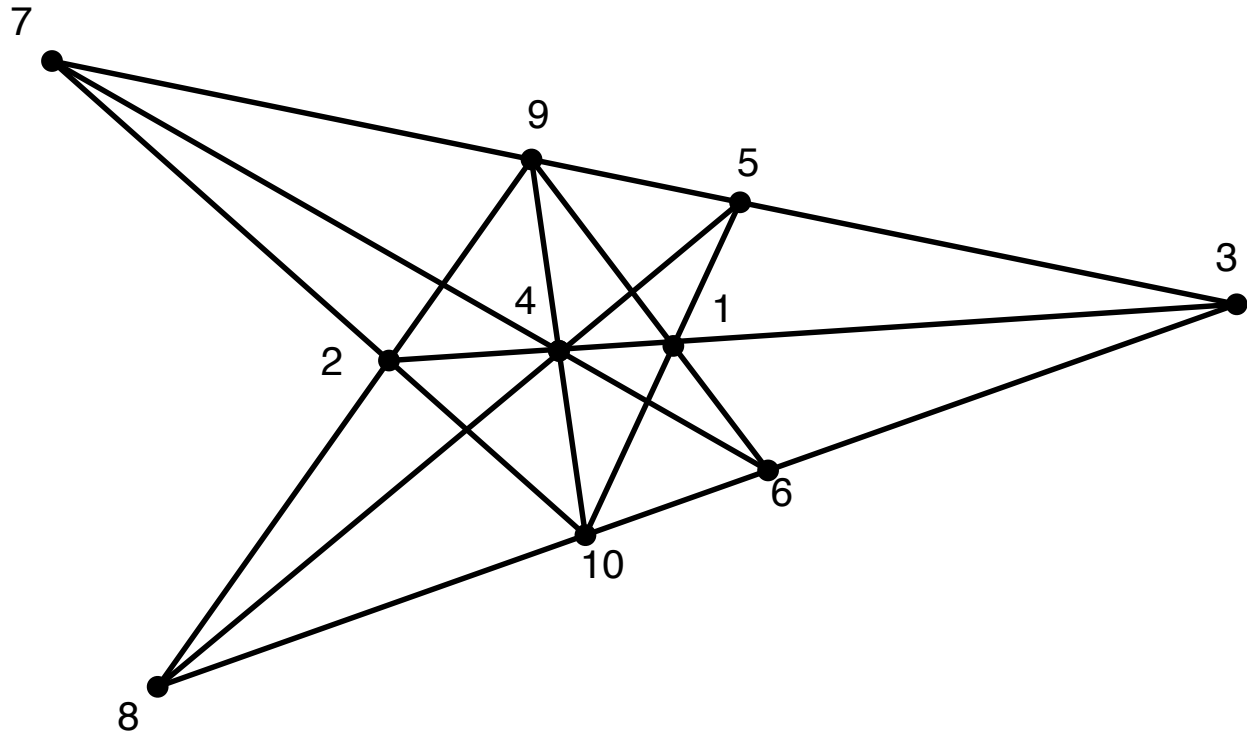
$$\mathcal{I}_3 = \{(4, 5, 9), (4, 6, 8), (5, 6, 7), (7, 8, 9)\}, \nu_3 = \frac{\sum c_i}{2(\gamma + \sum_{i=1}^3 c_i)}$$

Three 4-point lines:

$$\mathcal{I}_4 = \{(1, 2, 6, 9), (1, 3, 5, 8), (2, 3, 4, 7)\}, \nu_{4j} = \frac{\gamma - c_j + \sum c_i}{\gamma + \sum_{i=1}^3 c_i}, j=1,2,3$$

\vee -system (E_6, A_1^3)

$$\mathcal{A} = \begin{bmatrix} 1 & 2 & 3 & 4 & 5 & 6 & 7 & 8 & 9 & 10 \\ \sqrt{2} & \sqrt{2} & 2\sqrt{3} & 0 & \sqrt{2} & -\sqrt{2} & -\sqrt{2} & \sqrt{2} & 0 & 0 \\ \sqrt{2} & -\sqrt{2} & 0 & 2 & \frac{\sqrt{2}}{2} & -\frac{\sqrt{2}}{2} & \frac{\sqrt{2}}{2} & -\frac{\sqrt{2}}{2} & 1 & -1 \\ 0 & 0 & 0 & 0 & \frac{\sqrt{2}}{2} & \frac{\sqrt{2}}{2} & \frac{\sqrt{2}}{2} & \frac{\sqrt{2}}{2} & 1 & 1 \end{bmatrix}$$



$$G = \begin{bmatrix} 24 & 0 & 0 \\ 0 & 12 & 0 \\ 0 & 0 & 4 \end{bmatrix}$$

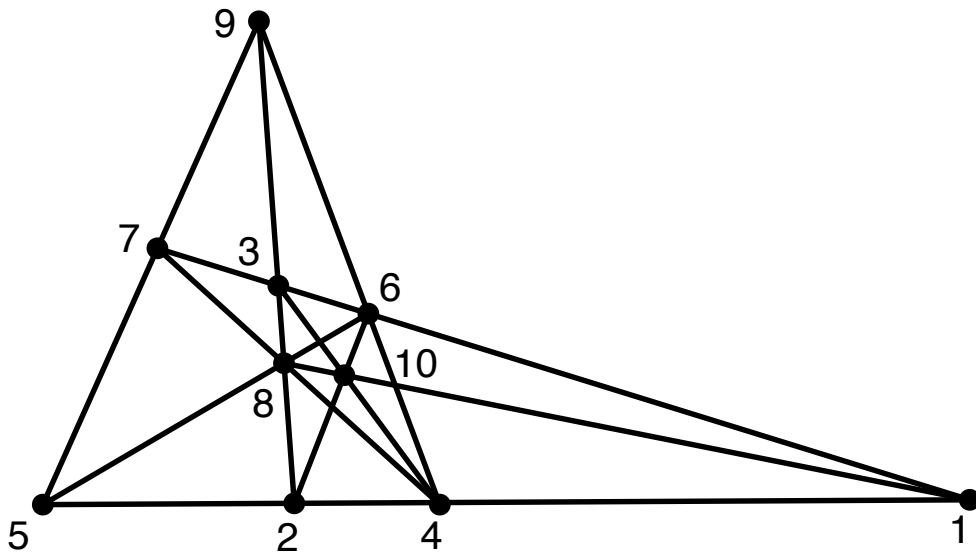
$$\mathcal{I}_2 = \{(1, 7), (1, 8), (2, 5), (2, 6), (5, 6), (7, 8)\}$$

$$\mathcal{I}_3 = \begin{cases} (10, 2, 7), (4, 6, 7), (9, 8, 2), (1, 5, 10), (4, 5, 8), (9, 1, 6), & \nu_{31} = \frac{5}{12} \\ (4, 9, 10), & \nu_{32} = \frac{1}{2} \end{cases}$$

$$\mathcal{I}_4 = \{(4, 1, 2, 3), (9, 5, 3, 7), (6, 3, 8, 10)\}, \nu_4 = \frac{2}{3}$$

\vee -system $(AB_4(t), A_1)_2$

$$A = \begin{bmatrix} 1 & 2 & 3 & 4 & 5 & 6 & 7 & 8 & 9 & 10 \\ \sqrt{2} & 0 & 0 & 1 & \frac{1}{\sqrt{4t^2+1}} & 1 & \frac{1}{\sqrt{4t^2+1}} & 0 & 0 & \frac{t\sqrt{2}}{\sqrt{(t^2+1)}} \\ 0 & \sqrt{2} & 0 & 1 & -\frac{1}{\sqrt{4t^2+1}} & 0 & 0 & 1 & \frac{1}{\sqrt{4t^2+1}} & \frac{t\sqrt{2}}{\sqrt{(t^2+1)}} \\ 0 & 0 & \sqrt{2} & 0 & 0 & 1 & -\frac{1}{\sqrt{4t^2+1}} & 1 & -\frac{1}{\sqrt{4t^2+1}} & \frac{t\sqrt{2}}{\sqrt{(t^2+1)}} \end{bmatrix}$$



$$G = \begin{bmatrix} 6 - \frac{2}{1+t^2} + \frac{2}{1+4t^2} & \frac{6(t^2+2t^4)}{1+5t^2+4t^4} & \frac{6(t^2+2t^4)}{1+5t^2+4t^4} \\ \frac{6(t^2+2t^4)}{1+5t^2+4t^4} & 6 - \frac{2}{1+t^2} + \frac{2}{1+4t^2} & \frac{6(t^2+2t^4)}{1+5t^2+4t^4} \\ \frac{6(t^2+2t^4)}{1+5t^2+4t^4} & \frac{6(t^2+2t^4)}{1+5t^2+4t^4} & 6 - \frac{2}{1+t^2} + \frac{2}{1+4t^2} \end{bmatrix}$$

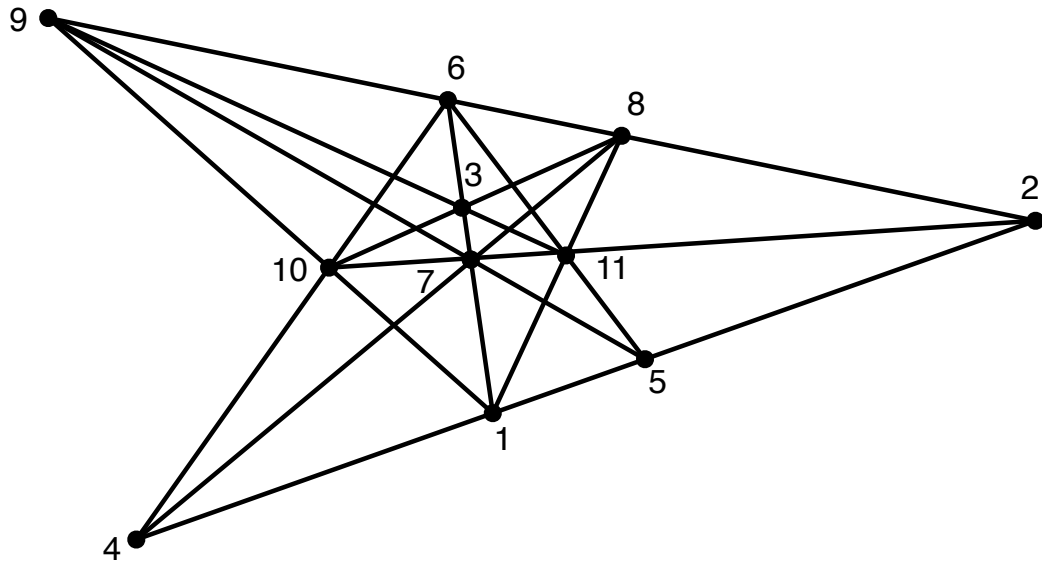
$$\mathcal{I}_2 = \{(1, 9), (2, 7), (3, 5), (5, 10), (7, 10), (9, 10)\}$$

$$\mathcal{I}_3 = \begin{cases} (1, 8, 10), (2, 6, 10), (3, 4, 10) & \nu_{31} = \frac{1+4t^2}{3(1+2t^2)} \\ (4, 6, 9), (4, 7, 8), (5, 6, 8) & \nu_{32} = \frac{3+4t^2}{6(1+2t^2)} \\ (5, 7, 9) & \nu_{33} = \frac{1}{2(1+2t^2)} \end{cases}$$

$$\mathcal{I}_4 = \{(1, 2, 4, 5), (1, 3, 6, 7), (2, 3, 8, 9)\}, \nu_4 = \frac{2}{3}$$

\vee -system $(AB_4(t), A_1)_1$

$$\mathcal{A} = \begin{bmatrix} 1 & 2 & 3 & 4 & 5 & 6 & 7 & 8 & 9 & 10 & 11 \\ \sqrt{2(2t^2+1)} & 0 & 0 & \sqrt{2} & \sqrt{2} & t\sqrt{2} & t\sqrt{2} & t & t & t & t \\ 0 & 2\sqrt{2(t^2+1)} & 0 & \sqrt{2} & -\sqrt{2} & 0 & 0 & 2t & -2t & 2t & -2t \\ 0 & 0 & t\sqrt{2(2t^2-1)} & 0 & 0 & t\sqrt{2} & -t\sqrt{2} & t & t & t & -t \end{bmatrix}$$



$$G = 6 \begin{bmatrix} 1+2t & 0 & 0 \\ 0 & 2+4t & 0 \\ 0 & 0 & \frac{t^2+2t^4}{1+t^2} \end{bmatrix}$$

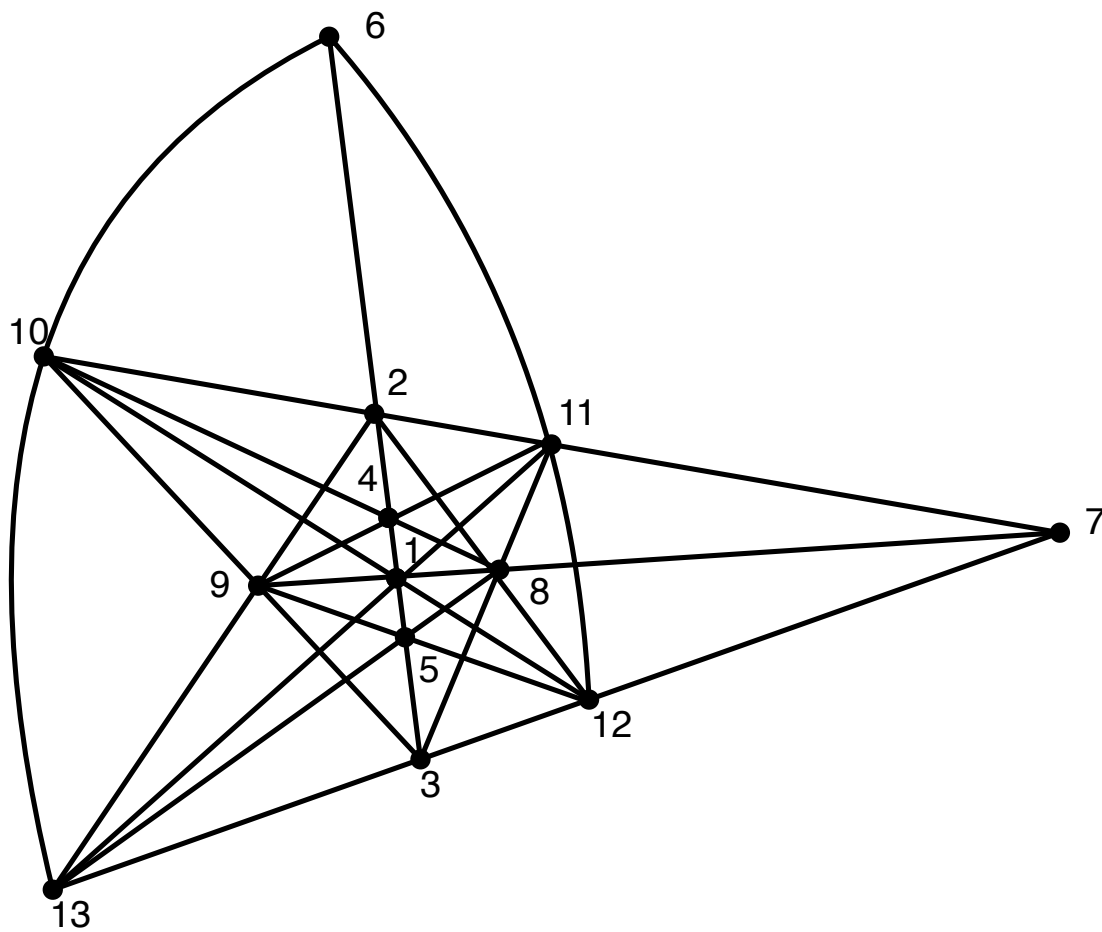
$$\mathcal{I}_2 = \{(2, 3), (3, 4), (3, 5), (4, 9), (4, 11), (5, 8), (5, 10)\}$$

$$\mathcal{I}_3 = \begin{cases} (4, 6, 10), (4, 7, 8), (5, 6, 11), (5, 7, 9) & \nu_{31} = \frac{3+4t^2}{6(1+2t^2)} \\ (1, 8, 11), (1, 9, 10) & \nu_{32} = \frac{1+3t^2}{3(1+2t^2)} \\ (3, 8, 10), (3, 9, 11) & \nu_{33} = \frac{t^2}{(1+2t^2)} \end{cases}$$

$$\mathcal{I}_4 = \begin{cases} (2, 6, 8, 9), (2, 7, 10, 11) & \nu_{41} = \frac{2}{3} \\ (1, 2, 4, 5) & \nu_{42} = \frac{3+2t^2}{3(1+2t^2)} \\ (1, 3, 6, 7) & \nu_{43} = \frac{1+4t^2}{3(1+2t^2)} \end{cases}$$

\vee -system $G_3(t)$

$$A = \begin{bmatrix} 1 & 2 & 3 & 4 & 5 & 6 & 7 & 8 & 9 & 10 & 11 & 12 & 13 \\ \sqrt{2t+1} & 0 & \sqrt{2t+1} & \sqrt{\frac{2t-1}{3}} & 2\sqrt{\frac{2t-1}{3}} & \sqrt{\frac{2t-1}{3}} & 0 & 1 & 1 & 0 & 0 & 1 & 1 \\ 0 & \sqrt{2t+1} & \sqrt{2t+1} & -\sqrt{\frac{2t-1}{3}} & \sqrt{\frac{2t-1}{3}} & 2\sqrt{\frac{2t-1}{3}} & 0 & 0 & 0 & 1 & 1 & 1 & 1 \\ 0 & 0 & 0 & 0 & 0 & 0 & \sqrt{\frac{3}{t}} & 1 & -1 & 1 & -1 & 1 & -1 \end{bmatrix}$$



$$G = \begin{bmatrix} 4(1+2t) & 2(1+2t) & 0 \\ 2(1+2t) & 4(1+2t) & 0 \\ 0 & 0 & 3(2+\frac{1}{t}) \end{bmatrix}$$

$$\mathcal{I}_2 = \{(4, 7), (4, 12), (4, 13), (5, 7), (5, 10), (5, 11), (6, 7), (6, 8), (6, 9)\}$$

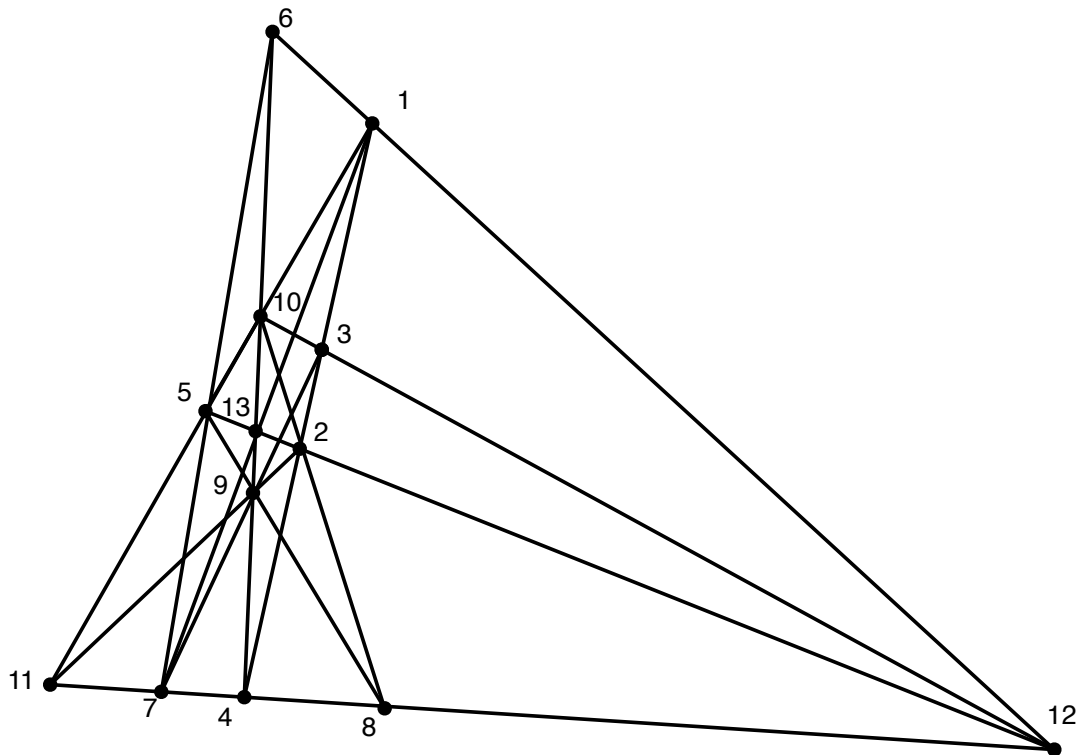
$$\mathcal{I}_3 = \begin{cases} (2, 9, 13), (2, 8, 12), (3, 8, 11), (1, 11, 13), (1, 10, 12), (3, 9, 10) & \nu_{31} = \frac{3+4t}{6(1+2t)} \\ (4, 8, 10), (6, 11, 12), (6, 10, 13), (5, 9, 12), (5, 8, 13), (4, 9, 11) & \nu_{32} = \frac{1+4t}{6(1+2t)} \end{cases}$$

$$\mathcal{I}_4 = \{(2,7,10,11), (1,7,8,9), (3,7,12,13)\}, \nu_4 = \frac{3+2t}{3+6t}$$

$$\mathcal{I}_6 = \{(1, 2, 3, 4, 5, 6)\}, \nu_6 = \frac{2t}{1+2t}$$

\vee -system $(E_7, A_1^2 \times A_2)$

$$\mathcal{A} = \begin{bmatrix} 1 & 2 & 3 & 4 & 5 & 6 & 7 & 8 & 9 & 10 & 11 & 12 & 13 \\ \sqrt{3} & \sqrt{3} & 2 & 0 & 0 & \frac{1}{\sqrt{2}} & -\frac{1}{\sqrt{2}} & -\frac{1}{\sqrt{2}} & \frac{1}{\sqrt{2}} & \sqrt{\frac{3}{2}} & -\sqrt{\frac{3}{2}} & -\sqrt{\frac{3}{2}} & \sqrt{\frac{3}{2}} \\ \sqrt{3} & -\sqrt{3} & 0 & 2\sqrt{6} & 0 & \frac{3}{\sqrt{2}} & -\frac{3}{\sqrt{2}} & \frac{3}{\sqrt{2}} & -\frac{3}{\sqrt{2}} & \sqrt{\frac{3}{2}} & -\sqrt{\frac{3}{2}} & \sqrt{\frac{3}{2}} & -\sqrt{\frac{3}{2}} \\ 0 & 0 & 0 & 0 & 1 & \frac{1}{\sqrt{2}} & \frac{1}{\sqrt{2}} & \frac{1}{\sqrt{2}} & \frac{1}{\sqrt{2}} & \sqrt{\frac{3}{2}} & \sqrt{\frac{3}{2}} & \sqrt{\frac{3}{2}} & \sqrt{\frac{3}{2}} \end{bmatrix}$$



$$G = 9 \begin{bmatrix} 2 & 0 & 0 \\ 0 & 6 & 0 \\ 0 & 0 & 1 \end{bmatrix}$$

$$\mathcal{I}_2 = \{(1, 8), (1, 9), (2, 6), (2, 7), (3, 5), (4, 5), (6, 11), (7, 10), (8, 13), (9, 12)\}$$

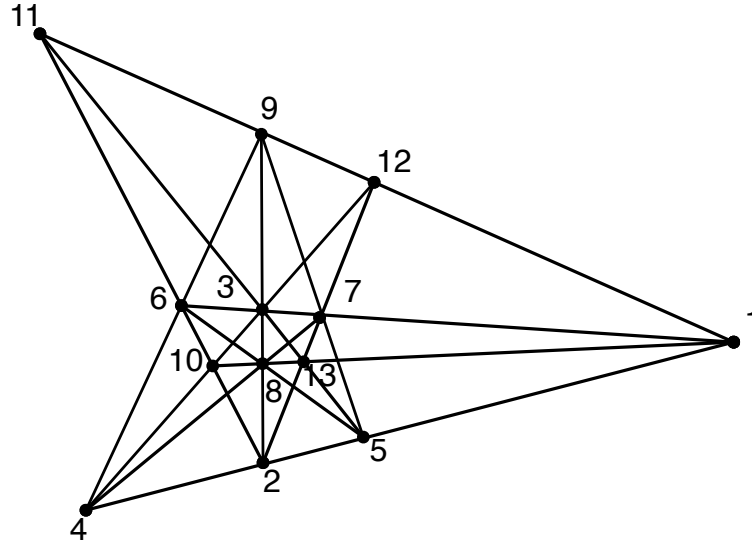
$$\mathcal{I}_3 = \begin{cases} (5, 9, 8), (7, 5, 6) & \nu_{31} = \frac{2}{9} \\ (10, 3, 12), (11, 13, 3) & \nu_{32} = \frac{7}{18} \\ (6, 3, 8), (7, 9, 3) & \nu_{33} = \frac{5}{18} \\ (6, 1, 12), (10, 2, 8), (7, 13, 1), (11, 9, 2) & \nu_{34} = \frac{1}{3} \end{cases}$$

$$\mathcal{I}_4 = \begin{cases} (5, 13, 2, 12), (11, 5, 10, 1) & \nu_{41} = \frac{4}{9} \\ (4, 2, 3, 1) & \nu_{42} = \frac{5}{9} \end{cases}$$

$$\mathcal{I}_5 = \{(11, 7, 4, 8, 12), (6, 10, 13, 9, 4)\}, \nu_5 = \frac{2}{3}$$

\vee -system $F_3(t)$

$$\begin{bmatrix} 1 & 2 & 3 & 4 & 5 & 6 & 7 & 8 & 9 & 10 & 11 & 12 & 13 \\ \sqrt{4t^2+2} & 0 & 0 & 1 & 1 & 1 & 1 & 0 & 0 & t\sqrt{2} & t\sqrt{2} & t\sqrt{2} & t\sqrt{2} \\ 0 & \sqrt{4t^2+2} & 0 & 1 & -1 & 0 & 0 & 1 & 1 & t\sqrt{2} & -t\sqrt{2} & t\sqrt{2} & -t\sqrt{2} \\ 0 & 0 & \sqrt{4t^2+2} & 0 & 0 & 1 & -1 & 1 & -1 & t\sqrt{2} & t\sqrt{2} & -t\sqrt{2} & -t\sqrt{2} \end{bmatrix}$$



$$G = (6 + 12t^2)I$$

$$\mathcal{I}_2 = \{(4,11), (4,13), (5,10), (5,12), (6,13), (7,10), (7,11), (8,11), (8,12), (9,10), (9,13)\}$$

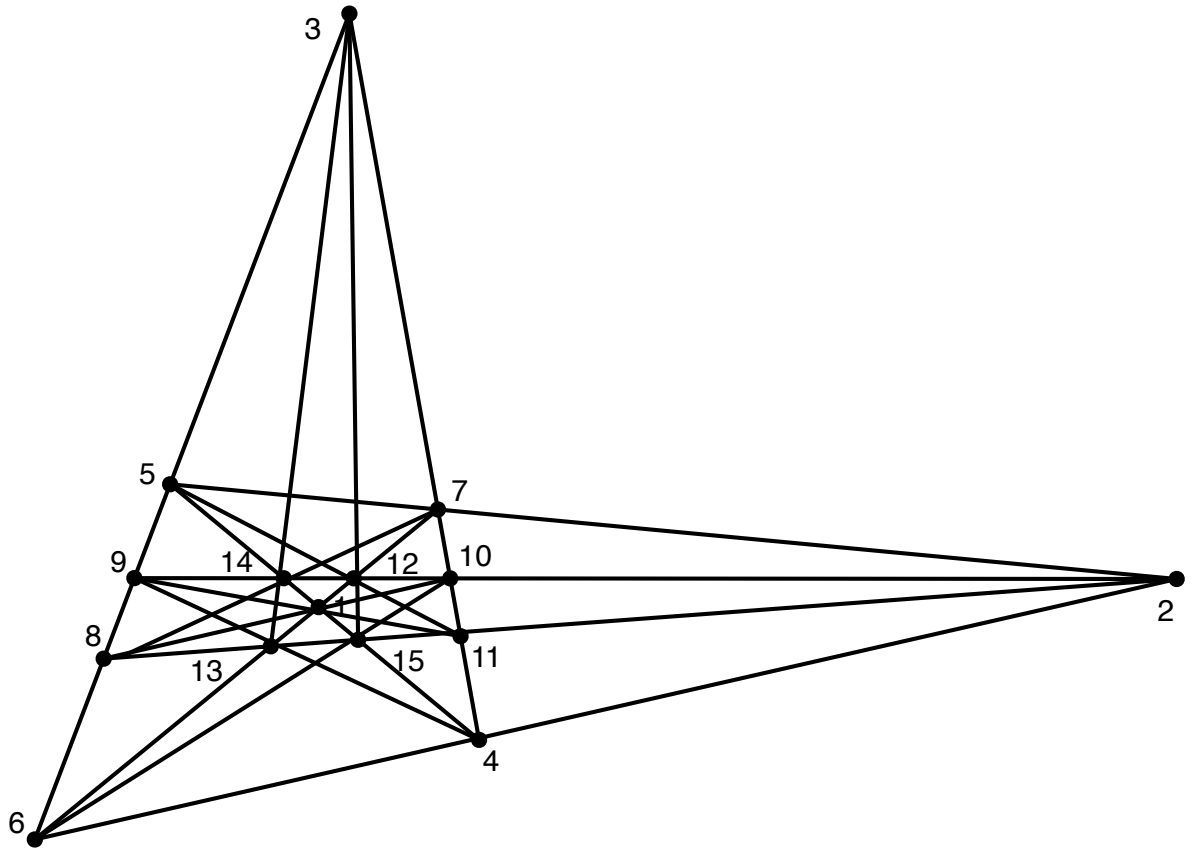
$$\mathcal{I}_3 = \{(4, 6, 9), (4, 7, 8), (5, 6, 8), (5, 7, 9), \quad \nu_{31} = \frac{1}{2+4t^2}\}$$

$$\mathcal{I}_4 = \begin{cases} (1, 2, 4, 5), (1, 3, 6, 7), (2, 3, 8, 9), & \nu_{32} = \frac{2(1+t^2)}{3+6t^2} \\ (1, 8, 10, 13), (1, 9, 11, 12), (2, 6, 10, 11), (2, 7, 12, 13), \\ (3, 4, 10, 12), (3, 5, 11, 13), & \nu_{33} = \frac{1+4t^2}{3+6t^2} \end{cases}$$

Coxeter \vee -system H_3

$$A = \begin{bmatrix} 1 & 2 & 3 & 4 & 5 & 6 & 7 & 8 & 9 & 10 & 11 & 12 & 13 & 14 & 15 \\ 2\phi & 0 & 0 & 1 & -1 & 1 & 1 & \phi & -\phi & \phi & \phi & \phi^2 & \phi^2 & -\phi^2 & \phi^2 \\ 0 & 2\phi & 0 & \phi & \phi & -\phi & \phi & -\phi^2 & \phi^2 & \phi^2 & \phi^2 & 1 & -1 & 1 & 1 \\ 0 & 0 & 2\phi & \phi^2 & \phi^2 & \phi^2 & -\phi^2 & 1 & 1 & -1 & 1 & -\phi & \phi & \phi & \phi \end{bmatrix}$$

with the golden mean $\phi = \frac{1+\sqrt{5}}{2}$ and $\phi^2 = \phi + 1$.



$$G = 10(3 + \sqrt{5})I$$

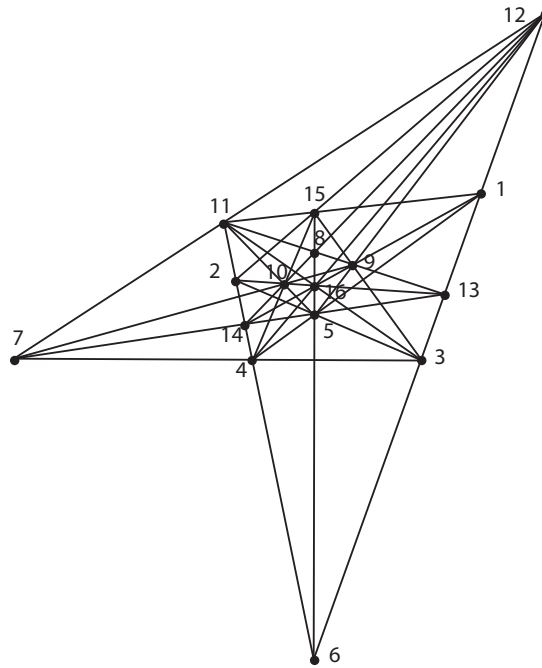
$$\mathcal{I}_2 = \left\{ (1, 2), (1, 3), (2, 3), (4, 8), (4, 12), (5, 10), (5, 13), (6, 11), \right. \\ \left. (6, 14), (7, 9), (7, 15), (8, 12), (9, 15), (10, 13), (11, 14). \right.$$

$$\mathcal{I}_3 = \left\{ (1, 8, 10), (1, 9, 11), (2, 4, 6), (2, 5, 7), (3, 12, 15), \right. \\ \left. (3, 13, 14), (4, 9, 13), (5, 11, 12), (6, 10, 15), (7, 8, 14) \right. \quad \nu_{31} = \frac{3}{10}$$

$$\mathcal{I}_5 = \left\{ (1, 4, 5, 14, 15), (1, 6, 7, 12, 13), (2, 8, 11, 13, 15), (2, 9, 10, 12, 14), \right. \\ \left. (3, 4, 7, 10, 11), (3, 5, 6, 8, 9) \right. \quad \nu_5 = \frac{1}{2}$$

V-system $(E_8, A_1 \times A_4)$

$$\mathcal{A} = \begin{bmatrix} 1 & 2 & 3 & 4 & 5 & 6 & 7 & 8 & 9 & 10 & 11 & 12 & & & \\ \sqrt{10} & \sqrt{10} & \sqrt{2} & \sqrt{2} & 0 & 0 & 2 & 0 & 1 & -1 & \sqrt{5} & -\sqrt{5} & \dots & & \\ \sqrt{10} & -\sqrt{10} & 0 & 0 & \sqrt{5} & \sqrt{10} & 0 & 2\sqrt{10} & \frac{2}{5} & \frac{5}{2} & -\frac{3\sqrt{5}}{2} & -\frac{3\sqrt{5}}{2} & & & \\ 0 & 0 & \sqrt{2} & -\sqrt{2} & \sqrt{5} & -\sqrt{10} & 0 & 0 & \frac{1}{2} & \frac{1}{2} & \frac{\sqrt{5}}{2} & \frac{\sqrt{5}}{2} & & & \\ & 13 & 14 & 15 & 16 & & & & & & & & & & \\ \dots & \sqrt{10} & -\sqrt{10} & 0 & 0 & & & & & & & & & & \\ & \frac{\sqrt{10}}{2} & \frac{\sqrt{10}}{2} & -\frac{5}{\sqrt{2}} & \frac{3\sqrt{10}}{2} & & & & & & & & & & \\ & \frac{\sqrt{10}}{2} & \frac{\sqrt{10}}{2} & \frac{1}{\sqrt{2}} & \frac{\sqrt{10}}{2} & & & & & & & & & & \end{bmatrix}$$



$$G = 30 \begin{bmatrix} 2 & 0 & 0 \\ 0 & 5 & 0 \\ 0 & 0 & 1 \end{bmatrix}$$

$$\mathcal{I}_2 = \{(1, 10), (2, 9), (3, 8), (3, 10), (3, 14), (4, 8), (4, 9), (4, 13), (6, 7), (6, 9), (6, 10), \\ (7, 15), (7, 16), (13, 15), (14, 15)\}$$

$$G = 30 \begin{bmatrix} 3 & 0 & 0 \\ 0 & 4 & 0 \\ 0 & 0 & 1 \end{bmatrix}$$

$$\mathcal{I}_2 = \{(1, 10), (2, 9), (3, 7), (3, 10), (3, 15), (4, 7), (4, 9), (4, 14),$$

$$(5, 11), (5, 12), (9, 11), (9, 17), (10, 12), (10, 16), (11, 15), (12, 14)\}$$

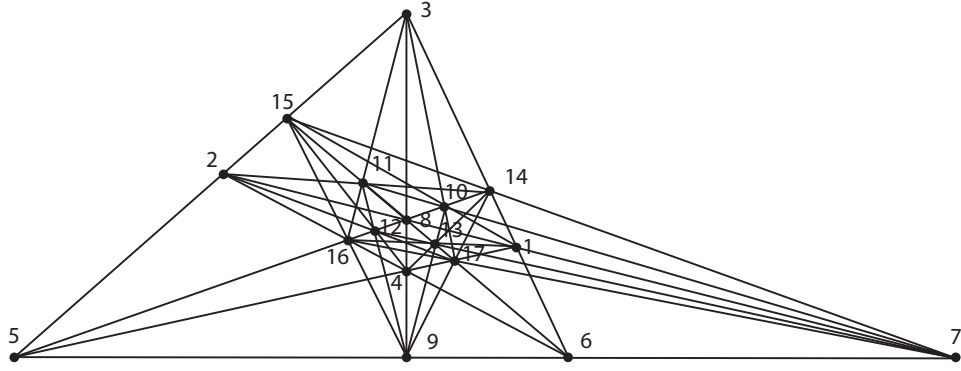
$$\mathcal{I}_3 = \begin{cases} \{(5, 9, 15), (5, 10, 14), (7, 9, 14), (7, 10, 15)\} & \nu_{31} = \frac{1}{6} \\ \{(3, 14, 17), (4, 12, 13), (4, 15, 16), (7, 11, 16), (7, 12, 17), (8, 11, 12), \\ (1, 4, 5), (1, 11, 14), (2, 3, 5), (2, 12, 15), (3, 4, 8), (3, 11, 13)\} & \nu_{32} = \frac{4}{15} \end{cases}$$

$$\mathcal{I}_4 = \begin{cases} (8, 9, 10, 13) & \nu_{41} = \frac{4}{15} \\ (1, 2, 7, 8), (1, 13, 15, 17), (2, 13, 14, 16), (5, 6, 7, 13), (5, 8, 16, 17), \\ (6, 8, 14, 15) & \nu_{42} = \frac{2}{5} \end{cases}$$

$$\mathcal{I}_6 = \{(1, 3, 6, 9, 12, 16), (2, 4, 6, 10, 11, 17)\}, \nu_6 = \frac{3}{5}$$

\vee -system $(E_8, A_1^2 \times A_3)$

$$\mathcal{A} = \begin{bmatrix} 1 & 2 & 3 & 4 & 5 & 6 & 7 & 8 & 9 & 10 & 11 & 12 & 13 \\ 2 & 2 & 0 & 0 & 2 & 2 & 2 & 0 & 0 & \frac{\sqrt{2}}{2} & \frac{\sqrt{2}}{2} & \frac{\sqrt{2}}{2} & \frac{\sqrt{2}}{2} & \dots \\ 2 & -2 & 2 & 2 & 0 & 0 & 0 & 2\sqrt{10} & 0 & 2\sqrt{2} & -2\sqrt{2} & -2\sqrt{2} & 2\sqrt{2} \\ 0 & 0 & 2 & -2 & 2 & -2 & 0 & 0 & 2 & \frac{\sqrt{2}}{2} & -\frac{\sqrt{2}}{2} & \frac{\sqrt{2}}{2} & -\frac{\sqrt{2}}{2} \\ & 14 & 15 & 16 & 17 \\ \dots & \sqrt{2} & \sqrt{2} & \sqrt{2} & \sqrt{2} \\ & 2\sqrt{2} & -2\sqrt{2} & -2\sqrt{2} & 2\sqrt{2} \\ & \sqrt{2} & -\sqrt{2} & \sqrt{2} & -\sqrt{2} \end{bmatrix}$$



$$G = 30 \begin{bmatrix} 1 & 0 & 0 \\ 0 & 4 & 0 \\ 0 & 0 & 1 \end{bmatrix}$$

$$\mathcal{I}_2 = \{(1, 9), (1, 11), (1, 12), (2, 9), (2, 10), (2, 13), (3, 7), (3, 12),$$

$$(3, 13), (4, 7), (4, 10), (4, 11), (5, 11), (5, 13), (6, 10), (6, 12)\}$$

$$\mathcal{I}_3 = \begin{cases} (7, 10, 11), (7, 12, 13), (9, 10, 13), (9, 11, 12) & \nu_{31} = \frac{1}{6} \\ (9, 15, 16), (9, 14, 17), (7, 16, 17), (7, 14, 15) & \nu_{32} = \frac{4}{15} \\ (1, 10, 15), (1, 13, 16), (2, 11, 14), (2, 12, 17), (3, 10, 17), \\ (3, 11, 16), (4, 12, 15), (4, 13, 14) & \nu_{33} = \frac{7}{30} \end{cases}$$

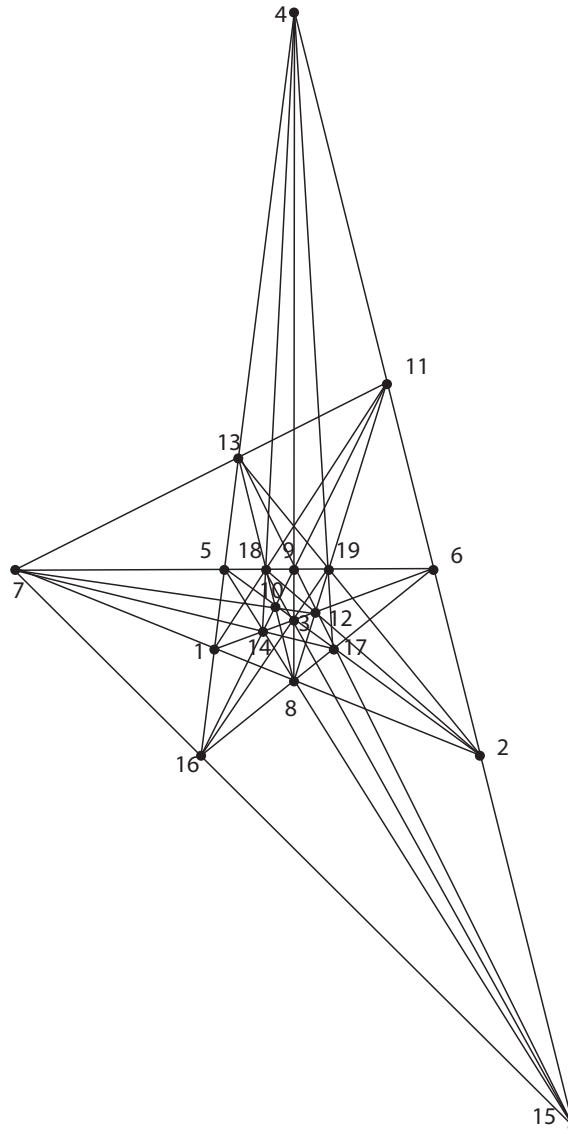
$$\mathcal{I}_4 = \{(1, 2, 7, 8), (1, 3, 6, 14), (1, 4, 5, 17), (2, 3, 5, 15), (2, 4, 6, 16), (3, 4, 8, 9), (5, 6, 7, 9)\},$$

$$\nu_4 = \frac{2}{5}$$

$$\mathcal{I}_6 = \{(6, 8, 11, 13, 15, 17), (5, 8, 10, 12, 14, 16)\}, \nu_6 = \frac{3}{5}$$

\vee -system $(E_8, A_1^3 \times A_2)$

$$\begin{bmatrix} 1 & 2 & 3 & 4 & 5 & 6 & 7 & 8 & 9 & 10 & 11 & 12 & 13 & 14 & 15 & 16 & 17 & 18 & 19 \\ \sqrt{3} & 3 & 0 & 1 & \sqrt{3} & 0 & \sqrt{6} & 0 & 0 & \sqrt{6} & \sqrt{3} & 3 & 1 & \sqrt{3} & 0 & 2 & \sqrt{6} & 0 & \sqrt{6} \\ \sqrt{3} & 0 & 3 & -1 & 0 & \sqrt{3} & 0 & \sqrt{6} & 0 & \sqrt{6} & \sqrt{3} & 3 & 2 & 0 & \sqrt{3} & 1 & 0 & \sqrt{6} & \sqrt{6} \\ 0 & 3 & 3 & 0 & -\sqrt{3} & -\sqrt{3} & 0 & 0 & 6\sqrt{2} & 3\sqrt{6} & 4\sqrt{3} & 6 & 3 & 3\sqrt{3} & 3\sqrt{3} & 3 & 2\sqrt{6} & 2\sqrt{6} & \sqrt{6} \end{bmatrix}$$



$$G = 30 \begin{bmatrix} 1 & 0 & 0 \\ 0 & 2 & 0 \\ 0 & 0 & 3 \end{bmatrix}$$

$$\begin{aligned} \mathcal{I}_2 = \{ & (1, 9), (1, 15), (1, 17), (2, 9), (2, 14), (2, 16), (3, 7), (3, 11), \\ & (3, 13), (4, 7), (4, 10), (4, 12), (5, 11), (5, 12), (6, 10), (6, 13), (10, 15), (11, 17), (12, 16), \\ & (13, 14), (14, 19), (15, 19), (16, 18), (17, 18) \} \end{aligned}$$

$$\mathcal{I}_3 = \begin{cases} (3, 15, 18), (3, 16, 19), (4, 14, 18), (4, 17, 19), (7, 14, 17), (7, 15, 16) & \nu_{31} = \frac{7}{30} \\ (7, 13, 11), (2, 12, 18), (2, 13, 19), (1, 10, 19), (1, 11, 18), (7, 10, 12) & \nu_{32} = \frac{1}{6} \end{cases}$$

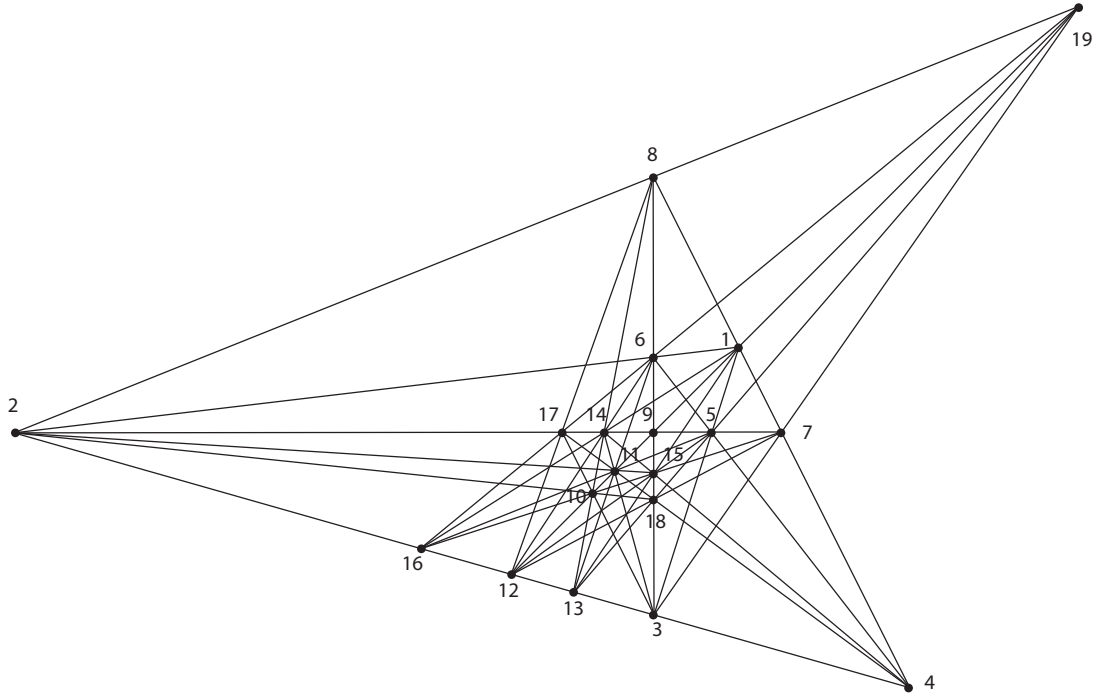
$$\mathcal{I}_4 = \begin{cases} (1, 2, 7, 8), (8, 10, 13, 18), (8, 11, 12, 19) & \nu_{31} = \frac{4}{15} \\ (3, 4, 8, 9), (5, 8, 14, 15), (6, 8, 16, 17) & \nu_{32} = \frac{2}{5} \end{cases}$$

$$\mathcal{I}_5 = \begin{cases} (9, 12, 13, 15, 17), (9, 10, 11, 14, 16), (2, 4, 6, 11, 15), \\ (2, 3, 5, 10, 17), (1, 4, 5, 13, 16), (1, 3, 6, 12, 14) & \nu_5 = \frac{2}{5} \end{cases}$$

$$\mathcal{I}_6 = \{(5, 6, 7, 9, 18, 19)\}, \nu_6 = \frac{3}{5}$$

\vee -system $(E_8, A_2^2 \times A_1)$

$$\mathcal{A} = \begin{bmatrix} 1 & 2 & 3 & 4 & 5 & 6 & 7 & 8 & 9 & 10 & 11 & 12 & 13 & 14 & 15 \\ \sqrt{3} & 3 & 0 & 1 & \sqrt{3} & 0 & \sqrt{6} & 0 & 0 & \sqrt{6} & \sqrt{3} & 3 & 1 & \sqrt{3} & 0 & \dots \\ \sqrt{3} & 0 & 3 & -1 & 0 & \sqrt{3} & 0 & \sqrt{6} & 0 & \sqrt{6} & \sqrt{3} & 3 & 2 & 0 & \sqrt{3} \\ 0 & 3 & 3 & 0 & -\sqrt{3} & -\sqrt{3} & 0 & 0 & 6\sqrt{2} & 3\sqrt{6} & 4\sqrt{3} & 6 & 3 & 3\sqrt{3} & 3\sqrt{3} \\ & 16 & 17 & 18 & 19 \\ \dots & 2 & \sqrt{6} & 0 & \sqrt{6} \\ & 1 & 0 & \sqrt{6} & \sqrt{6} \\ & 3 & 2\sqrt{6} & 2\sqrt{6} & \sqrt{6} \end{bmatrix}$$



$$G = 30 \begin{bmatrix} 2 & 1 & 3 \\ 1 & 2 & 3 \\ 3 & 3 & 12 \end{bmatrix}$$

$$\mathcal{I}_2 = \{(1, 17), (1, 18), (4, 9), (4, 10), (4, 19), (5, 8), (5, 10), (6, 7), (6, 10), (7, 11), (7, 13), \\ (8, 11), (8, 16), (9, 13), (9, 16), (13, 17), (14, 18), (14, 19), (15, 17), (15, 19), (16, 18)\}$$

$$\mathcal{I}_3 = \begin{cases} (1, 2, 6), (1, 3, 5), (2, 11, 15), (3, 11, 14), (5, 12, 15), (6, 12, 14) & \nu_{31} = \frac{7}{30} \\ (7, 12, 18), (8, 12, 17), (3, 10, 17), (3, 7, 19), (2, 10, 18), (2, 8, 19) & \nu_{32} = \frac{4}{15} \\ (1, 13, 15), (1, 14, 16), (4, 5, 6), (4, 14, 15), (5, 11, 16), (6, 11, 13) & \nu_{33} = \frac{1}{6} \end{cases}$$

$$\mathcal{I}_4 = \begin{cases} (1, 4, 7, 8), (4, 11, 17, 18), (5, 13, 18, 19), (6, 16, 17, 19), \\ (7, 10, 15, 16), (8, 10, 13, 14) \end{cases} \quad \nu_4 = \frac{4}{15}$$

$$\mathcal{I}_6 = \begin{cases} (2, 3, 4, 12, 13, 16); & \nu_{61} = \frac{2}{5} \\ (2, 5, 7, 9, 14, 17), (1, 9, 10, 11, 12, 19), (3, 6, 8, 9, 15, 18) & \nu_{62} = \frac{3}{5} \end{cases}$$

\vee -system (H_4, A_1)

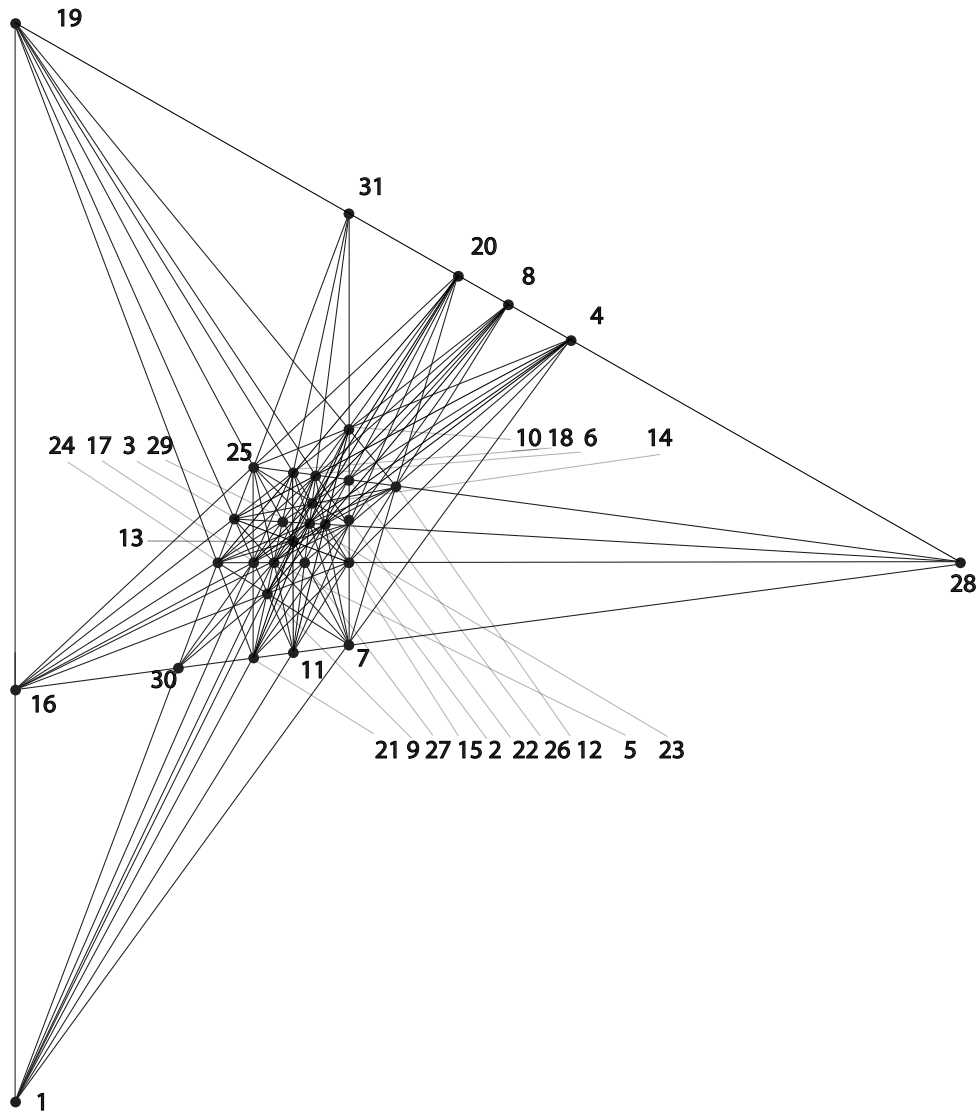
$$\mathcal{A} = \begin{bmatrix} 1 & 2 & 3 & 4 & 5 & 6 & 7 & 8 & 9 & 10 & 11 & 12 & 13 & 14 & 15 & 16 \\ 1 & 0 & 0 & \frac{\sqrt{2}}{2} & \frac{\sqrt{2}}{2} & \frac{\sqrt{2}}{2} & \frac{\sqrt{2}}{2} & a & a & a & a & b & b & b & b & \frac{1}{2} & \dots \\ 0 & 1 & 0 & \frac{\sqrt{2}}{2} & \frac{\sqrt{2}}{2} & -\frac{\sqrt{2}}{2} & -\frac{\sqrt{2}}{2} & \frac{1}{2} & \frac{1}{2} & -\frac{1}{2} & -\frac{1}{2} & a & a & -a & -a & b \\ 0 & 0 & 1 & \frac{\sqrt{2}}{2} & -\frac{\sqrt{2}}{2} & \frac{\sqrt{2}}{2} & -\frac{\sqrt{2}}{2} & b & -b & b & -b & \frac{1}{2} & -\frac{1}{2} & \frac{1}{2} & -\frac{1}{2} & a \\ 17 & 18 & 19 & 20 & 21 & 22 & 23 & 24 & 25 & 26 & 27 \\ \dots & \frac{1}{2} & \frac{1}{2} & \frac{1}{2} & a\sqrt{2} & a\sqrt{2} & 0 & 0 & b\sqrt{2} & b\sqrt{2} & \sqrt{b\sqrt{5}} & \sqrt{b\sqrt{5}} & \dots \\ & b & -b & -b & b\sqrt{2} & -b\sqrt{2} & a\sqrt{2} & a\sqrt{2} & 0 & 0 & 2a\sqrt{b\sqrt{5}} & -2a\sqrt{b\sqrt{5}} \\ & -a & a & -a & 0 & 0 & b\sqrt{2} & -b\sqrt{2} & a\sqrt{2} & -a\sqrt{2} & 0 & 0 \\ & & & & 28 & 29 & 30 & 31 \\ \dots & & 0 & 0 & 2a\sqrt{b\sqrt{5}} & -2a\sqrt{b\sqrt{5}} \\ & & \sqrt{b\sqrt{5}} & \sqrt{b\sqrt{5}} & 0 & 0 \\ & & 2a\sqrt{b\sqrt{5}} & -2a\sqrt{b\sqrt{5}} & \sqrt{b\sqrt{5}} & \sqrt{b\sqrt{5}} \end{bmatrix}$$

with $a = \frac{1+\sqrt{5}}{4}$ and $b = \frac{-1+\sqrt{5}}{4}$.

$$G = I$$

$$\begin{aligned} \mathcal{I}_2 = & \{(1, 22), (1, 23), (1, 28), (1, 29), (2, 24), (2, 25), (2, 30), (2, 31), (3, 20), \\ & (3, 21), (3, 26), (3, 27), (4, 11), (4, 13), (4, 18), (5, 10), (5, 12), (5, 19), \\ & (6, 9), (6, 15), (6, 16), (7, 8), (7, 14), (7, 17), (8, 25), (8, 29), (8, 27), \\ & (9, 25), (9, 26), (9, 28), (10, 24), (10, 27), (10, 28), (11, 24), (11, 26), \\ & (11, 29), (12, 29), (12, 31), (13, 20), (13, 28), (13, 31), (14, 21), \\ & (14, 28), (12, 21), (14, 30), (15, 20), (15, 29), (15, 30), (16, 23), \\ & (16, 27), (16, 31), (17, 22), (17, 26), (17, 31), (18, 22), (18, 27), \end{aligned}$$

$(18, 30), (19, 23), (19, 26), (19, 30)\}$



$$\mathcal{I}_3 = \left\{ \begin{array}{l} \{(1, 4, 7), (1, 5, 6), (2, 4, 5), (2, 6, 7), (3, 4, 6), (3, 5, 7), (4, 10, 25), (4, 15, 21), (4, 17, 23), \\ (5, 11, 25), (17, 21, 25), (8, 21, 22), (18, 20, 24), (16, 20, 25), (19, 21, 24) \\ (5, 14, 20), (5, 16, 22), (6, 8, 24), (6, 13, 21), (6, 19, 22), (7, 9, 24), (7, 12, 20), (7, 18, 23), \\ (9, 20, 23), (10, 21, 23), (11, 20, 22), (12, 23, 24), (13, 22, 24), (14, 22, 25), (15, 23, 25)\} \quad \nu_{31} = \frac{2}{15} \\ \{(1, 16, 19), (1, 17, 18), (2, 8, 9), (2, 10, 11), (3, 12, 14), (3, 13, 15), (8, 14, 17), \\ (11, 13, 18), (9, 15, 16), (10, 12, 19)\} \quad \nu_{32} = \frac{1}{10} \end{array} \right.$$

$$\mathcal{I}_5 = \{(1, 8, 11, 12, 15), (1, 9, 10, 13, 14), (2, 12, 13, 16, 17), (2, 14, 15, 18, 19),$$

$$(3, 8, 10, 16, 18), (3, 9, 11, 17, 19)\}$$

$$\nu_5 = \frac{1}{6}$$

$$\begin{aligned} \mathcal{I}_6 = & \{(1, 2, 20, 21, 26, 27), (1, 3, 24, 25, 30, 31), (2, 3, 22, 23, 28, 29), (4, 8, 19, 20, 28, 31), \\ & (5, 8, 13, 23, 26, 30), (5, 9, 18, 21, 29, 31), (5, 15, 17, 24, 27, 28), (6, 10, 17, 20, 29, 30), \\ & (6, 11, 14, 23, 27, 31), (6, 12, 18, 25, 26, 28), (4, 9, 12, 22, 27, 30), (4, 14, 16, 24, 26, 29), \\ & (7, 10, 15, 22, 26, 31), (7, 11, 16, 21, 28, 30), (7, 13, 19, 25, 27, 29)\} \end{aligned}$$

$$\nu_6 = \frac{1}{3} \}$$

Appendix B

Mathematica implementation of linearised \vee -conditions

The purpose of this appendix is to demonstrate how the linearised \vee -conditions derived in section 3.2 can be implemented in Mathematica [55]. Here we use a modified version of the Mathematica program developed by K. Schwerdtfeger in [41].

```
all2Flats[A_] := Block[{At, n, Ids},
  At = Transpose[A]; n = Length[At]; Ids = {};
  Do[If[! pairListedQ[Ids, i, j], AppendTo[Ids, {i, j}]];
  Do[If[MatrixRank[{At[[i]], At[[j]], At[[k]]}] == 2,
    AppendTo[Ids[[Length[Ids]], k]],
    {k, j + 1, n}]],
  {i, 1, n - 1}, {j, i + 1, n}];
  Ids[[2 ;;]]];
```

gives a list of all 2-flats of a given system. Here the command

```
pairListedQ[L_, i_, j_] :=
  Catch[If[i == j, Throw[False]]];
  Do[If[MemberQ[l, i] && MemberQ[l, j], Throw[True]], {l, L}];
  False];
```

is used. The command

```
large2Flats[A_] := Select[all2Flats[A], Length[#] > 2 &];
```

gives only flats with more than 2 elements.

In order to check the \vee -conditions and compute the values of the ν -function one can use the following command [41]

```

checkV[A_] := Block[{At, G, Gi, mults, m, i = 1},
  At = Transpose[A]; G = A.At; Gi = Inverse[G];
  Do[mults = {};
  Do[m =
    Solve[Sum[At[[i]].Gi.At[[id]]*At[[i]], {i, ids}] == 1*At[[id]],
    1];
  AppendTo[mults, If[m == {}, False, Simplify[m[[1, 1, 2]]]],
  {id, ids}];
  Print[{i++, ids,
    If[Do[If[m != mults[[1]], Return[True]], {m, mults}] === True,
    mults, mults[[1]]}],
  {ids, all2Flats[A]}}];

```

Interested in the number of parameters on which the solutions of the infinitesimal constraints depend (see section 3.2) we add the extension

```

G = FullSimplify[vt.vectors];
Gi = Inverse[G];
x = Table[a[i], {i, n}]
vectorsx = Table[Sqrt[x[[k]]]*vectors[[k]], {k, 1, n}];
X = FullSimplify[Transpose[vectorsx].vectorsx];
gorth = {};
mults = {};

gorth = Table[
  Simplify[Gi.vectors[[12i[[1]]]].X.Gi.vectors[[12i[[2]]]],
  {12i, 12}];
Do[m = Simplify[
  Solve[Sum[
    Simplify[
      Simplify[vectors[[i]].Gi.vectors[[ids[[1]]]]*
      Simplify[Gi.vectors[[i]]], {i, ids}] ==
      1*Simplify[Gi.vectors[[ids[[1]]]], 1];
    AppendTo[mults, Simplify[m[[1, 1, 2]]], {ids, llarge}];
  mults

Block[{Xp, vp, m1, m2},
  Do[vp = Table[vectorsx[[id]], {id, llarge[[i]]}];
  Xp = Simplify[Transpose[vp].vp];
  V1 = Simplify[Gi.vectors[[llarge[[i]][[1]]]];
  V2 = Simplify[Gi.vectors[[llarge[[i]][[3]]]];
  m1 = Simplify[
    Numerator[
      Simplify[(Simplify[(V1.(Xp - mults[[i]]*X).V1)/
        Simplify[(V1.G.V1)]] -
        Simplify[(Simplify[(V2.(Xp - mults[[i]]*X).V2)/
        Simplify[(V2.G.V2)]])]];
  m2 = Simplify[
    Numerator[
      Simplify[
        FullSimplify[(Simplify[(V1.(Xp - mults[[i]]*X).V1)]/

```

```
Simplify[(V1.G.V1))] -  
Simplify[(Simplify[(V1.(Xp - mults[[i]]*X).V2)]/  
Simplify[(V1.G.V2)])]]];  
AppendTo[gorth, Simplify[m1]]; AppendTo[gorth, Simplify[m2]],  
{i, Length[l1arge]}}];  
  
MatrixForm[Transpose[vectorsx]]  
MatrixRank[  
NullSpace[  
Table[Coefficient[gorth[[1]], x[[j]], 1], {1, Length[gorth]}, {j,  
Length[vectors]}]]]
```

The results obtained using this approach are listed in section [3.2](#).

Bibliography

- [1] MOSAIC 11. *Journal of Asprom*, 1984.
- [2] E. R. Berlekamp, E. N. Gilbert, and F. W. Sinden. A Polygon Problem. *The American Mathematical Monthly*, *Mathematical Association of America*, 72(3):pp. 233–241, 1965.
- [3] Nicolas Bourbaki. *Éléments de mathématique*. Masson, Paris, 1981. Groupes et algèbres de Lie. Chapitres 4, 5 et 6. [Lie groups and Lie algebras. Chapters 4, 5 and 6].
- [4] O.A. Chalykh, M.V. Feigin, and A.P. Veselov. New integrable generalizations of Calogero-Moser quantum problem. *J. Math. Phys.*, 39:695–703, 1998.
- [5] O.A. Chalykh and A.P. Veselov. Locus configurations and \vee -systems. *Phys.Lett.A*, 285:339–349, 2001.
- [6] Yves Colin de Verdière. Sur un nouvel invariant des graphes et un critre de planarité. *J. Comb. Theory, Ser. B*, 50(1):11–21, 1990.
- [7] J.H. Conway, H. Burgiel, and C. Goodman-Strass. *The Symmetries of Things*. A.K. Peters, Ltd, 2008.
- [8] D. Cvetković, P. Rowlinson, and S. Simić. *An Introduction to the Theory of Graph Spectra*. Cambridge: Cambridge University Press, 2010.
- [9] Boris Dubrovin. Geometry of 2D topological field theories. In Mauro Francaviglia and Silvio Greco, editors, *Integrable Systems and Quantum Groups*, volume 1620 of *Lecture Notes in Mathematics*, pages 120–348. Springer Berlin Heidelberg, 1996.
- [10] Boris Dubrovin. On almost duality for Frobenius manifolds. *Amer. Math. Soc. Transl.* 212, 2004.
- [11] J. R. Edmundson. The arrangement of point charges with tetrahedral and octahedral symmetry on the surface of a sphere with minimum Coulombic potential energy. *Acta Cryst.*, A49:648–654, 1993.

-
- [12] K. Ehly and G. Gordon. Matroid automorphisms of the root system H_3 . *Geom. Dedicata*, 130:149–161, 2007.
- [13] M. Feigin. On the logarithmic solutions of the WDVV equations. *Czechoslovak J. Phys*, 56:1149–1153, 2006.
- [14] M.V. Feigin and A.P. Veselov. Logarithmic Frobenius structures and Coxeter discriminants. *Adv. Math.*, 212:143–162, 2007.
- [15] M.V. Feigin and A.P. Veselov. On the geometry of \vee -systems. *Amer. Math. Soc. Transl. (2)*, 224:111–123, 2008.
- [16] M. Fiedler. Algebraic connectivity of graphs. *Czechoslovak Mathematical Journal*, 23(98):298–305, 1973.
- [17] W. Fulton and J. Harris. *Representation Theory*. Springer, 1991.
- [18] Branko Grünbaum. Graphs of polyhedra; polyhedra as graphs. *Discrete Mathematics*, 307(3-5):445–463, 2007.
- [19] F. Harari. *Graph Theory*. AddisonWesley, Reading, MA, 1969.
- [20] G. Huisken. Flow by mean curvature of convex surfaces into spheres. *J. Differential Geom.*, 20:237–266, 1984.
- [21] I. Ivriissimtzis and N. Peyerimhoff. Spectral representations of vertex transitive graphs, Archimedean solids and finite Coxeter groups. *Groups Geom. Dyn.*, 7, 2011.
- [22] Ivan Izmestiev. Colin de Verdière number and graphs of polytopes. *Israel J. Math.*, 178:427–444, 2010.
- [23] S. Kobayashi and K. Nomizu. *Foundations of differential geometry, Vol. II*. ohn Wiley and Sons, Inc., New York-London- Sydney, 1969.
- [24] A. Kotlov, L. Lovász, and S. Vempala. The Colin de Verdière Number and Sphere Representations of a Graph. *Combinatorica*, 17(4):483–521, 1997.
- [25] P. Kurasov, G. Malenová, and S. Naboko. Spectral gap for quantum graphs and their edge connectivity. *Journal of Physics A Mathematical General*, 46(26):A265309, July 2013.
- [26] O. Lechtenfeld, K. Schwertfeger, and J. Thueringen. $N = 4$ multi-particle mechanics, WDVV equation and roots. *SIGMA*, 7:21, 2011.
- [27] L. Lovász. Steinitz representations of polyhedra and the Colin de Verdière number. *J. Comb. Theory, Ser. B*, 82:223–236, 2000.

- [28] L. Lovász. Geometric representations of graphs, 2009.
- [29] L. Lovász and A. Schrijver. On the null space of a Colin de Verdière matrix. *Symposium la Mémoire de Francois Jaeger, Grenoble*, 1998.
- [30] P. Mani. Automorphismen von polyedrischen Graphen. *Mathematische Annalen*, 192:279–303, 1971.
- [31] A. Marshakov, A. Mironov, and A. Morozov. WDVV-like equations in $N = 2$ SUSY Yang-Mills theory. *Phys.Lett. B*, 389:43–52, 1996.
- [32] Y. Matsumoto, S. Moriyama, H. Imai, and D. Bremner. Matroid Enumeration for Incidence Geometry. *Discrete & Computational Geometry*, 47(1):17–43, 2012.
- [33] B.D.S. McConnell. Spectral realizations of graphs. <http://daylateanddollarshort.com/mathdocs/Spectral-Realizations-of-Graphs.pdf>.
- [34] J. Morgan and G. Tian. Ricci flow and the Poincare conjecture. *Clay Mathematics Monographs*, 3, 2007.
- [35] A. Mowshowitz. The group of a graph whose adjacency matrix has all distinct eigenvalues. *Proof Techniques in Graph Theory, Academic Press, New York*, pages 109–110, 1969.
- [36] J. Oxley. *Matroid Theory*. Oxford Graduate Texts in Mathematics, Oxford, 1993.
- [37] J. Richter-Gebert and G. M. Ziegler. Oriented matroids. *In Handbook of discrete and computational geometry, 111132, CRC Press Ser. Discrete Math. Appl., CRC, Boca Raton, FL*, 1997.
- [38] N.C. Saldanha and C. Tomei. Spectra of regular polytopes. *Discrete Comput. Geom.*, 7(4):403–414, 1992.
- [39] V. Schreiber and A. P. Veselov. On deformation and classification of \vee -systems. *ArXiv:1404.4552*, 2014.
- [40] V. Schreiber, A. P. Veselov, and J. P. Ward. In search for a perfect shape of polyhedra: Buffon transformation. *ArXiv:1402.5354*, 2014.
- [41] K.W. Schwerdtfeger. Ueber Loesungen zu der WDVV-Gleichungen, Diploma Thesis, unpublished. <http://www.itp.uni-hannover.de/lechtenf/Theses/schwerdtfeger.pdf>.
- [42] V. Serganova. On generalization of root systems. *Commun. in Algebra*, 24:4281–4299, 1996.

-
- [43] A.N. Sergeev and A.P. Veselov. Deformed quantum Calogero-Moser problems and Lie superalgebras. *Comm. Math. Phys.*, 245:249–278, 2004.
- [44] Paul D. Seymour. Decomposition of regular matroids. *J. Comb. Theory, Ser. B*, 28(3):305–359, 1980.
- [45] T. Takahashi. Minimal immersions of Riemannian manifolds. *J. Math. Soc. Japan*, 18:4:380–385, 1966.
- [46] H. van der Holst. A short proof of the planarity characterization of Colin de Verdière. *J. Comb. Theory Ser. B*, 65(2):269–272, 1995.
- [47] H. van der Holst, L. Lovász, and A. Schrijver. The Colin de Verdière graph parameter. *Graph Theory and Combinatorial Biology, Bolyai Soc. Math. Stud.*, 7:29–85, 1999.
- [48] A. P. Veselov. On geometry of a special class of solutions to generalised WDVV equations. *Integrability: the Seiberg-Witten and Whitham equations (Edinburgh, 1998), Gordon and Breach (2000)*.
- [49] A.P. Veselov. Deformations of root systems and new solutions to generalised WDVV equations. *Phys. Lett.*, A 261:297, 1999.
- [50] A.P. Veselov and J.P. Ward. Buffon transformation for polyhedra. *Unpublished*, 2004.
- [51] J. P. Ward. Experimental mathematics in the curriculum (part I). *Teaching Mathematics and its Applications*, 25(4):205–215, December 2006.
- [52] J.P. Ward. Experimental mathematics in the curriculum (part II). *Teaching Mathematics and its Applications*, 26(1):27–37, March 2007.
- [53] D. S. Watkins. *The Matrix Eigenvalue Problem: GR and Krylov Subspace Methods*. SIAM, 2007.
- [54] Walter Wenzel. Projective equivalence of matroids with coefficients. *J. Comb. Theory, Ser. A*, 57(1):15–45, 1991.
- [55] Inc. Wolfram Research. Mathematica.
- [56] G. Ziegler. *Lectures on Polyhedra*. Springer, 2007.